Study and Development of an "Electronic Nose" and Comparison with Mammalian Olfaction

Thesis by

Brett James Doleman

In Partial Fulfillment of the Requirements

for the Degree of

Doctor of Philosophy

California Institute of Technology

Pasadena, California

1999

(Submitted April 5, 1999)

Acknowledgements

In keeping with my custom of brevity, I will broadly state that I want to deeply thank all those who have helped me along in reaching this point in my life. This includes my friends and family, and those with whom I have worked within and outside Caltech. Specifically, Prof. Nate Lewis, my research advisor, provided an environment full of interesting research ideas and the material resources to pursue them, and he consistently encouraged the pursuit of my own research ideas and interests. I also want to specifically thank Erik Severin, with whom I have worked for over four years now, for his useful ideas and for the helpful advancements he has made in automating our experimental equipment.

Ironically, while Caltech is a place known predominantly for its science and engineering excellence, it has also furnished opportunities for me to develop strong non-scientific interests which will likely guide my future career. For the diversity of my learning and growth experiences here, I owe much to Caltech.

Abstract

Arrays of broadly responsive vapor detectors (i.e., electronic noses) are receiving an increasing amount of scientific attention for their potential as analytical devices, as models for studying mammalian olfaction, and perhaps for someday ultimately duplicating or surpassing the mammalian olfactory sense. Herein, research was primarily focused on an electronic nose composed of an array of carbon black-polymer composite detectors while arrays of tin oxide detectors and organic conducting polymer detectors were used only in a comparison study. The research determined the odorant resolving power of electronic nose sensor arrays, explored the dependence of the electronic nose array response intensity on odorant vapor pressure, compared the odorant detection thresholds and odorant classification properties of the electronic nose to the mammalian olfactory sense, and attempted to predict human odor quality judgements using electronic nose detector responses.

The Fisher linear discriminant statistical metric was utilized to quantify the performance of arrays composed of carbon black-insulating polymer composite detectors, tin oxide detectors and bulk conducting organic polymer detectors in resolving nineteen odorant vapors. The odorant resolving power of the sensor arrays as a function of the chemical composition of the detectors and the number of detectors they contained was studied. The results provided insights into optimizing the chemical diversity and size of a chemical vapor sensor array for various tasks.

Response data were collected for a carbon black-polymer composite electronic nose array during exposure to homologous series of 1-alcohol and n-alkane odorants. The mean response intensity of the electronic nose detectors, and the response intensity of the most strongly-driven set of electronic nose detectors, was essentially constant for members of a chemically homologous odorant series when the concentration of each odorant in the gas phase was maintained at a constant fraction of the odorant's vapor pressure. A similar

trend is observed in human odor detection threshold values for these same odorants. The data imply that the trends in detector responses and human detection thresholds can be understood based on the thermodynamic tendency to establish a relatively constant concentration of sorbed odorant into each of the polymeric films of the electronic nose and into the olfactory epithelium of humans at a constant fraction of the odorant's vapor pressure.

Experiments were performed to compare the detection thresholds and trends in discrimination abilities of the electronic nose to those of the mammalian olfactory sense, and to develop models predicting human odor quality judgements from electronic nose detector responses. The detection thresholds for the electronic nose and the human nose were compared for series of n-alkanes and 1-alcohols. Trends in the odorant-discriminating abilities of an electronic nose and mammalian noses were compared for series of esters, alcohols and carboxylic acids. Electronic nose response data were collected for a diverse set of odorants which had previously been quantitatively characterized by human panelists according to many categories of odor quality. The responses of the electronic nose detectors were then used in attempts at predicting the human odor quality judgements.

Table of Contents

List of Figures and Tables

Chapter 1: Introduction

BACKGROUND

Conventional approaches to chemical sensors have traditionally made use of a "lock-and-key" design, wherein a specific receptor is synthesized in order to bind strongly and with high selectivity to the analyte of interest. The selectivity is achieved through precise chemical design of the receptor site. Such approaches are appropriate when a specific target compound is to be identified in a controlled or known environment. However, this type of approach is tedious since it requires the synthesis of a different, highly selective detector for each analyte to be detected.

An alternative approach to chemical sensing is conceptually closer to a design believed to be present in the mammalian sense of olfaction.[1-5] In such an approach, the strict "lock-and-key" design criterion of traditional sensing devices is abandoned. Instead, an array of incrementally different detectors is used, with every detector in the array chosen to respond to a number of different chemicals or classes of chemicals.[6-9] The individual detectors of such an array should contain as much chemical diversity as possible, so that the array responds to the largest possible cross section of odorants. In this design, the identification of an odorant cannot be accomplished from the response of a single detector, but a distinct pattern of responses produced over the collection of detectors in the array provides a fingerprint that identifies the odorant. The advantage of this approach is that it yields responses to a variety of different odorants, including those for which the array was not originally designed. In addition, the broadly responsive detectors need not contain synthetically challenging, custom-designed, "lock-and-key" receptor sites in order to generate a response to an odorant. Also, an array of detectors naturally performs an integration to yield a unique signal for complex but distinctive odors (e.g., cheeses, beers, etc.) without requiring that the mixture be broken down into its individual components prior to, or during, the analysis.

Array-based vapor sensing has been demonstrated previously in several systems, including those using surface acoustic wave devices,[10-13] tin oxide detectors,[14-16] and conducting organic polymers.[17-19] In general, desirable design criteria for the detectors in such an array are as follows: (1) they should readily transduce chemical stimuli into an easily monitored signal using a minimum of hardware and energy; (2) they should exhibit reversible and reproducible responses with a minimum of baseline drift; (3) they should be broadly tunable to respond in a predictable manner to a wide range of chemical species and concentrations; (4) they should be easily fabricated from inexpensive, commercially available materials using well-established techniques; (5) they should permit miniaturization to facilitate the construction of compact sensor arrays with a large number of detectors; and (6) they should be robust and stable in many different environments.

The primary sensor array system studied in this thesis is based on detectors composed of conducting carbon black dispersed in a variety of insulating organic polymer films.[20] The carbon black endows electrical conductivity to the films, whereas the different organic polymers are the source of chemical diversity between detectors in the sensor array. Individual carbon black-polymer composite detectors, but not arrays with multiple detectors, have been explored as humidity detectors[21-24] and as detectors for organic vapors or liquids such as gasoline.[25-28] The mechanism by which the chemical vapor stimuli are transduced into an easily monitored electrical signal is based on percolation theory.[20,21,26,29-32] According to percolation theory, swelling of the polymer film as it sorbs odorant molecules increases the resistance of the film by breaking a fraction of the conductive pathways. As shown in Figure 1.1, this provides an extraordinarily simple means for monitoring the presence of odorant vapors by monitoring the electrical resistance of the polymer film within a detector.[20] Since a different polymer is present in each detector, the detectors respond differentially to a given odorant, resulting in an odorant-identifying response pattern.[20] A hypothetical example of such a response pattern is shown in Figure 1.2. An array of detectors will respond to a wide variety of odorant

vapors to yield distinctive response patterns. In many cases, the differences in the response patterns for different odorants can be discerned with the naked eye; however, it is often preferable to transform the data into an optimized coordinate system to emphasize the relative positions and separations of the odorants. For example, in Figure 1.3, response data has been processed using principal component analysis[33] and plotted in multiple dimensions to qualitatively depict the ability of the electronic nose to resolve odorants.[20] These, along with other early results,[20] have shown that an electronic nose based on carbon black-polymer composite detectors appears to be a promising new chemical vapor sensing technology worthy of further study.

Of additional interest, the electronic nose mimics several of the behavioral phenomena and design characteristics associated with mammalian olfaction. For example, the behavioral phenomena of adaptation (i.e., the progressive reduction in the perceived intensity of an odorant exposed at a constant concentration for a prolonged time period) and cross-adaptation (i.e., the reduction in the perceived intensity of one odorant due to a prolonged exposure to a prior odorant) are naturally built-in to the electronic nose. As shown in Figure 1.1, the slope of a detector response decreases as a function of time as the detector adapts to the exposed odorant. Furthermore, if the electronic nose detectors were allowed to adapt to an odorant immediately before replacing the odorant with another, then each detector response to the second odorant would be reduced to the differential response between the two odorants which is analogous to mammalian olfactory cross-adaptation. In terms of design characteristics, recent data suggests that the mammalian nose contains $\approx 10^3$ incrementally different types of olfactory receptors which each recognize multiple odorants and that each odorant is recognized by a distinct combination of receptors which encode the odorant identity.[1-5] This design is conceptually analogous to the electronic nose. Despite the similarities between electronic and mammalian olfaction, the electronic nose cannot yet approach the sensitivity or discrimination capability of the mammalian olfactory sense for certain odorant classes such as pheromones, thiols and amines.

Figure 1.1: Schematic diagram showing how an individual carbon black-polymer composite detector changes resistance upon exposure to an odorant vapor. Before the odorant exposure starts, the carbon black-polymer film has an initial volume and resistance. During exposure to an odorant vapor, the film sorbs odorant molecules and swells to a larger volume which breaks a fraction of the conductive carbon black pathways and in turn increases the resistance. Once the exposure stops, the film relaxes back to its initial volume and resistance as odorant molecules diffuse out.

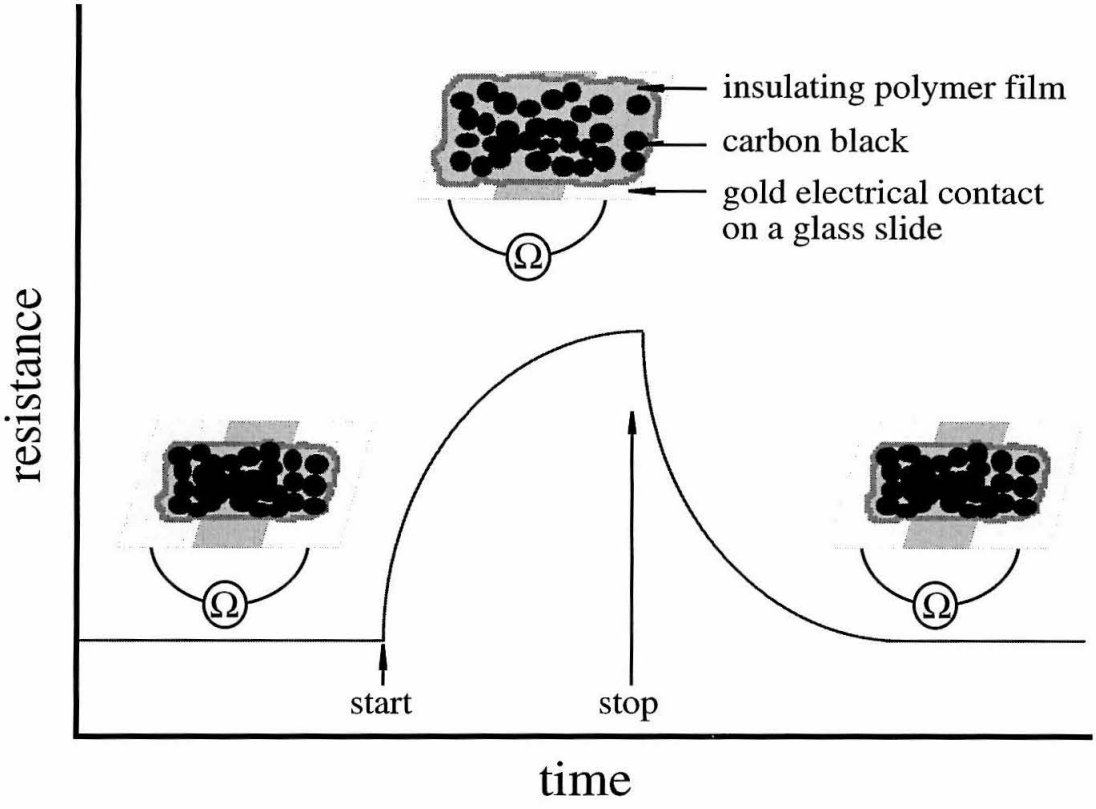
insulating polymer film
carbon black
gold electrical contact
on a glass slide
Ω
resistance
start
stop
time

Figure 1.1

Figure 1.2: Schematic diagram showing how an odorant-identifying response pattern is obtained from the combination of all the detector responses in the array.[20] A detector response is generally defined as the maximum odorant-induced resistance change relative to the baseline resistance, $\Delta R_{max}/R$. Typically even nearly identical odorants will have slightly different response patterns as long as the selected detectors are reasonably diverse.

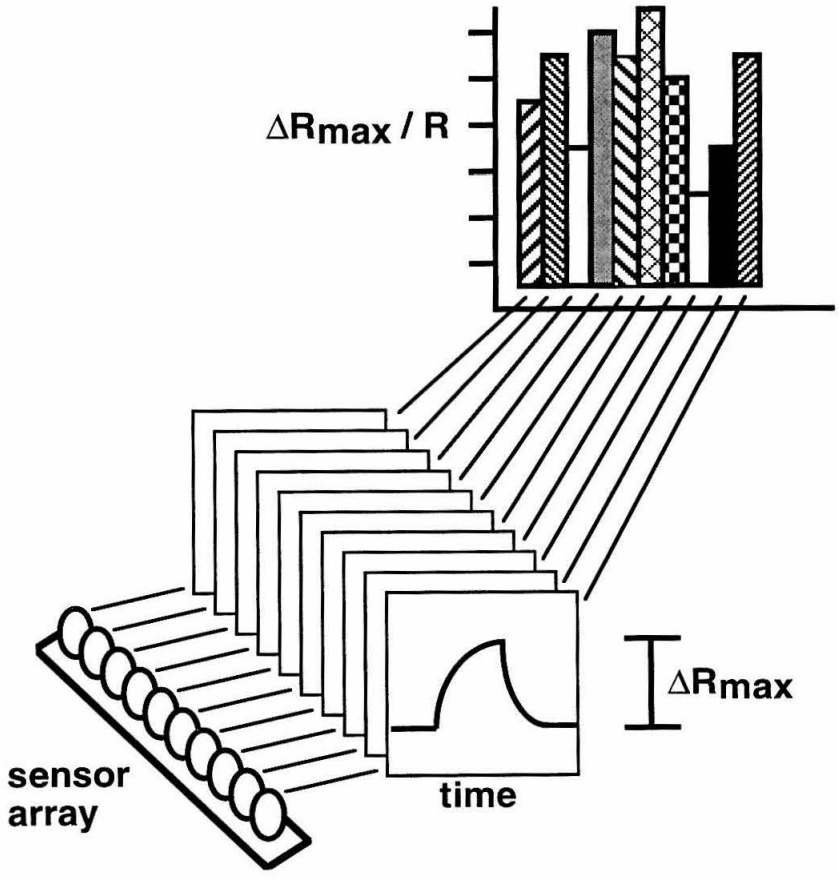

Figure 1.2

Figure 1.3: Three-dimensional plots showing the relative positions and separations of various odorants in principal component (PC) space.[20] The patterned regions contain multiple data points corresponding to the array responses to the specified odorants. (a) The first three principal components (PC1, PC2 and PC3) contain the most information but still leave some odorants unresolved. (b) All the odorants are shown to be resolved in a three-dimensional plot of PC3, PC4 and PC5.

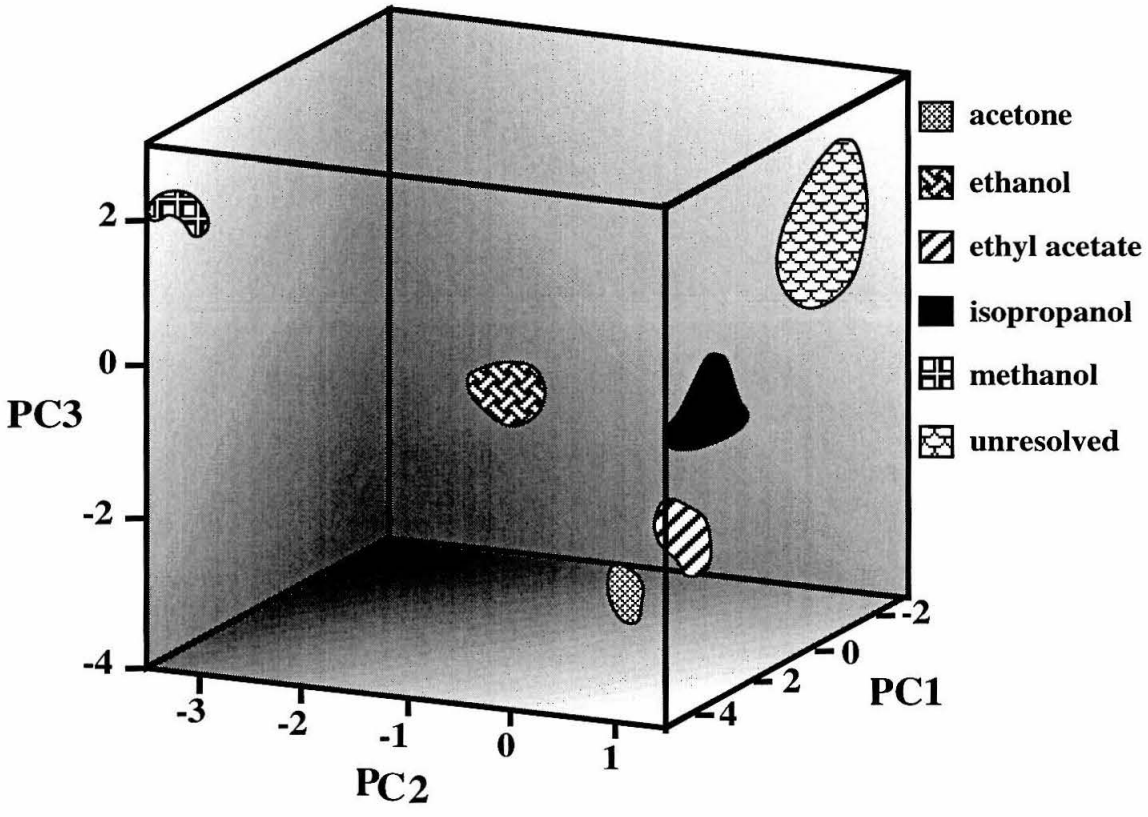
acetone
ethanol
ethyl acetate
isopropanol
methanol
unresolved
PC3
2
0
-2
-4
PC2
-3
-2
-1
0
1
PC1
-2
0
2
4

Figure 1.3a

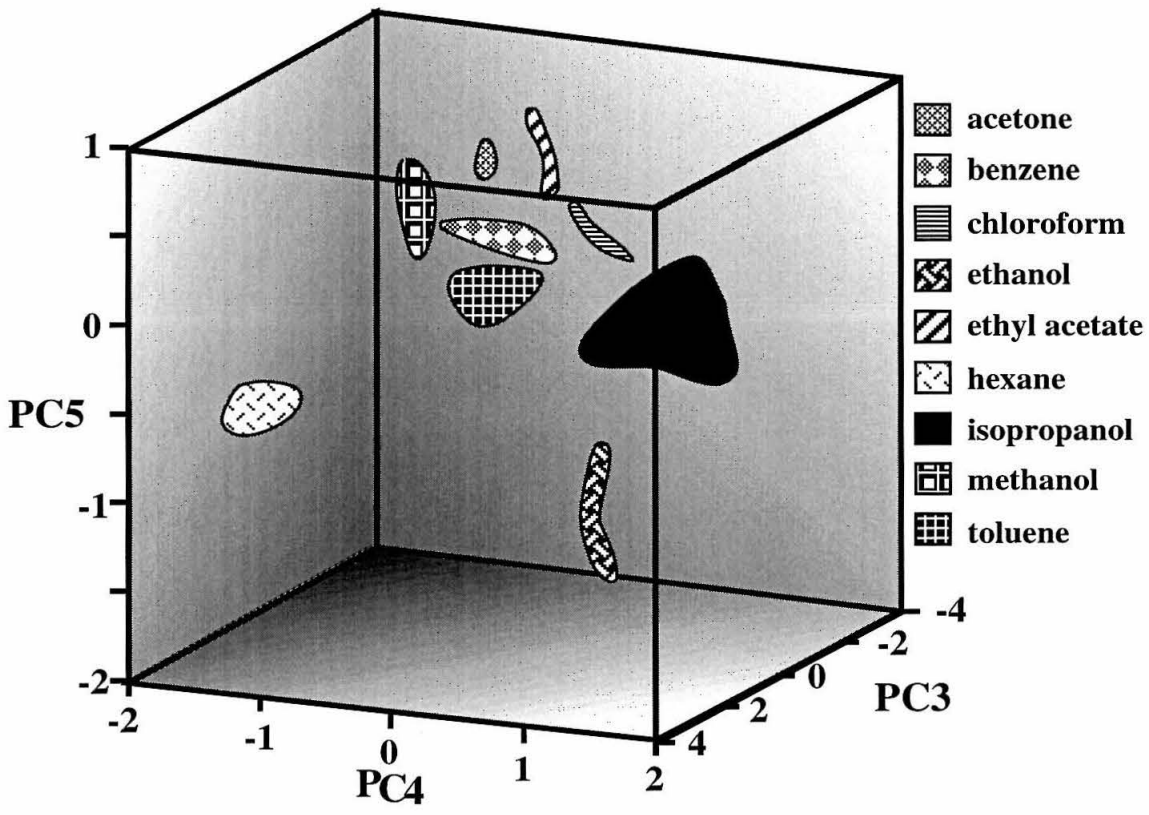
1
0
-1
-2
PC5
-2
-1
0
1
2
PC4
-4
-2
0
2
4
PC3
acetone
benzene
chloroform
ethanol
ethyl acetate
hexane
isopropanol
methanol
toluene

Figure 1.3b

THESIS OVERVIEW

The goal of the research described in this thesis was to build upon the initial work on electronic noses based on arrays of carbon black-polymer detectors[20] by focusing on various important aspects such as quantifying odorant resolving power, studying the dependence of response intensities on thermodynamic parameters, and comparing the abilities of the electronic nose with the abilities of the mammalian olfactory sense.

In Chapter 2, the research focused on statistically quantifying the performance of electronic noses in resolving odorant pairs and applying this toward answering questions about array performance as a function of the chemical composition of detectors and the number of detectors in the array. It is possible to determine with the untrained eye, by comparing odorant response patterns such as those in Figure 1.2 or by using plots such as those in Figure 1.3, that the electronic nose can distinguish between many odorant pairs.[20] However, a more advanced method is required in cases where odorants are chemically similar and thus elicit similar response patterns. Also, a statistically consistent methodology is necessary to quantify the resolution of odorants before studies on the performance of arrays as a function of various variables of interest can begin. Thus, the Fisher linear discriminant methodology[34] was implemented to statistically quantify and study the performance of electronic noses as a function of the chemical composition of the detectors and the number of detectors they contained.

In Chapter 3, the research focused on answering the question of whether the response intensities of the electronic nose can be understood and thus predicted based on simple thermodynamic properties of the test odorant vapors. The results show that, to a first order approximation, the electronic nose responds with a constant signal intensity to odorant vapors which are delivered at a constant ratio of their partial pressure to their vapor pressure. This is explained based on the thermodynamic tendency to establish an approximately constant concentration on average of sorbed odorant into the polymeric films of the electronic nose when odorants are exposed at a constant fraction of their vapor

pressure.[35] Furthermore, the same concepts are proposed to account for trends in human odorant detection thresholds. In the case of the electronic nose, the additional knowledge that response signal intensities vary linearly[20] with the partial pressure of a given odorant allows for estimates of the absolute array response intensity to be made from only the vapor pressure and exposed partial pressure of almost any odorant.

In Chapter 4, the research focused on comparing the electronic nose to the mammalian olfactory sense. There is a growing intellectual interest in comparing the behavior of electronic noses to the mammalian olfactory system, especially as scientific understanding of the mammalian olfactory system begins to suggest it comprises an array of broadly and differentially responsive receptors which is conceptually analogous to electronic noses.[1-5] Thus, identifying and quantifying any behavioral similarities would be useful toward furthering the development of an electronic analogue to mammalian olfaction. In this chapter, the detection thresholds of an electronic nose and human noses were compared. Trends in the abilities of the electronic nose and mammalian noses in distinguishing odorants were also compared. In each case, interesting similarities were observed. In addition, electronic nose response data were used in attempts to develop models predicting human odor quality judgements.

Overall, the research contained in this thesis has contributed to the general understanding of the current generation of the electronic nose, contributed to further developing its abilities and provided a foundation for future progress. These contributions, coupled with contributions from colleagues, are providing the necessary steps toward fulfilling the promise of this technology as an important analytical tool and realizing the ambitious goal of creating an electronic nose which is behaviorally analogous to the mammalian olfactory sense.

REFERENCES

(1) Reed, R. R. *Neuron* **1992**, *8*, 205.

(2) Lancet, D.; Ben-Arie, N. *Curr. Biol.* **1993**, *3*, 668.

(3) Malnic, B.; Hirono, J.; Sato, T.; Buck, L. B. *Cell* **1999**, *96*, 713.

(4) Axel, R. *Sci. Am.* **1995**, *273*, 154.

(5) Breer, H.; Wanner, I.; Strotmann, J. *Behav. Genet.* **1996**, *26*, 209.

(6) Zaromb, S.; Stetter, J. R. *Sens. Actuators* **1984**, *6*, 225.

(7) Lundstrom, I.; Erlandsson, R.; Frykman, U.; Hedborg, E.; Spetz, A.; Sundgren, H.; Welin, S.; Winquist, F. *Nature* **1991**, *352*, 47.

(8) Shurmer, H. V.; Gardner, J. W. *Sens. Actuators B* **1992**, *8*, 1.

(9) Gardner, J. W.; Bartlett, P. N. *Sens. Actuators B* **1994**, *18*, 211.

(10) Ballantine, D. S.; Rose, S. L.; Grate, J. W.; Wohltjen, H. *Anal. Chem.* **1986**, *58*, 3058.

(11) Grate, J. W.; Abraham, M. H. *Sens. Actuators B* **1991**, *3*, 85.

(12) Grate, J. W.; Rosepehrsson, S. L.; Venezky, D. L.; Klusty, M.; Wohltjen, H. *Anal. Chem.* **1993**, *65*, 1868.

(13) Nakamoto, T.; Fukuda, A.; Moriizumi, T. *Sens. Actuators B* **1993**, *10*, 85.

(14) Gardner, J. W.; Shurmer, H. V.; Corcoran, P. *Sens. Actuators B* **1991**, *4*, 117.

(15) Gardner, J. W.; Shurmer, H. V.; Tan, T. T. *Sens. Actuators B* **1992**, *6*, 71.

(16) Corcoran, P.; Shurmer, H. V.; Gardner, J. W. *Sens. Actuators B* **1993**, *15*, 32.

(17) Shurmer, H. V.; Corcoran, P.; Gardner, J. W. *Sens. Actuators B* **1991**, *4*, 29.

(18) Pearce, T. C.; Gardner, J. W.; Friel, S.; Bartlett, P. N.; Blair, N. *Analyst* **1993**, *118*, 371.

(19) Freund, M. S.; Lewis, N. S. *Proc. Natl. Acad. Sci. U.S.A.* **1995**, *92*, 2652.

(20) Lonergan, M. C.; Severin, E. J.; Doleman, B. J.; Beaber, S. A.; Grubbs, R. H.; Lewis, N. S. *Chem. Mater.* **1996**, *8*, 2298.

(21) Norman, R. H. *Conductive Rubbers and Plastics*; Elsevier: Amsterdam, 1970.

(22) Boyd, J.; Bulgin, D. *J. Text. Inst. Proc.* **1957**, *48*, 66.

(23) Newton, R. G. *J. Rubber Res.* **1946**, *15*, 35.

(24) Sands, A. G.; McDowell, M. V. *Rubber Age, New York* **1956**, *80*, 500.

(25) Ford, C. J., U.S. Patent 2,691,134.

(26) Lundberg, B.; Sundqvist, B. *J. Appl. Phys.* **1986**, *60*, 1074.

(27) Ruschau, G. R.; Newnham, R. E.; Runt, J.; Smith, B. E. *Sens. Actuators* **1989**, *20*, 269.

(28) Talik, P.; Zabkowskawaclawek, M.; Waclawek, W. *J. Mater. Sci.* **1992**, *27*, 6807.

(29) Kirkpatrick, S. *Rev. Mod. Phys.* **1973**, *45*, 574.

(30) Jachym, B. J. In *Carbon Black-Polymer Composites*; E. K. Sichel, Ed.; Marcel Dekker, Inc.: New York, 1982.

(31) Reboul, J. P. In *Carbon Black-Polymer Composites*; E. K. Sichel, Ed.; Marcel Dekker, Inc.: New York, 1982.

(32) Medalia, A. I. *Rubber Chem. Tech.* **1986**, *59*, 432.

(33) Hecht, H. G. *Mathematics in Chemistry: An Introduction to Modern Methods*; Prentice Hall: Englewood Cliffs, NJ, 1990.

(34) Duda, R. O.; Hart, P. E. *Pattern Classification and Scene Analysis*; John Wiley & Sons: New York, 1973.

(35) Schwarzenbach, R. P.; Gschwend, P. M.; Imboden, D. M. *Environmental Organic Chemistry*; John Wiley & Sons: New York, 1993.

Chapter 2: A Quantitative Study of the Resolving Power of Arrays of Carbon Black-Polymer Composites in Various Vapor Sensing Tasks

This chapter is based on the publication: Doleman, B. J.; Lonergan, M. C.; Severin, E. J.; Vaid, T. P.; Lewis, N. S. *Anal. Chem.* **1998**, *70*, 4177.

ABSTRACT

A statistical metric, based on the magnitude and standard deviations along linear projections of clustered array response data, was utilized to facilitate an evaluation of the performance of detector arrays in various vapor classification tasks. This approach allowed quantification of the ability of a fourteen-element array of carbon black-insulating polymer composite chemiresistors to distinguish between members of a set of 19 solvent vapors, some of which vary widely in chemical properties (e.g., methanol and benzene) and others of which are very similar (e.g., n-pentane and n-heptane). The data also facilitated evaluation of questions such as the optimal number of detectors required for a specific task, whether improved performance is obtained by increasing the number of detectors in a detector array, and how to assess statistically the diversity of a collection of detectors in order to understand more fully which properties are underrepresented in a particular set of array elements. In addition, the resolving power of arrays of carbon black-polymer composites was compared to the resolving power of specific collections of bulk conducting organic polymer or tin oxide detector arrays in a common set of vapor classification tasks.

INTRODUCTION

Arrays of broadly cross-reactive detectors have attracted widespread interest from a practical viewpoint and from researchers attempting to construct functional analogues to the mammalian olfactory sense. For example, "electronic nose" detector arrays have been used to evaluate the quality of foodstuffs, perfumes, and plastic packaging, as well as in a variety of other vapor-sensing tasks.[1,2] In addition, recent work has focused on developing analogies between several aspects of artificial and mammalian olfaction.[3-5] In the artificial olfaction approach, analyte classification and identification is not achieved primarily through use of a "lock-and-key" design in which a detector responds in a highly selective fashion to a specific target compound or class of target compounds. Instead, each detector responds to a broad class of stimuli, with the collective response of the many different members of the detector array providing a fingerprint for an analyte of interest. The signal processing required to classify and identify the stimulus from the array output data is either performed statistically using standard chemometric methods or through hardware and/or software implementations of neural networks. Sensing modalities for arrays developed to date include surface acoustic wave (SAW) devices,[6-9] tin oxide detectors,[10-12] conducting organic polymers,[13-15] dye-impregnated polymer films on fiber optic detectors,[16] polymer-coated micromirrors,[17,18] quartz crystal microbalances (QCMs),[19,20] electrochemical gas detectors,[21] chemically sensitive field-effect transistors,[22] and carbon black-polymer composite chemiresistors.[23]

Given the plethora of possible combinations of broadly responsive detectors, it is of interest to evaluate the relative performance of various possible implementations of a given sensing modality. For example, given two different arrays comprised of a fixed number of organic polymers to be used in a given detector modality (SAWs, carbon black-polymer composites, conducting organic polymers, dye-impregnated polymer films on fiber optic detectors, polymer-coated micromirrors or QCMs), it is desirable to evaluate quantitatively whether one array is more diverse than another array. Such data has been obtained, with

emphasis on the performance of carbon black-polymer composite detectors, as a focus of this work. Similarly, it would be desirable to identify which types of vapors were not well-resolved by a particular array and thereby be guided to modify the array constituents to improve the array performance in areas that are underrepresented in the initial collection of detectors. As described in this work, such an evaluation is facilitated by quantitative measurement of the resolving power of an array in response to a diverse set of vapor resolution tasks.

It is also useful to evaluate how many detectors are needed, or are optimal, for a given task. It has been hypothesized that a fairly small number of detectors is sufficient to span odor space[7] (a multi-dimensional space, containing all odorants, where every possible orthogonal chemical difference between any two odorants is represented by a separate dimension). Small numbers of carefully chosen detectors are thought to be optimal because it is hypothesized that additional detectors add noise, but not classifying ability, to the data produced by a well-designed detector array. In contrast, others have hypothesized that it is desirable to have as many detectors as possible in an array.[24,25] Current research suggests that in human olfaction there are approximately 10^3 different receptor genes and approximately 10^7 total receptor cells.[26] Thus, it is not clear whether functional models of the mammalian olfactory system can be satisfactorily constructed with a small detector basis set or whether such models will require thousands, or even millions, of different detector compositions. A quantitative measure (i.e., a metric) of the resolving power of a detector array as a function of the number of detectors (referred to as detector elements) in the system can allow evaluation of some of these questions in a meaningful fashion.

Finally, despite the presence of various options for constructing detector arrays, little attention seems to have been devoted to performing a quantitative assessment of the relative performance of various detector array types. For example, bulk organic conducting polymers,[13-15] carbon black-insulating polymer composites,[23] and tin oxide detectors[10-12] all use electrical conductance to transduce environmental information into an output signal.

However, the functional requirements to obtain an operational vapor detector impose constraints on the types of materials that can be used in each detector modality. As part of our study, we have applied the Fisher linear discriminant method[27] to evaluate quantitatively the performance of these various systems for certain test sensing tasks, and we have used this metric to enhance our understanding of the limitations in classification and identification of different vapors that are imposed by each type of detector modality.

EXPERIMENTAL

A. Materials

The carbon black used to fabricate the carbon black-polymer composite detectors[23] was Black Pearls 2000, a furnace black made by the Cabot Corporation. The polymers used in the carbon black-polymer detectors (Table 2.1, Figure 2.1) were purchased from Aldrich and Polysciences, and were used as received. Eight tin oxide detectors (model numbers TGS813, TGS842, TGS822, TGS830, TGS800, TGS880, TGS882 and TGS883), selected from literature provided by the vendor as those most relevant to the task of distinguishing organic solvent vapors, were purchased from Figaro USA, Inc. A 12-element conducting polymer detector array manufactured by Neotronics, Inc. was used as received. All 19 test solvents (1,2-dimethoxyethane, acetone, acetonitrile, anisole, benzene, butylamine, chloroform, cyclohexane, dichloromethane, ethanol, ethyl acetate, isopropanol, methanol, n-heptane, n-pentane, tetrahydrofuran, toluene, triethylamine and α,α,α-trifluorotoluene) were reagent grade from either EM Scientific or Aldrich Chemical Co., and were used as received.

Table 2.1: Polymers used in the carbon black-polymer composite detector array.

Detector #	Polymer
1	poly(4-vinyl phenol)
2	poly(vinyl chloride-*co*-vinyl acetate), 10% vinyl acetate
3	poly(*N*-vinylpyrrolidone)
4	poly(vinyl acetate)
5	poly(methyl vinyl ether-*co*-maleic anhydride)
6	poly(carbonate bisphenol A)
7	poly(styrene)
8	poly(sulfone)
9	poly(methyl methacrylate)
10	poly(vinylidene chloride-*co*-acrylonitrile), 80% vinylidene chloride
11	poly(caprolactone)
12	poly(ethylene-*co*-vinyl acetate), 82% ethylene
13	poly(ethylene oxide)
14	poly(9-vinylcarbazole)

Table 2.1

Figure 2.1: Structures of the 14 polymers used in the carbon black-polymer composite detectors. The numbering corresponds to the polymer names given in Table 2.1.

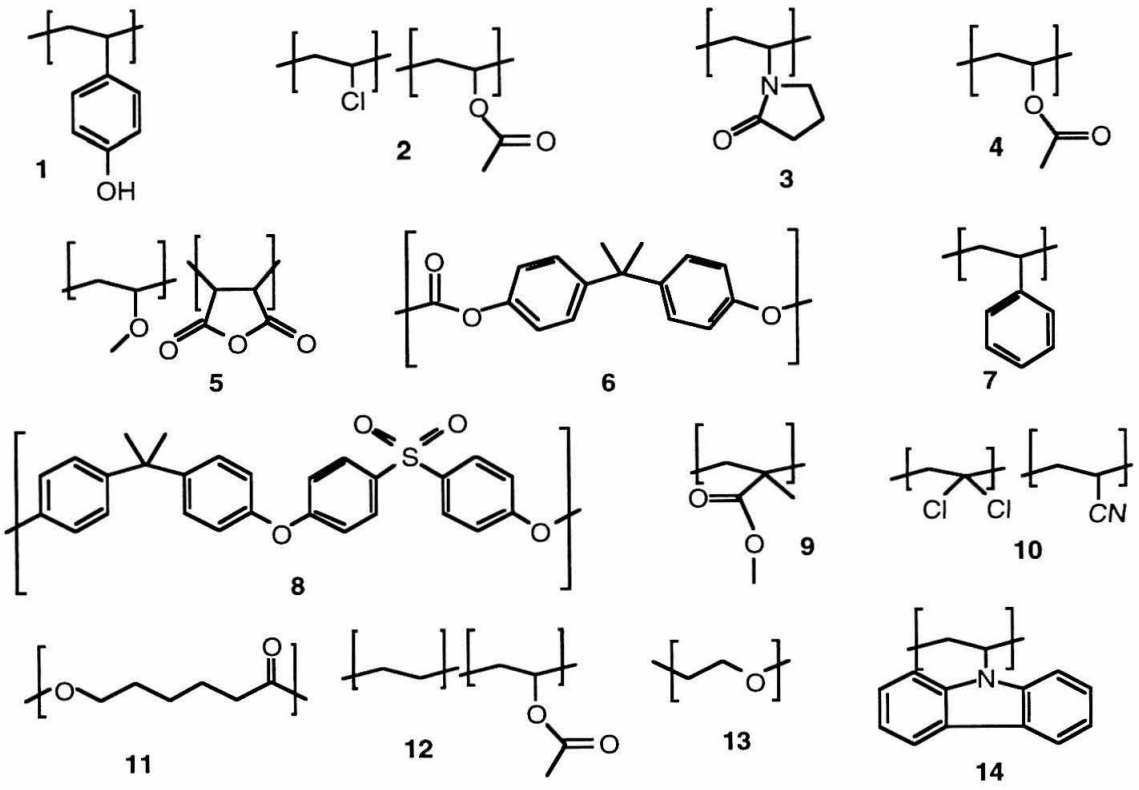

Figure 2.1

B. Instrumentation and Apparatus

An automated flow system consisting of LabVIEW software, a pentium computer, and electronically controlled solenoid valves and mass flow controllers was used to produce and deliver selected concentrations of solvent vapors to the detectors. To obtain the desired analyte concentration, a stream of carrier gas was passed through a bubbler that had been filled with the solvent of choice. Saturation of the carrier gas with the solvent vapor was verified through measurement of the rate of mass loss of the solvent in the bubbler.[28] The vapor-saturated carrier gas was then diluted with pure carrier gas through the use of mass flow controllers (MKS Instruments). The carrier gas for all experiments was oil-free air, obtained from the general compressed air lab source, containing 1.10 ± 0.15 ppth (parts per thousand) of water vapor. The air was filtered to remove particulates but deliberately was not dehumidified nor otherwise purified, in order to reproduce a range of potential "real world" operating environments. Calibrations of the flow system using a flame ionization detector (Model 300 HFID, California Analytical Instruments, Inc.) indicated that the delivered analyte concentrations were: 5.7 ppth for dichloromethane, n-pentane and acetone; 6.1 ppth for chloroform; 6.2 ppth for tetrahydrofuran, butylamine, methanol and cyclohexane; 6.4 ppth for ethyl acetate, benzene and acetonitrile; 6.8 ppth for n-heptane; 6.9 ppth for α,α,α-trifluorotoluene, ethanol, anisole and 1,2-dimethoxyethane, triethylamine and isopropanol; and 7.1 ppth for toluene. Fluctuations in laboratory temperature, 21.5 ± 1.5 °C, could cause a 10% error in setting and controlling the vapor concentrations between nominally identical exposures over the course of the data collection analyzed in this work. No temperature control of the apparatus or of the conducting organic polymer or carbon black-polymer composite detectors was performed, in an attempt to mimic the performance of the detectors under operating environments where such temperature control would not be available. The detectors were multiplexed through a Keithley model 7001 channel switcher to a Keithley model 2002 multimeter that measured the dc resistance of each detector once every 3 seconds. Because the tin oxide detectors

required active heating, heat was supplied to these detectors for a period beginning one week before the experiment and was maintained throughout the duration of the experiment. The tin oxide detectors were heated by applying a constant voltage of 5.000 ± 0.005 V across their heating electrodes using a Lambda Electronics Corp. power supply (model LCS-B-5-OV; 5 Volt, 5.8 Amp).

C. Fabrication of Carbon Black-Polymer Composite Detectors

Substrates for the carbon black-polymer detectors were made by cutting Corning micro glass slides into 10 mm x 25 mm strips. Two gold electrodes, each $\approx$ 50 nm thick, 10 mm wide and 10 mm long, were evaporated onto the ends of each slide. A gap of 5 mm was left between the electrodes and this region was used to probe the resistance of the carbon black-polymer composite films.

To prepare the carbon black-polymer composites, 40 mg of carbon black and 160 mg of one of the insulating polymers (Table 2.1, Figure 2.1) were added to 20 mL of solvent. The solvent was generally tetrahydrofuran, but benzene was the solvent for detectors prepared from poly(ethylene-*co*-vinyl acetate) and poly(ethylene oxide), and dichloromethane was the solvent for the detector made from poly(caprolactone). The solutions were sonicated for 5 min to suspend the carbon black, and the films were then cast by dipping a modified glass slide substrate into the solution and then removing the slide into air. The dipping procedure was repeated 2 or 3 times until a measurable film resistance was obtained. Before use, the detectors were dried in open air for 12-24 h and then placed in air flowing at 7.5 $L \cdot min^{-1}$ for 5 hours.

D. Measurements

The dc electrical resistance of each detector was monitored in response to the presence of various test vapors. Resistance measurements were performed using a simple two-point configuration across the gold leads that bridged the sensing element.

To initiate an experiment, the detectors were placed into the flow chamber and a background flow of compressed air was introduced until the resistance of the detectors stabilized. The tin oxide, conducting organic polymer and carbon black-polymer composite detectors were each tested separately but were subjected to identical protocols in terms of the concentration of, and order of exposure to, the various solvents used during a test run. The duty cycle of exposure to carrier gas vs. exposure to solvent vapor was different for the tin oxide detectors than for the conducting organic polymer and carbon black-polymer composite detectors, although the total time for an exposure cycle was the same for all detector sets. Each exposure for the carbon black-polymer composite detectors and the conducting organic polymer detectors consisted of a three step process that began with 300 s of air flow to achieve a smooth baseline resistance. After this period, solvent vapor at a controlled concentration in flowing air was introduced over the detectors for 240 s. The solvent exposure was then followed by 300 s of air flow to restore the baseline resistance values. At the film thicknesses employed in this work, the tin oxide detectors showed a more rapid response time than either type of polymer-based vapor detector. Hence the exposure protocol for the tin oxide-based detectors was 390 s of flowing air, 60 s exposure to solvent vapor, followed by 390 s of flowing air, again to reach a total of 840 s in an entire exposure cycle.

The array of 14 carbon black-polymer composite detectors, and then later and separately the arrays of tin oxide detectors and bulk conducting organic polymer detectors, were exposed to 19 different solvent vapors (1,2-dimethoxyethane, acetone, acetonitrile, anisole, benzene, butylamine, chloroform, cyclohexane, dichloromethane, ethanol, ethyl acetate, isopropanol, methanol, n-heptane, n-pentane, tetrahydrofuran, toluene, triethylamine and α,α,α-trifluorotoluene), one vapor at a time, with 12 exposures being performed for each vapor except n-heptane which was presented 11 times. Data collection from each detector class required an elapsed period of seven days. Since only eight bubblers were available for the 19 solvents, the solvents were exposed in random order

within three groups of solvents. Solvent groups A (anisole, n-pentane, toluene, methanol, ethanol, acetonitrile and acetone), B (benzene, α,α,α-trifluorotoluene, butylamine, dichloromethane and n-heptane) and C (tetrahydrofuran, ethyl acetate, isopropanol, chloroform, cyclohexane, 1,2-dimethoxyethane and triethylamine) were exposed in the order A, B, C, C, B, A. All data for a set of detectors responding to a given solvent were treated together regardless of when during the experiment the solvent was exposed to the detectors. Laboratory temperature and barometric pressure conditions were 21.5 ± 1.5 °C and 748 ± 3 Torr, respectively.

In order to study the response properties as a function of analyte concentration, the array of carbon black detectors was exposed three times each to approximately 15%, 45%, 82%, 120% and 150% of the analyte concentrations used in the vapor classification study. This data set was collected for 15 of the analytes (acetone, benzene, toluene, acetonitrile, isopropanol, tetrahydrofuran, cyclohexane, ethyl acetate, 1,2-dimethoxyethane, anisole, α,α,α-trifluorotoluene, chloroform, dichloromethane, triethylamine, butylamine). Linearity in detector response was also validated for the other four analytes, and will be reported separately as part of a comprehensive study of the response of these types of detectors to variations in analyte concentration.[29] The solvent trials were performed in the order the solvents are listed above, but within each solvent trial the ordering of the 15 concentration exposures was randomized. The time protocol for each exposure was 300 s of air flow followed by 240 s of solvent in air flow ending with another 300 s of air flow.

E. Data Processing

Although the resistance of each detector was sampled once every 3 seconds during each exposure, only the maximum relative differential resistance change, $\Delta R_{ij,max}/R_b$ where $\Delta R_{ij,max}$ is the maximum resistance change of the j^{th} detector during the i^{th} exposure and R_b is the baseline resistance of the detector prior to the exposure, was used in analysis of the data. Sample responses for a carbon black-polymer composite detector, a tin oxide

detector, and a conducting organic polymer detector are shown in Figures 2.2a, 2.2b and 2.2c respectively. The maximum relative differential resistance changes for the detectors in Figures 2.2a, 2.2b and 2.2c are 1.96%, -51.72% and 0.69%, respectively.

Figure 2.2: Resistances as a function of time during an exposure of (a) a carbon black-poly(*N*-vinylpyrrolidone) composite detector, (b) a tin oxide (TGS883) detector and (c) a bulk organic conducting polymer detector. All three detectors were exposed to 6.9 ppth ethanol in air. The carbon black composite and bulk organic conducting polymer detectors were given 300 s before and after the exposure to achieve a stable baseline in air and 240 s to respond to the ethanol. The tin oxide detectors generally needed less time to reach steady state responses and thus they were given 390 s before and after a 90 s exposure to ethanol to establish steady baselines.

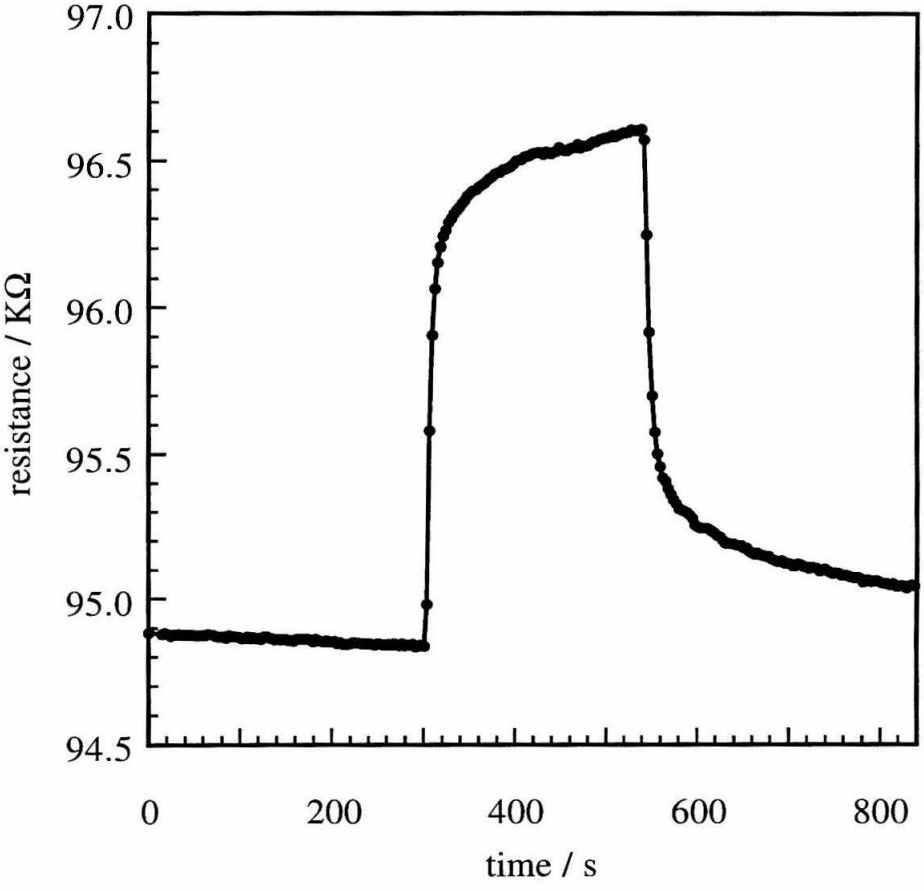

Figure 2.2a

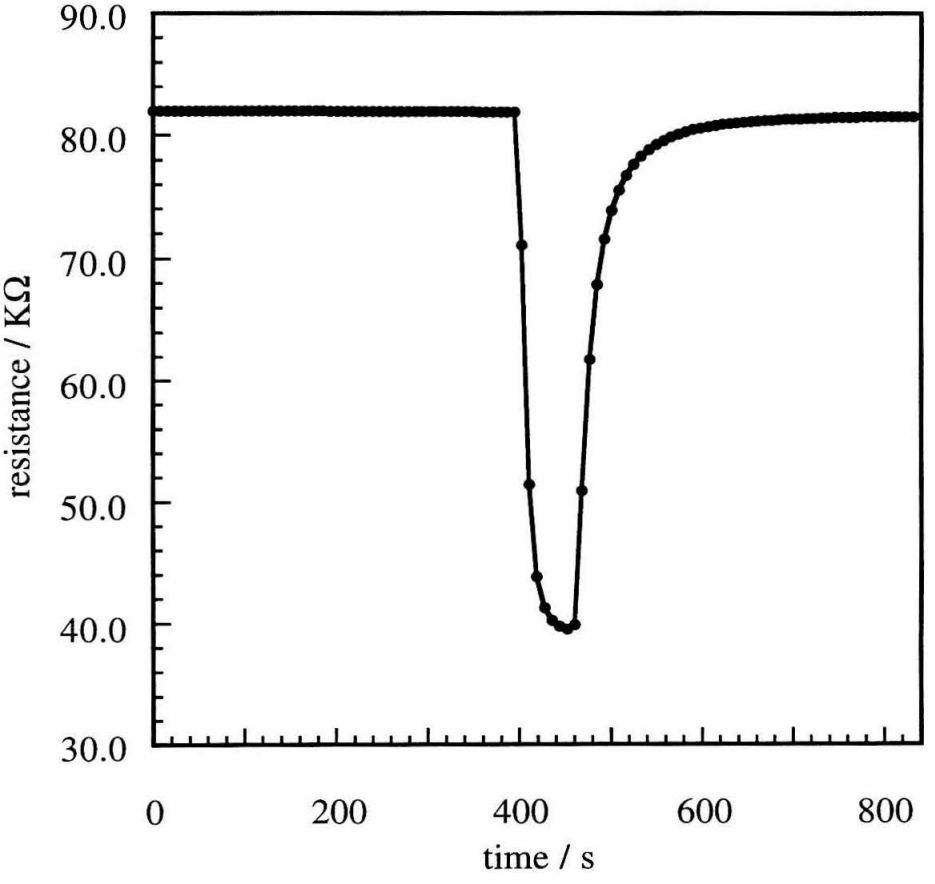
90.0
80.0
70.0
60.0
50.0
40.0
30.0
resistance / KΩ
0
200
400
600
800
time / s

Figure 2.2b

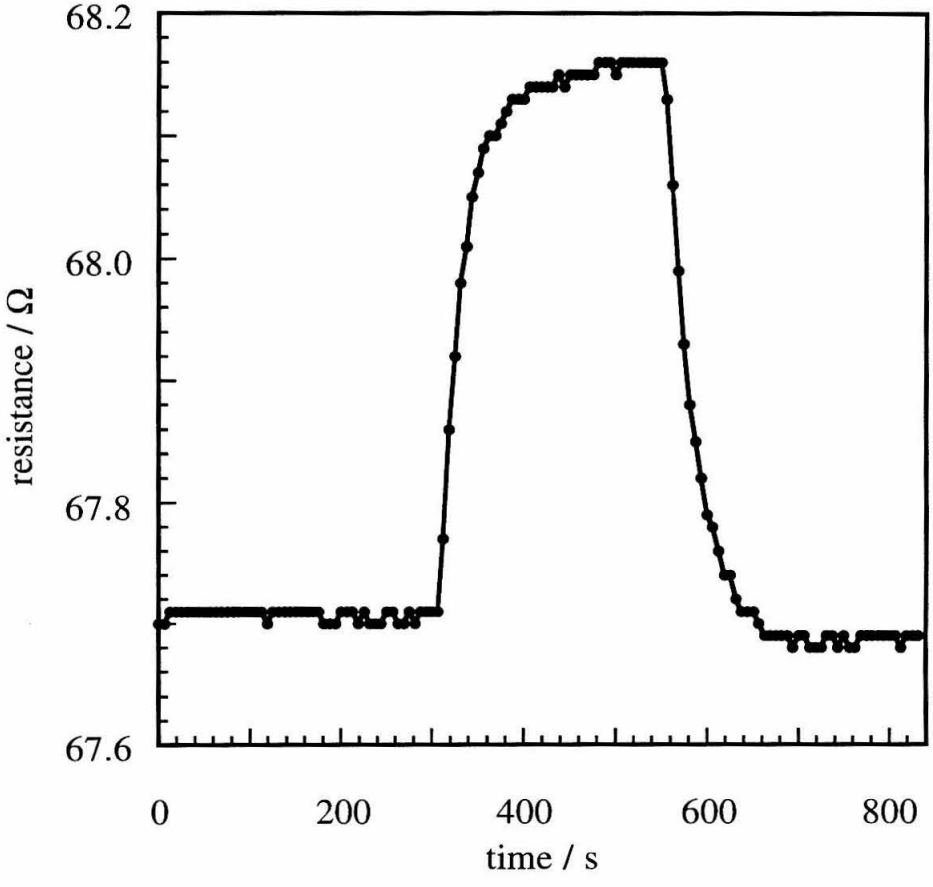

Figure 2.2c

RESULTS

A. Quantifying Detector Array Performance

The autoscaled[30] detector response patterns that resulted from exposure of the carbon black-polymer composite, tin oxide, and conducting polymer detectors to chloroform, isopropanol and triethylamine are depicted in Figures 2.3a, 2.3b and 2.3c respectively. The autoscaled response of the j^{th} detector to the i^{th} exposure of chloroform, isopropanol or triethylamine, A_{ij}, was calculated from

$$A_{ij} = \frac{(\Delta R_{ij,max} / R_b) - \alpha_j}{\beta_j} \quad . \tag{1}$$

The terms α_j and β_j represent the mean and standard deviation, respectively, of the maximum relative differential resistance response of the j^{th} detector to the group of three analytes. Although the patterns in Figure 2.3 are obviously different even to the untrained human eye, the goal of this work was to assess in a quantitative fashion the differences between such patterns.

Neural networks were not used to analyze these differences because although the performance of neural networks in pattern classification can be superior to that of statistically-based chemometric methods, the use of a neural network intimately couples the performance of a specific training/learning algorithm to the detector response data. Another approach to analyze the data is through statistical methods based on cluster analysis.[27] The Fisher linear discriminant method[27] was used to analyze the data collected in this work. A resolution factor for any solvent pair can be obtained along any vector, $\vec{w}$, from the vector projection onto $\vec{w}$ of the distance between the cluster centroids, $d_{\vec{w}}$, divided by the sum of the projected standard deviations, $\sigma_{a,\vec{w}}$ and $\sigma_{b,\vec{w}}$, for the data arising from repeated exposures to the two vapors, *a* and *b* (Figure 2.4). The resulting numerical resolution factor along $\vec{w}$ is defined as:

$$\text{rf} = \frac{d_{\vec{w}}}{\sqrt{\sigma^2_{a,\vec{w}} + \sigma^2_{b,\vec{w}}}} \quad . \tag{2}$$

The Fisher linear discriminant searches for the projection vector, $\vec{w}$, in detector space which maximizes the pairwise resolution factor for each set of analytes, and reports the value of rf along this optimal linear discriminant vector. It can be shown that this rf value is an inherent property of the data set and does not depend on whether principal component space or original detector space is used to analyze the response data. This resolution factor is basically a multi-dimensional analogue to the separation factors used to quantify the resolving power of a column in gas chromatography, and thus the rf value serves as a quantitative indication of how distinct two patterns are from each other, considering both the signals and the distribution of responses upon exposure to the analytes that comprise the solvent pair of concern.

Assuming a Gaussian distribution relative to the mean value of the data points that are obtained from the responses of the array to any given analyte, the probabilities of correctly identifying an analyte as *a* or *b* from a single presentation when *a* and *b* are separated with resolution factors of 1.0, 2.0 or 3.0 are approximately 76%, 92% and 98% respectively. Since the multiple exposures to each analyte allow only an estimate of the statistical distributions of the clustered data, the resolution factors can be overestimated. The overestimations will typically be less than 30% in the cases involving a 14-detector array, decreasing to approximately 3% in the cases involving single-detector arrays. However, especially large rf's should be interpreted cautiously as these could be overestimated by larger amounts. Autoscaling has no effect, and thus was not used, in the evaluation of the array resolving power using the Fisher linear discriminant methodology.

Figure 2.3: Autoscaled responses, A_{ij}, of (a) the 14 carbon black-polymer composite, (b) the 8 tin oxide and (c) the 12 conducting polymer detector arrays to 6.1 ppth of chloroform, and 6.9 ppth of isopropanol and triethylamine. Each bar represents the average autoscaled response over 12 exposures and the error bars represent the standard deviation in the responses.

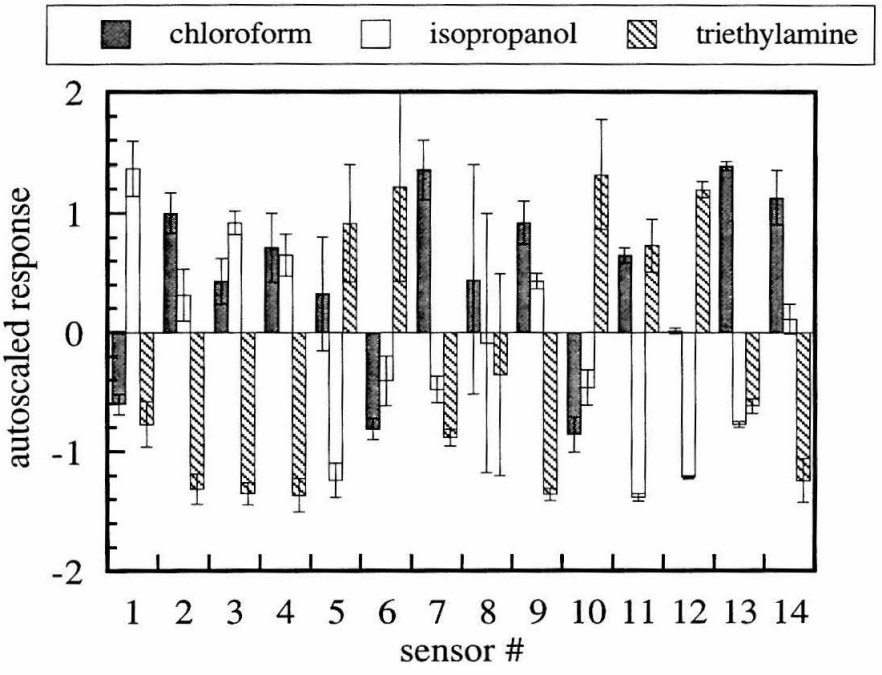
chloroform
isopropanol
triethylamine
autoscaled response
2
1
0
-1
-2
1 2 3 4 5 6 7 8 9 10 11 12 13 14
sensor #

Figure 2.3a

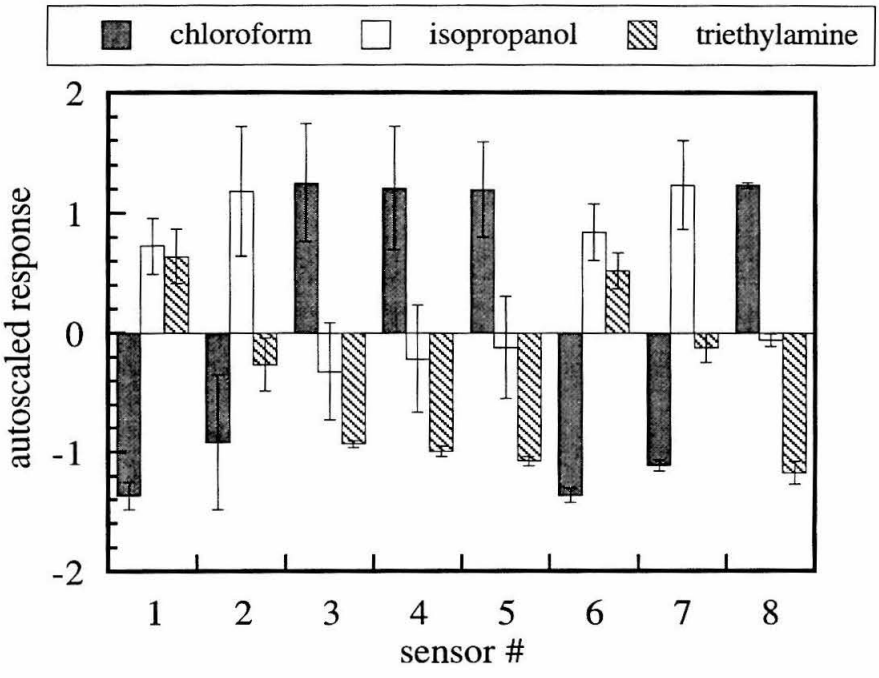
chloroform
isopropanol
triethylamine
autoscaled response
2
1
0
-1
-2
1
2
3
4
5
6
7
8
sensor #

Figure 2.3b

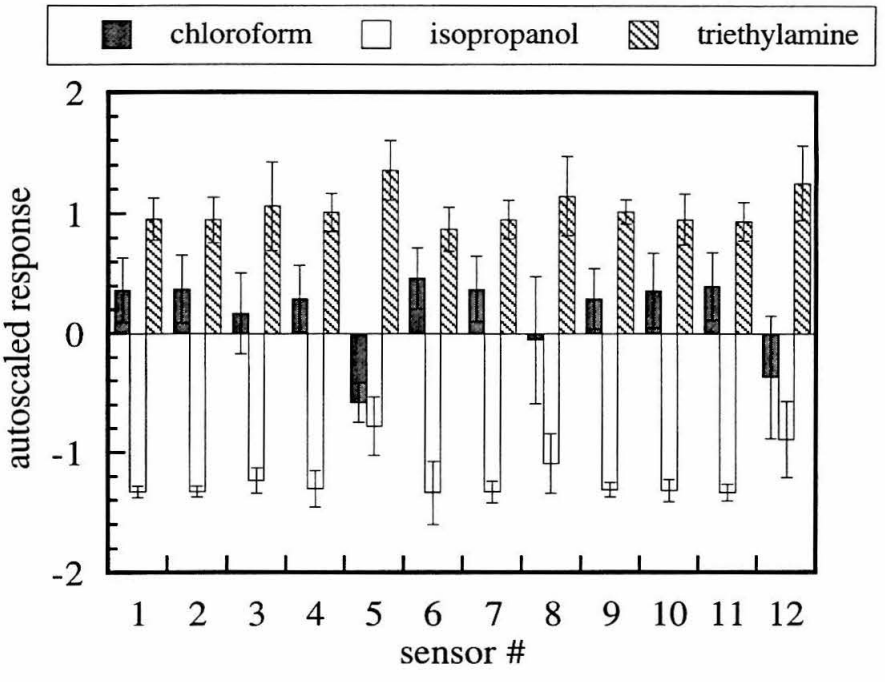
chloroform
isopropanol
triethylamine
autoscaled response
2
1
0
-1
-2
1 2 3 4 5 6 7 8 9 10 11 12
sensor #

Figure 2.3c

Figure 2.4: Mathematical representation of the resolution factor, rf, in resolving analytes *a* and *b* in multi-dimensional space, obtained using the Fisher linear discriminant method.

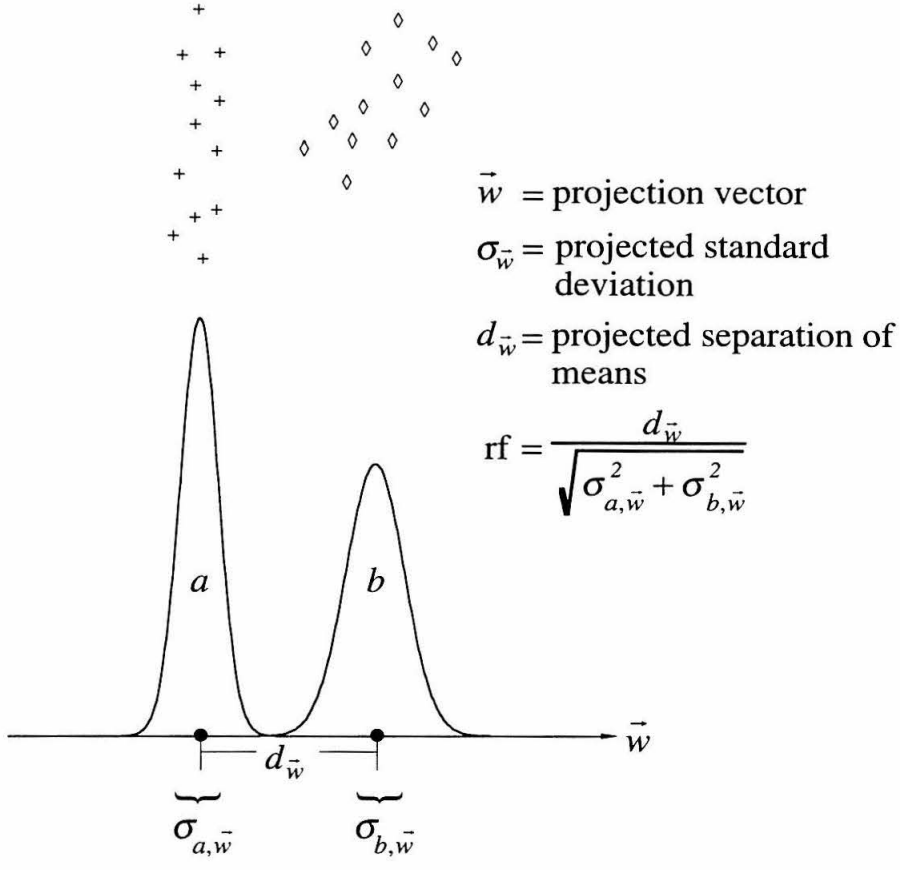
$\vec{w}$ = projection vector
$\sigma_{\vec{w}}$ = projected standard deviation
$d_{\vec{w}}$ = projected separation of means
$\text{rf} = \frac{d_{\vec{w}}}{\sqrt{\sigma^2_{a,\vec{w}} + \sigma^2_{b,\vec{w}}}}$
a
b
$\vec{w}$
$d_{\vec{w}}$
$\sigma_{a,\vec{w}}$
$\sigma_{b,\vec{w}}$

Figure 2.4

B. Evaluation of Array Performance in Various Tasks

1. Comparison of the Resolving Power of Different Detector Arrays at Fixed Analyte Concentrations

Tables 2.2, 2.3 and 2.4 display the pairwise resolution factors for three different types of detector arrays. Table 2.2 presents the resolution factors obtained from an array of the 14 carbon black-polymer composite detectors for all 171 pairs of the 19 vapors. Tables 2.3 and 2.4 display similar data for the eight tin oxide detectors and for the 12 available bulk conducting organic polymer detectors that had all been exposed to the 19 test solvent vapors. Histograms showing the distributions of the resolution factors are given in Figure 2.5.

These resolution factors allow assessment of the performance of the different arrays, or of the performance of subsets of the arrays, in various sensing tasks. Two criteria were chosen as measures of array performance: (1) the average ability to resolve all analyte pairs, $\overline{rf}$, and (2) the ability of the array to resolve the worst-resolved analyte pair, rf_{worst}. The $\overline{rf}$'s and standard deviations across all analyte pairs for the full carbon black-polymer composite, tin oxide, and conducting polymer arrays (Tables 2.2, 2.3 and 2.4) evaluated in this work were 145 ± 93, 27 ± 23 and 18 ± 16 respectively, while the rf_{worst} values were 23, 3.8 and 1.4, respectively. Based on this analysis, the carbon black-polymer composite array yielded the largest mean statistical separation of the response patterns produced by exposure of this particular collection of available detectors to this particular collection of test solvent vapors exposed at fixed concentrations. Using the same experimental conditions, the carbon black composite detector array also yielded the largest separation between the worst-resolved pair of analytes.

Table 2.2: Resolution factors quantifying the ability of the 14 element carbon black-polymer composite detector array to resolve pairwise each of the 19 vapors, at fixed concentrations, from any other vapor in the test set. The average and worst pairwise resolution factors are 145 and 23, respectively.

	acetone	acetonitrile	anisole	benzene	butylamine	chloroform	cyclohexane	dichloromethane	ethanol	ethyl acetate	isopropanol	methanol	n-heptane	n-pentane	tetrahydrofuran	toluene	triethylamine	α,α,α-trifluorotoluene
1,2-dimethoxyethane	121	194	71	49	58	95	287	130	135	164	184	230	156	354	130	179	73	119
acetone		51	102	98	44	106	88	42	58	93	107	41	95	172	42	227	138	198
acetonitrile			154	173	54	153	152	73	58	171	207	75	119	135	88	317	174	200
anisole				106	23	178	146	130	107	126	131	129	140	182	145	59	78	60
benzene					52	65	177	132	117	58	140	202	112	195	102	229	47	82
butylamine						55	63	53	48	36	82	86	76	54	48	41	57	65
chloroform							123	102	122	133	126	204	92	231	159	303	146	180
cyclohexane								109	103	180	108	151	202	152	153	528	132	312
dichloromethane									57	121	60	72	132	54	63	489	246	384
ethanol										119	102	57	77	77	51	279	125	137
ethyl acetate											88	201	123	181	59	253	122	151
isopropanol												135	161	119	73	313	218	206
methanol													107	58	87	401	308	260
n-heptane														177	161	380	156	90
n-pentane															217	556	171	343
tetrahydrofuran																359	93	178
toluene																	246	180
triethylamine																		168

Table 2.2

Table 2.3: Resolution factors quantifying the ability of the eight element tin oxide detector array to resolve pairwise each of the 19 vapors, at fixed concentrations, from any other vapor in the test set. The average and worst resolution factors are 27 and 3.8, respectively.

	acetone	acetonitrile	anisole	benzene	butylamine	chloroform	cyclohexane	dichloromethane	ethanol	ethyl acetate	isopropanol	methanol	n-heptane	n-pentane	tetrahydrofuran	toluene	triethylamine	α,α,α-trifluorotoluene
1,2-dimethoxyethane	18	48	102	10	7.3	120	44	106	7.3	35	18	15	5.5	64	33	26	7.2	22
acetone		36	59	6.5	11	50	10	47	8.1	15	11	12	10	11	17	27	16	19
acetonitrile			57	7.3	29	103	13	94	49	14	26	21	21	26	23	15	33	49
anisole				23	45	53	37	53	67	54	57	48	43	56	41	54	66	51
benzene					13	9.7	7.0	12	7.8	8.6	8.3	6.9	4.9	5.2	5.1	11	14	9.7
butylamine						37	36	36	10	26	16	12	9.1	31	22	22	3.8	30
chloroform							37	20	24	34	47	44	27	38	16	149	38	7.9
cyclohexane								25	10	13	22	19	12	6.6	8.8	19	24	8.9
dichloromethane									25	32	48	35	27	25	20	116	36	4.9
ethanol										16	12	11	7.2	20	20	34	11	12
ethyl acetate											13	14	19	17	12	21	21	17
isopropanol												15	7.7	53	25	16	16	19
methanol													11	14	11	16	20	26
n-heptane														23	25	9.1	12	28
n-pentane															14	29	27	16
tetrahydrofuran																17	26	9.6
toluene																	26	48
triethylamine																		23

Table 2.3

Table 2.4: Resolution factors quantifying the ability of the 12 element bulk conducting organic polymer detector array to resolve pairwise each of the 19 vapors, at fixed concentrations, from any other vapor in the test set. The average and worst resolution factors are 18 and 1.4 respectively.

	acetone	acetonitrile	anisole	benzene	butyl amine	chloroform	cyclohexane	dichloromethane	ethanol	ethyl acetate	isopropanol	methanol	n-heptane	n-pentane	tetrahydrofuran	toluene	triethylamine	α,α,α-trifluorotoluene
1,2-dimethoxyethane	5.7	24	9.7	7.3	10	9.5	8.7	6.5	46	5.5	25	29	9.8	11	9.5	7.7	21	8.4
acetone		22	15	14	11	16	19	6.7	64	12	35	29	20	18	14	10	19	8.7
acetonitrile			36	35	23	45	32	23	54	27	36	28	41	39	45	31	43	34
anisole				3.1	12	4.4	7.1	12	26	6.9	17	42	8.5	9.5	14	3.5	9.9	5.0
benzene					13	2.7	2.8	4.3	18	5.0	7.9	31	3.3	4.4	8.8	3.5	9.8	2.0
butylamine						12	14	11	35	17	12	40	12	11	11	12	18	12
chloroform							6.1	6.8	37	6.2	8.4	35	7.3	12	10	3.4	10	5.1
cyclohexane								3.5	66	7.5	22	27	1.6	4.3	9.8	4.5	12	2.6
dichloromethane									57	4.0	15	31	4.0	5.7	4.8	5.2	14	3.5
ethanol										62	78	55	49	46	42	16	49	24
ethyl acetate											20	29	11	9.4	11	4.9	14	5.2
isopropanol												39	12	21	10	8.0	39	6.4
methanol													35	41	38	30	38	34
n-heptane														4.4	5.5	4.7	9.2	1.4
n-pentane															9.3	5.2	15	4.2
tetrahydrofuran																4.9	16	5.5
toluene																	13	4.4
triethylamine																		9.7

Table 2.4

Figure 2.5: Histograms showing the distribution of resolution factors, in resolving all 171 pairs of the 19 analyte set, for (a) the 14 element carbon black-polymer composite detector array, (b) the eight element tin oxide detector array and (c) the 12 element bulk conducting organic polymer detector array.

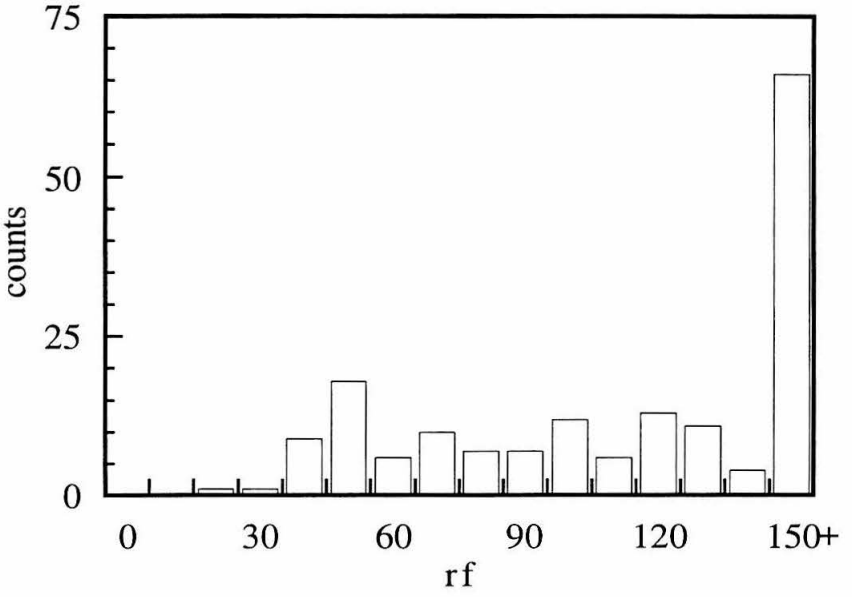

Figure 2.5a

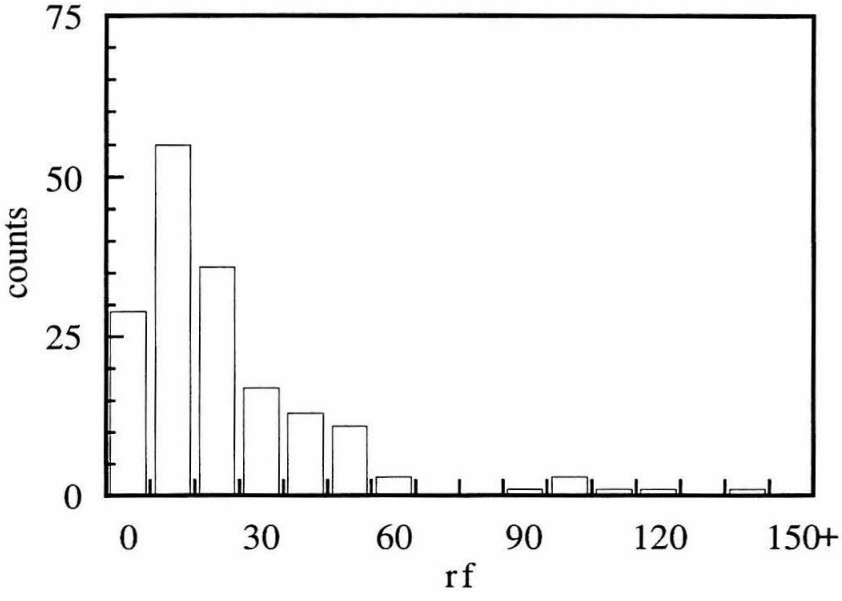

Figure 2.5b

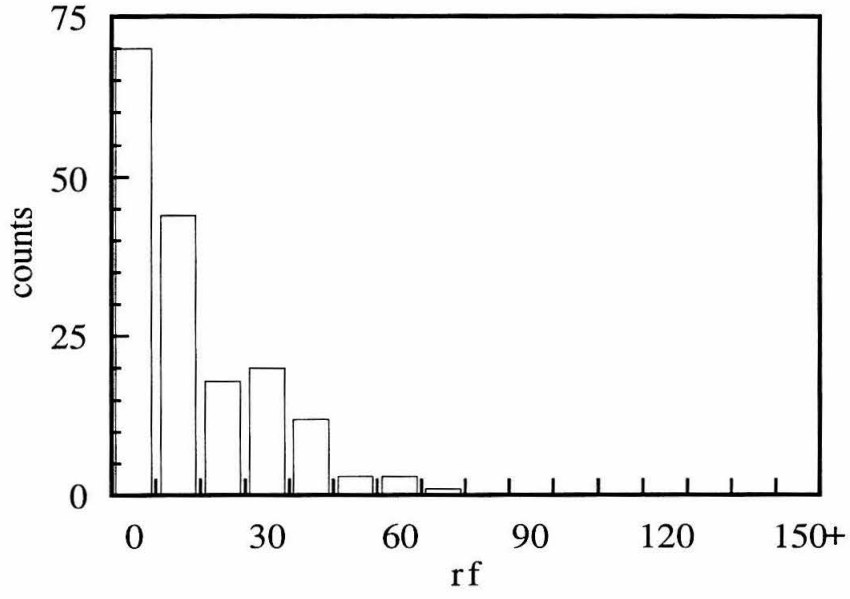

Figure 2.5c

2. Resolving Power of Carbon Black-Polymer Composite Detectors at Variable Analyte Concentrations

The analysis above serves as one quantitative measure of the classification ability of different detector arrays. However, this metric also includes any separation between data clusters that arises from differences in the amplitudes of the array response to the vapors in the test analyte set. Thus, two solvents that produced nearly identical patterns, but with very different absolute detector response amplitudes, would produce two well-separated clusters. The large pairwise rf value for such a solvent pair produced by the data analysis method described above is relevant for tasks in which the concentration of an analyte is known, or when only detection of changes over time in an otherwise relatively constant analyte composition is of interest. However, such a data analysis procedure is clearly not appropriate for assessing array classification performance in applications where the concentration of the analyte is not known, or not known to be fixed, in advance.

A measure of array performance under such conditions requires that the fundamental differences in patterns produced by the various vapors be determined without considering differences in the mean magnitude of the detector responses. Carbon black-polymer composite detectors containing ≥ 20% by weight carbon black have been shown to respond linearly to the concentration of several test analytes over at least an order of magnitude of analyte concentration.[23] This linear dependence was verified for 15 of the 19 vapors used in this work, whereas the linear response to the other solvents has been verified separately.[29] Figure 2.6 displays representative data showing the response of a poly(ethylene oxide) detector exposed to cyclohexane and the response of a poly(carbonate bisphenol A) detector exposed to toluene. These responses yielded straight lines with correlation coefficients of 0.99 and 0.98, respectively. The median value of all 210 straight line correlation coefficients for all the tested solvents on all 14 polymers was 0.98. Hence, a measure of the concentration-independent ability of the array to classify the various solvents in our test set can be obtained for the carbon black-polymer composite detectors by

normalizing the array responses. This procedure is equivalent to adding an extra degree of freedom, analyte concentration, to the classification task.

The normalized response, N_{ij}, of the j^{th} detector in an n detector array to the i^{th} of k exposures of a specific analyte is defined as

$$N_{ij} = \frac{\Delta R_{ij,max} / R_b}{\frac{1}{n \cdot k} \sum_{j,i} (\Delta R_{ij,max} / R_b)} , \qquad (3)$$

where the summation is over the response of all n detectors to all k exposures of the specific analyte. For the carbon black-polymer composite vapor detectors, a comparison of the 171 pairwise resolution factors obtained from normalized responses (Table 2.5) to those obtained only from raw response data (Table 2.2) shows that allowing the vapor concentration to be a floating variable slightly reduces, but does not remove, the array's ability to resolve the various test analytes at the concentrations used in this study. Thus, the $\overline{rf}$ decreased from 145 ± 93 to 102 ± 50 when the data were normalized. This procedure was only performed for the carbon black composite detectors, which have been the subject of extensive investigation in our laboratory.[23] It was not performed for the other detector modalities because some of these detectors do not exhibit responses that are linear with changes in analyte concentration.[31]

Figure 2.6: Plots showing representative examples of the linear relationship between the detector response and analyte concentration for (a) poly(ethylene oxide) exposed to cyclohexane and (b) poly(carbonate bisphenol A) exposed to toluene. Straight lines fit through the data yielded correlation coefficients of (a) 0.99 and (b) 0.98.

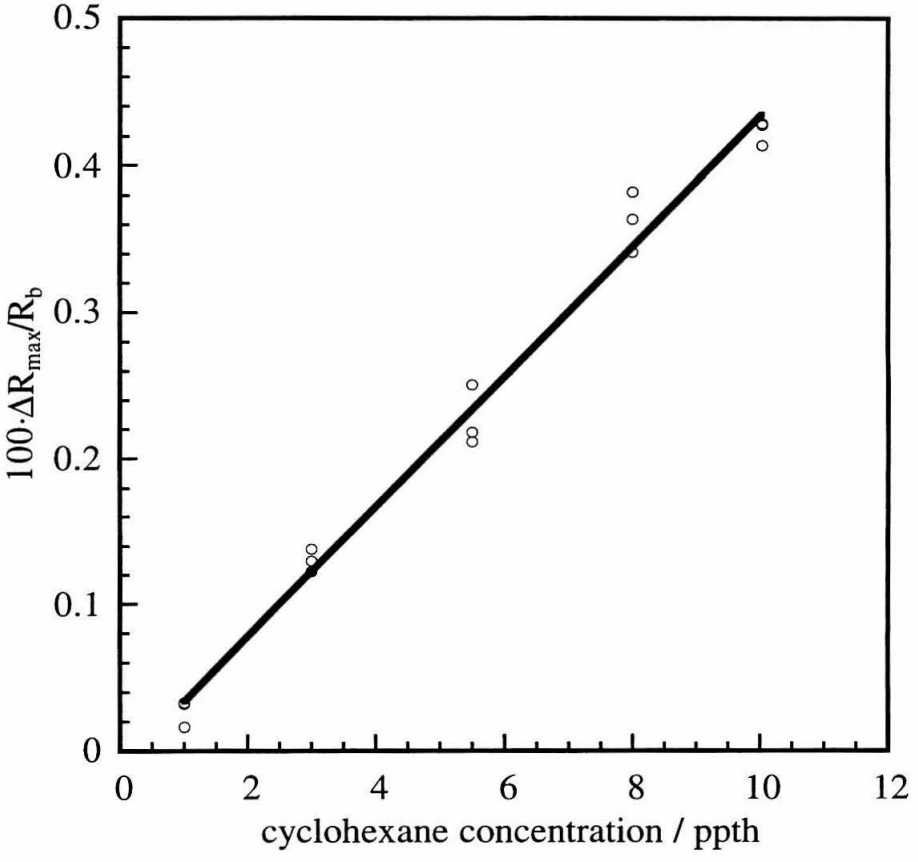
0.5
0.4
0.3
0.2
0.1
0
100·ΔR_max/R_b
0
2
4
6
8
10
12
cyclohexane concentration / ppth

Figure 2.6a

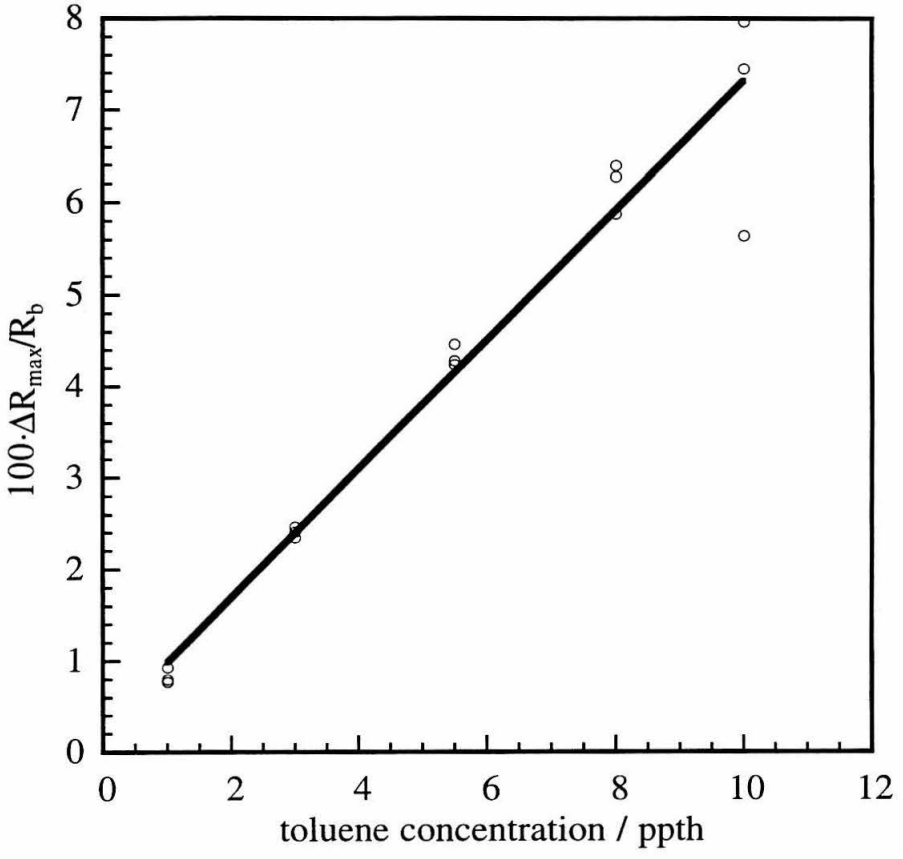
8
7
6
5
4
3
2
1
0
100·ΔR_max/R_b
0
2
4
6
8
10
12
toluene concentration / ppth

Figure 2.6b

Table 2.5: Resolution factors quantifying the ability of the 14 element carbon black-polymer composite detector array to resolve pairwise each of the 19 vapors, using normalized data, from any other vapor in the set. The average and worst resolution factors are 102 and 21, respectively.

	acetone	acetonitrile	anisole	benzene	butylamine	chloroform	cyclohexane	dichloromethane	ethanol	ethyl acetate	isopropanol	methanol	n-heptane	n-pentane	tetrahydrofuran	toluene	triethylamine	α,α,α-trifluorotoluene
1,2-dimethoxyethane	59	107	76	61	59	110	120	41	68	103	58	61	157	129	74	111	97	138
acetone		30	74	88	29	86	103	56	47	59	77	32	93	64	58	82	105	148
acetonitrile			154	176	70	145	167	81	63	107	208	40	133	99	91	225	171	182
anisole				40	23	134	91	117	90	106	88	126	128	100	119	48	102	58
benzene					54	92	100	88	115	84	144	168	113	99	136	31	51	43
butylamine						55	75	65	37	35	67	54	116	21	31	30	74	77
chloroform							74	89	97	139	95	166	154	89	146	118	142	156
cyclohexane								111	159	120	107	151	85	107	107	141	40	71
dichloromethane									63	48	59	70	110	45	42	229	197	256
ethanol										55	90	30	79	60	50	189	112	111
ethyl acetate											124	149	185	50	42	157	158	143
isopropanol												89	181	55	84	123	203	141
methanol													74	54	71	187	240	149
n-heptane														98	221	187	203	82
n-pentane															56	119	70	109
tetrahydrofuran																184	112	149
toluene																	82	27
triethylamine																		96

Table 2.5

3. Comparison of the Resolving Power of the Different Detector Modalities, with the Same Number of Detectors, at Known Analyte Concentrations

a. Average Resolving Power

It is also of interest to compare the performance of different detector modalities at a constant array size. This allows comparison between the performance of different types of arrays without possible biases due to differing numbers of detectors in each type of system. Thus, the data obtained from the specific carbon black-polymer composite detector array having the median $\overline{rf}$ of all possible combinations of 12 of the 14 carbon black-polymer composite detectors studied in this work were compared to the data produced by the available 12 element conducting polymer detector array. Similarly, arrays of carbon black-polymer composite, bulk organic conducting polymer, and tin oxide detectors were compared at a common array size of eight detector elements. In these comparisons, unnormalized data were used because the lack of linearity with varying analyte concentration of some of the detector modalities prevented meaningful normalization of the detector response data in those instances.

The carbon black-polymer composite detector array having the median $\overline{rf}$ of all possible combinations of 12 of the 14 carbon black-polymer composite detectors consisted of polymers #2 and 4-14 (Table 2.1 and Figure 2.1). This particular array displayed $\overline{rf}$ = 117± 79 for the unnormalized response patterns to the set of test analytes at the fixed concentrations used in this study. For comparison, the available 12 element bulk organic conducting polymer array produced $\overline{rf}$ = 18 ± 16 for this same task.

The three detector array modalities were also compared in resolving power using eight element arrays. The $\overline{rf}$ value using unnormalized data for the eight tin oxide detectors was 27 ± 23, while that for the median-performing eight element carbon black-polymer composite array (detectors #3, 6-10, 12 and 13 from Table 2.1 and Figure 2.1) was 62 ± 32 and that of the median-performing eight element bulk conducting organic polymer array (detectors #1-4, 6, 7, 10 and 11 as labeled by the manufacturer) was 13 ± 10. The trends

in $\overline{rf}$ values observed for 12 element arrays were thus also present at smaller array sizes, for the set of tasks and sets of detectors evaluated in this study.

b. Resolving the Worst-Resolved Analyte Pair

Another possible measure of array performance is to maximize the resolution between the two poorest-resolved solvent pairs in the test set. To obtain this type of comparison, the array having the median rf_{worst} of all possible combinations of 12 of the 14 carbon black-polymer composite detectors was compared to the rf_{worst} value of the available 12 detector conducting polymer array. The selected 12 element carbon black-polymer array contained detectors #1-3, 5 and 7-14 and displayed $rf_{worst} = 20$ (for anisole vs. butylamine), whereas the 12 element conducting polymer array yielded $rf_{worst} = 1.4$ (for n-heptane vs. α,α,α-trifluorotoluene). Using a set of only eight detectors allowed a comparison between all three types of detector modalities. Using this metric, the median-performing eight element carbon black-polymer composite array (detectors #2, 4, 5 and 8-12) had an $rf_{worst} = 11$ (anisole vs. butylamine) and the eight element tin oxide array had an rf_{worst} of 3.8 (for butylamine vs. triethylamine), while the median-performing eight element bulk conducting organic polymer array (detectors #1, 2, 4-6, 9, 10 and 12) had an $rf_{worst} = 1.0$ (n-heptane vs. α,α,α-trifluorotoluene).

C. Evaluation of Array Performance as a Function of the Number of Detector Elements

1. Resolving All Analyte Pairs at Fixed Concentrations

It is also of interest to investigate the performance of a particular type of detector modality as a function of the number of elements in the detector array, to determine how many detectors are required for various tasks. Both $\overline{rf}$ and rf_{worst} were evaluated for all possible combinations of 1 through 14 detectors in the carbon black-polymer composite detector array, 1 through 8 detectors in the tin oxide array, and 1 through 12 detectors in

the bulk organic conducting polymer array. This procedure was first performed using raw response data arising from all exposures of the detector elements to each of the 19 solvent vapors. In addition, normalized data were investigated for the various different array sizes of the carbon black-polymer composite detectors.

a. Average Resolution Between All Analyte Pairs as a Function of Array Size

One scenario would be to construct the array that has the best average resolution between any pair of vapors that it might encounter. This criterion is closely related to the goal of constructing the array with the most chemical diversity, so that it best separates any set of vapors that is likely to be in the environment. To assess the diversity of the detector elements in a given detector modality, for all possible combinations of every n-element array of each detector type, the average pairwise resolution factor, $\overline{rf}(n)$, was computed for all 171 different solvent pairs of the 19 solvents. The value of $\overline{rf}(n)$ for each allowed combination was tabulated, and the average value of $\overline{rf}(n)$ for all possible combinations having the specified number of detectors was plotted vs. the number of detectors in the array. The computed quantity is thus a statistically-based measure of the average pairwise resolution of the solvents in the 19 vapor test set that would be obtained from the average, unbiased and unsorted data arising from an n-element detector array of a given detector modality.

As displayed in Figure 2.7a, these data show that, for all three detector modalities, the average resolving power of the array increased as the numbers of detectors in the array increased. Thus, for situations in which the sensing task is not known in advance, such as in quality control applications or in complex environments with varying backgrounds, the average performance of these tested detector arrays improved as the number of different detectors increased. For both raw response data and normalized data for the carbon black-polymer composite detectors, whose signal linearity vs. analyte concentration behavior

permitted such an analysis to be performed in this test system, the same trend was observed for this particular array with this particular set of test analytes (Figure 2.7b).

b. Maximizing the Average Resolution Between All Analyte Pairs

At any array size and for any of the detector modalities investigated, subsets of the full array that can outperform the mean $\overline{rf}(n)$ performance of all possible combinations of elements having that specific array size can, of course, always be identified. The question of interest is whether, given that the task is to best resolve on average all 19 specific test vapors, the best performing array contains the full collection of available detectors or instead only contains subsets of each detector modality.

The quantity that was evaluated was the average pairwise resolution factor, determined using the Fisher linear discriminant method, of the best-performing set of detectors in an array, $\overline{rf}_{max}(n)$, at each number of detectors, *n*. Figure 2.7c depicts the $\overline{rf}_{max}(n)$ data for each of the three detector modalities using raw response data. For each of the three detector modalities, a larger number of detectors provides increased resolving power according to the $\overline{rf}_{max}(n)$ criterion.

In the case of the carbon black-polymer composite detectors, it was also possible to evaluate the concentration-independent performance using normalized data. As displayed in Figure 2.7d, the optimum set of detectors obtained under these criteria once again was the full 14-detector array.

Figure 2.7: (a) The average ability, of all array combinations of the specified number of detectors, of tin oxide, carbon black-polymer composite or bulk organic conducting polymer detectors to resolve all 171 possible pairwise combinations of the 19 analytes. (b) The average ability, of all array combinations of the specified number of carbon black-polymer composite detectors to resolve all 171 possible pairwise combinations of the 19 analytes using normalized data. (c) The data points corresponding to the maximum average rf refer to the specific set of the specified number of detectors which has the largest ability on average to resolve all solvent vapor pairs. (d) The average resolution factor, in resolving all 171 possible pairwise combinations of the 19 analytes, for the carbon black-polymer composite detector combination with the maximum average using normalized data. The error bars in (a) and (b) represent the standard deviations in the distributions of resolution factors for different combinations of detectors.

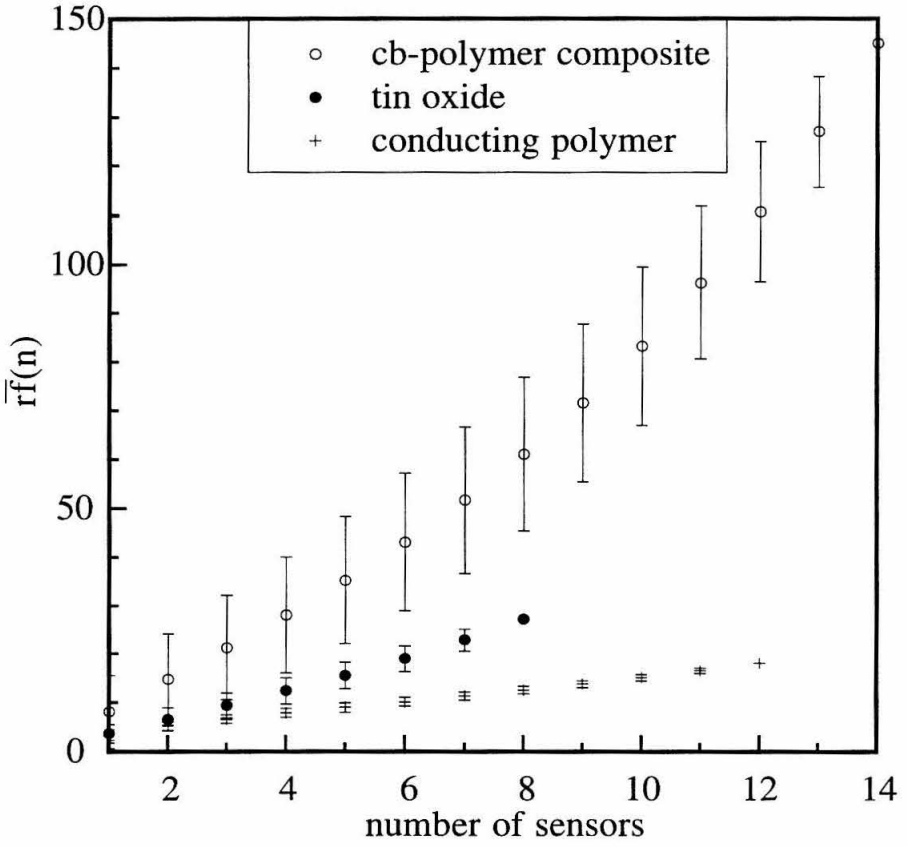
150
100
50
0
$\overline{rf}(n)$
cb-polymer composite
tin oxide
conducting polymer
2
4
6
8
10
12
14
number of sensors

Figure 2.7a

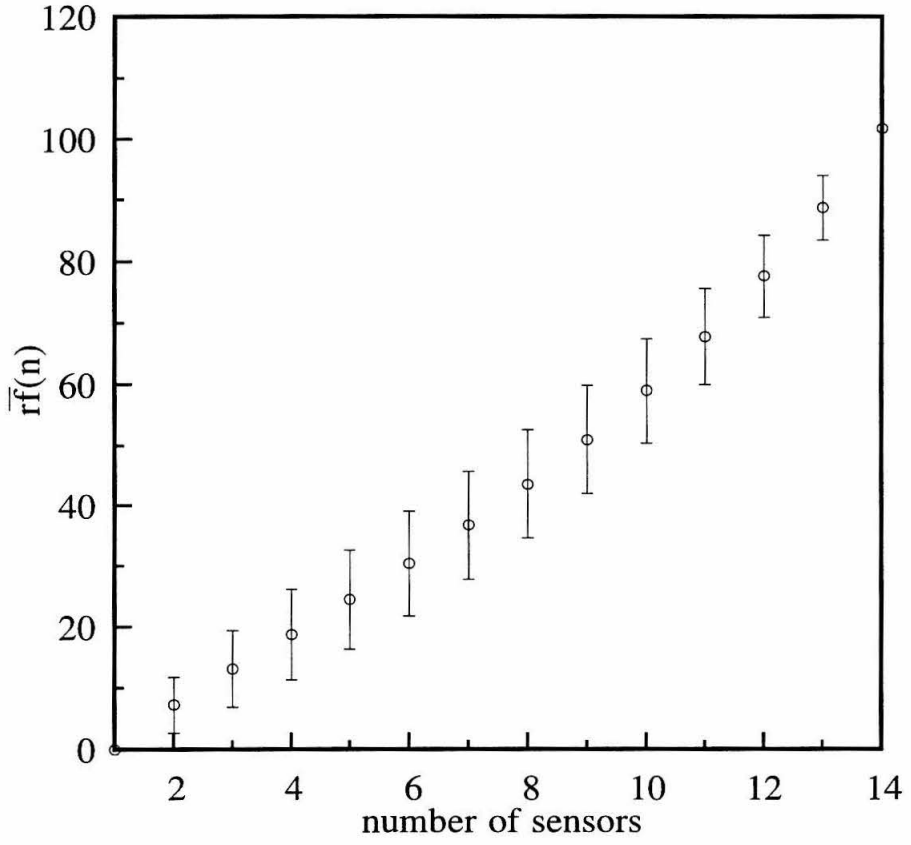
120
100
80
60
40
20
0
$\overline{rf}(n)$
2
4
6
8
10
12
14
number of sensors

Figure 2.7b

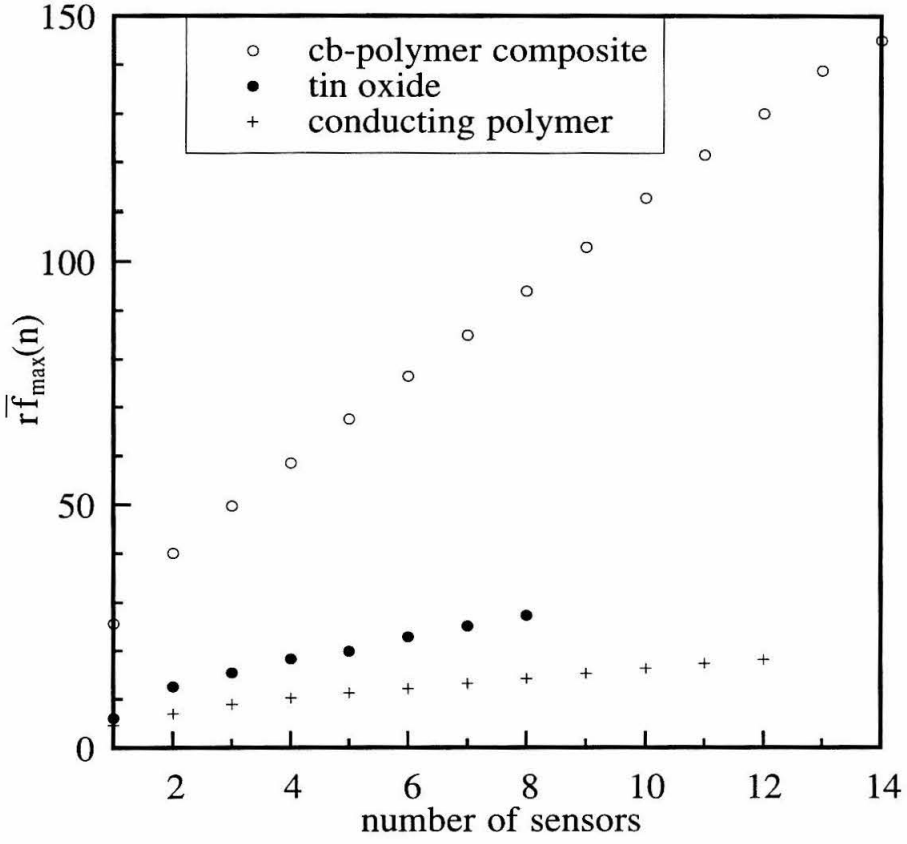
150
100
50
0
cb-polymer composite
tin oxide
conducting polymer
$\overline{rf}_{max}(n)$
2
4
6
8
10
12
14
number of sensors

Figure 2.7c

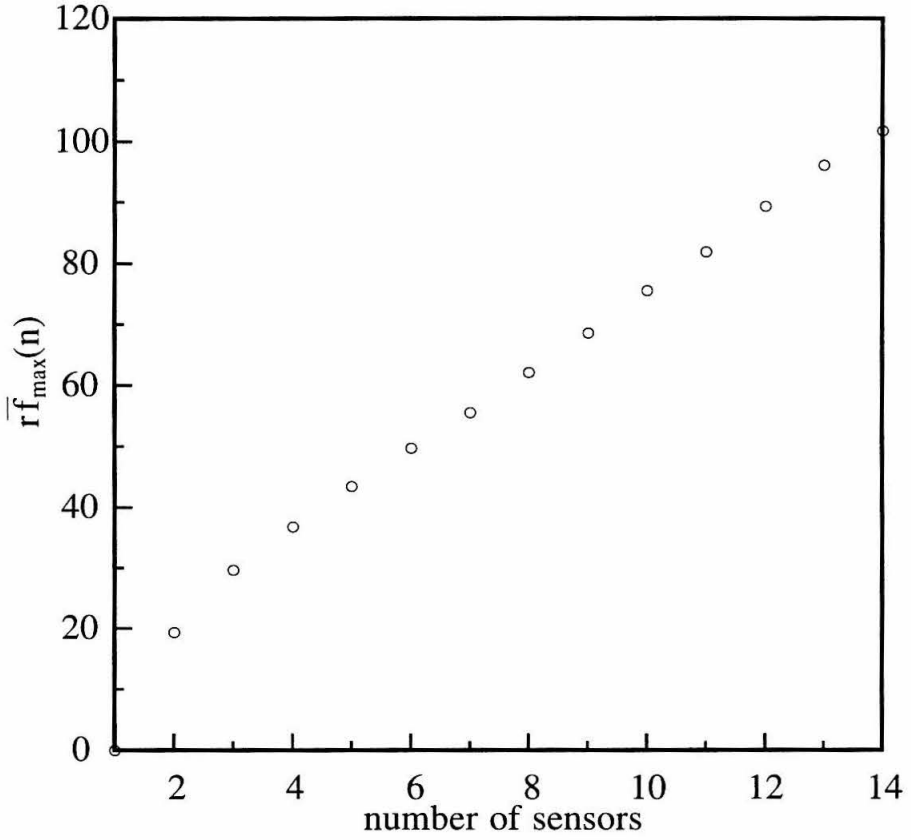
120
100
80
60
40
20
0
$\overline{rf}_{max}(n)$
2
4
6
8
10
12
14
number of sensors

Figure 2.7d

c. Maximizing the Resolution of the Worst-Resolved Solvent Pair

Another performance criterion would be to select the subset of detectors that maximized the smallest pairwise solvent resolution factor for the analytes in the test set. The data in Figure 2.8a describe the ability of each array type to resolve the worst-resolved analyte pair as a function of the size of the detector array. For each of the three detector modalities, the resolving power increases rapidly and then appears to plateau at large numbers of detectors. However, in none of the three cases, using raw response data to analytes at fixed concentrations, does the addition of an extra detector diminish the resolving power of the array.

The array of eight tin oxide detectors maximized the rf_{worst} at 3.8 (for butylamine vs. triethylamine). This rf_{worst} corresponded to approximately a 99% confidence in correctly distinguishing between the two analytes in a single presentation of either analyte to the array. The array of twelve bulk conducting organic polymer detectors maximized the rf_{worst} at 1.4 (for n-heptane vs. α,α,α-trifluorotoluene). This corresponds to approximately an 84% confidence in correctly distinguishing between the two analytes on a single presentation to the array. The array of 14 carbon black-polymer detectors maximized rf_{worst} at 23. For this best set of 14 detectors, the worst resolved analyte pair was anisole and butyl amine. The rf_{worst} of 23 essentially corresponds to a 100% confidence in distinguishing between the two analytes in a single presentation to the detector array.

Figure 2.8b depicts rf_{worst} values for normalized data for the carbon black-polymer composite detectors. Again, the best resolution was maximized by the full fourteen detector array, although the data appeared to plateau for sets containing more than eleven detectors. The full 14-detector set maximized rf_{worst} at 21 (for butylamine vs. n-pentane), which essentially corresponds to a 100% resolution probability. This full set of 14 carbon black-polymer composite detectors contains polymers which vary widely in chemical properties, from the polar poly(*N*-vinylpyrrolidone) to the comparatively non-polar poly(ethylene-*co*-vinyl acetate), and includes polymers having halogenated and aromatic

functional groups such as those in poly(vinylidene chloride-*co*-acrylonitrile) and poly(9-vinylcarbazole). The diversity in the detector component properties, which matches well with the diversity in the analytes, leads to the ability to resolve all the 19 analytes in the test set quite effectively.

Figure 2.8: (a) The ability of arrays of carbon black-polymer composite, bulk conducting organic polymer, or tin oxide detectors to resolve the worst-resolved analyte pair as a function of the number of detectors in the array. All combinations within each class of detectors were studied, and only the combination giving the largest resolution factor for its worst-resolved pair, at each specific number of detectors, was plotted. (b) The ability of arrays of carbon black-polymer composite detectors to resolve the worst-resolved analyte pair, independently of concentration, as a function of the number of detectors in the array. All combinations of detectors were studied and only the combination giving the largest resolution factor for its worst-resolved pair, at each specific number of detectors, was plotted.

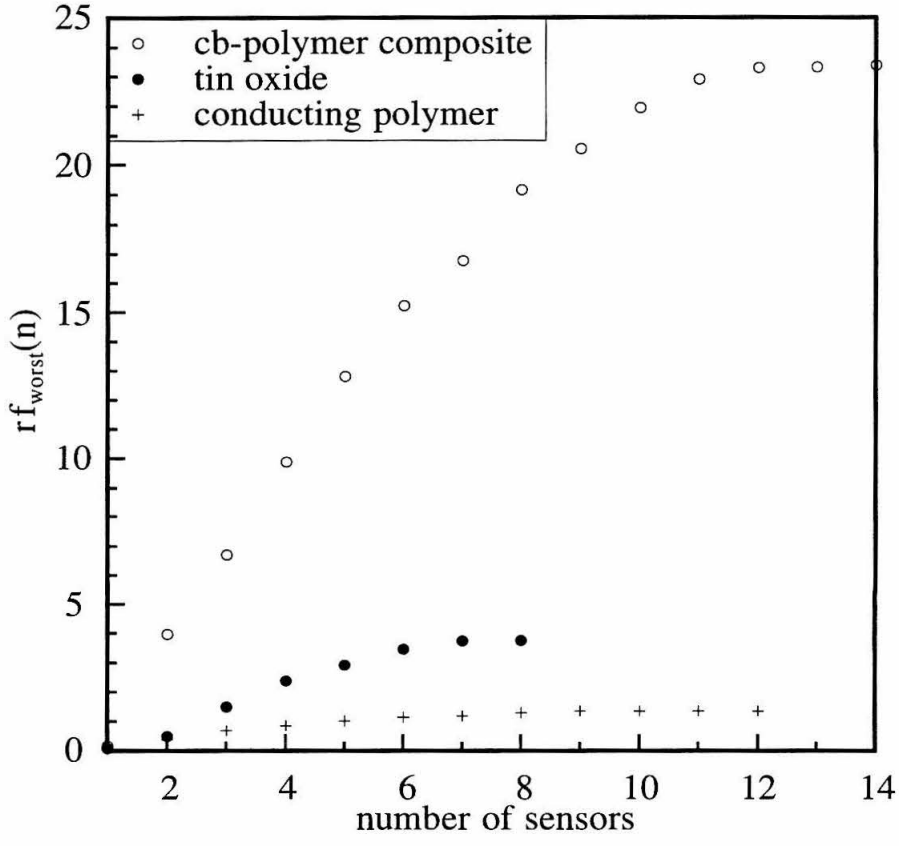
cb-polymer composite
tin oxide
conducting polymer
rf worst(n)
number of sensors
0
5
10
15
20
25
2
4
6
8
10
12
14

Figure 2.8a

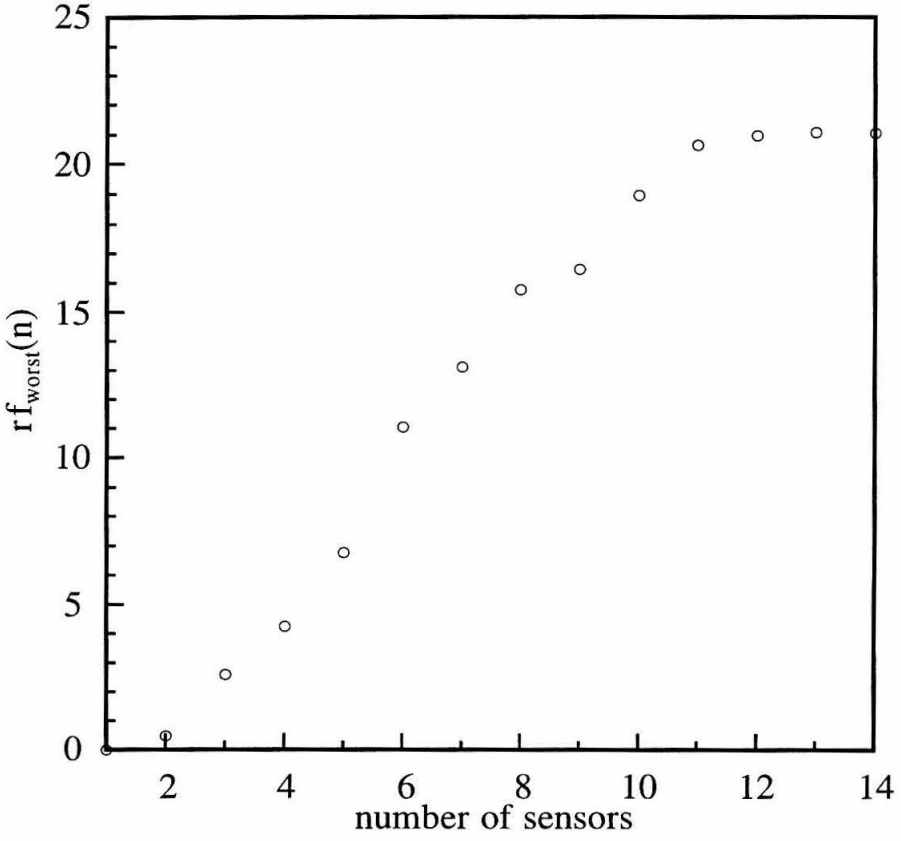

Figure 2.8b

2. Maximizing the Resolution Between a Single Analyte Pair

In this scenario, the task is known and can be specified precisely in advance of array construction. Members of the detector array can, in principle, be pre-selected to provide the optimum performance for the task of concern. The issue to be addressed is whether the optimal resolution of a specific solvent pair, at a fixed concentration, is obtained through use of the data produced by the full array, or whether it is advantageous, for that particular pair of analytes, to use only the data produced by a subset of the full detector array. Ideally, all detectors would be orthogonal and one detector would probe exactly along the direction that is associated with maximizing the chemical differences between the two specific analytes. This single detector, and duplicates of it, would form the best "array" for resolving the two test analytes, under controlled conditions, at fixed concentrations. However, since in reality the vapor detectors are not generally mutually orthogonal, nor do they probe exactly the chemical differences between a specific analyte pair, it is probable that a few specific, partially correlated, detectors will combine to resolve a specific analyte pair better than any single detector in the array.

As a representative example, Figure 2.9 depicts the results for resolving an arbitrarily chosen solvent pair, ethyl acetate from tetrahydrofuran, as a function of the size of the detector array, using only raw response data. All possible combinations of n detectors in the array were investigated for the 14 detector carbon black-polymer composite array, the eight detector tin oxide array, and the 12 detector bulk conducting organic polymer array. Only elements from a given detector modality were allowed to form the desired detector array (i.e., carbon black composites, tin oxide detectors, and bulk conducting organic polymers were restricted to be in mutually separate arrays for this analysis). For each specific number of detectors in the array, only the best resolution factors that resulted from the optimal array for the task of separating ethyl acetate from tetrahydrofuran, $rf_{best}(n)$, were plotted.

In each of the three cases, the ability of the arrays to resolve ethyl acetate from tetrahydrofuran increases as additional detectors are included. From Figure 2.9, it is apparent that beyond approximately the first six carbon black-polymer detectors (#8-13 from Table 2.1 and Figure 2.1), additional detectors provide minimal increases in the resolution of ethyl acetate from tetrahydrofuran. Five of these six carbon black-polymer composite detectors contain polymers with one or both of the ether and ketone functionalities present in the ethyl acetate and tetrahydrofuran analytes, which explains chemically why the detectors perform well in this specific task. The other detectors in the array produced response data along vectors that did not lie as close to the vector that best separated these two solvents in detector space.

A similar metric was evaluated for all other solvent pairs as well. For each array class, using raw response data, the full array maximizes the resolution of each analyte pair. The best resolution factor that was obtained between any vapor pair, using any set of detectors of the same class, was obtained for distinguishing n-pentane from toluene using the carbon black-polymer composite detector array which had rf = 556 using unnormalized data for this task. Similarly, using normalized data from the carbon black-polymer composite detector array, the best resolved analyte pair was dichloromethane from α,α,α-trifluorotoluene with rf = 256. The largest resolution factors obtained between any analyte pair, using raw response data, for the conducting polymer or tin oxide detectors were 77 (for ethanol vs. isopropanol) and 148 (for chloroform vs. toluene), respectively, again for unnormalized data.

Figure 2.9: The ability of the carbon black-polymer composite, tin oxide and bulk conducting organic polymer detectors to resolve ethyl acetate from tetrahydrofuran at fixed concentrations. All combinations of either carbon black-polymer composite, bulk organic conducting polymer, or tin oxide detectors were studied for each number of detectors, and only the sets giving the best resolution for each specified number of detectors were plotted.

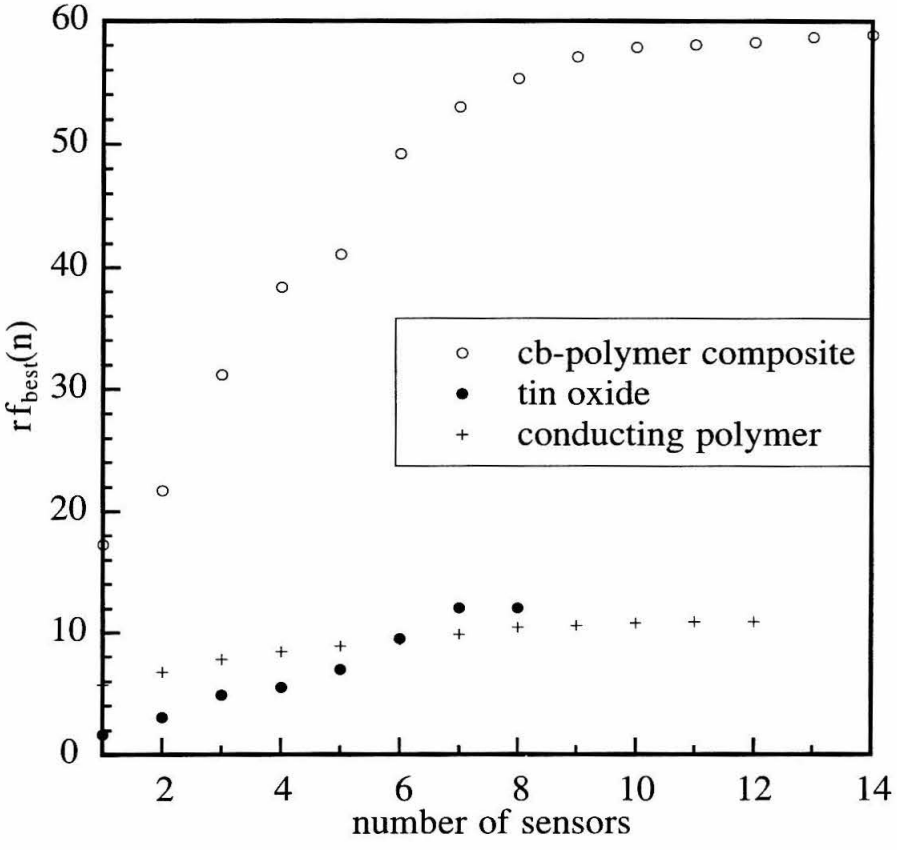
60
50
40
30
20
10
0
$rf_{best}(n)$
2
4
6
8
10
12
14
number of sensors
cb-polymer composite
tin oxide
conducting polymer

Figure 2.9

DISCUSSION

A. Number of Broadly Responsive Detectors Needed for a Generalized Sensing Task

One of the key findings of this work is that array performance increased, in general, as the number of detectors increased. This makes intuitive sense because addition of new detectors should always increase, or at worst keep constant, the information content in the output signals of the detector array. Prior efforts to analyze detector response data have generally used resolution factors which involve projecting the standard deviations of exposures to various analyte pairs along the line in detector space that runs through the mean response values of the various exposures to both of the solvents in the test pair of concern.[32,33] When such a metric is used, noisy detectors can actually produce a decrease in resolution factor when the detectors are added to the array, because even though new detectors add to the overall information content of the array output signal, the additional detectors contribute noise along a direction that is defined by the vector that runs through the mean response points of a specific analyte pair. If the noise along this direction is greater than the increased resolving power along this direction, then the computed resolution factor will decrease. The use of such a metric, however, possesses the drawback that the best line for separating two clusters may not be the line that connects their mean response points. This drawback is mitigated by use of the Fisher linear discriminant analysis method, which instead chooses a projection vector such that array resolving power is maximized for each analyte pair. Thus, artifacts from new detectors transferring noise to certain directions in detector space are minimized, and detectors which provide significant noise, rather than resolving power, for a given task are not strongly weighted along the optimum vector that is identified by the Fisher linear discriminant methodology.

In this work, a set of 14 carbon black-polymer composite detectors was found to be sufficient for the task of resolving the 19 analytes at fixed and variable concentrations under

laboratory conditions. However, it is expected that for more complex, undefined or variable tasks, incorporation of as many different detectors as possible into a broadly responsive detector array would likely be beneficial. A larger number of detectors will increase the probability that the dimensionality of odor space is fully spanned by the array (i.e., that the array will be able to probe all chemical differences between analytes), since each detector could contribute new chemical information. This conclusion has been confirmed by the analysis using the Fisher linear discriminant method described herein.

The number of meaningful orthogonal dimensions probed by the 14 carbon black-polymer composite detectors in sensing the 19 analytes can be estimated using principal component analysis.[30] This is expected to be less than 14 due to correlation between the various detectors in this non-optimally chosen set of polymers. To evaluate such correlations, the full data set was used, the exposures to each analyte were averaged (to reduce random response noise), the data were mean-centered but not normalized, and then the principal components and their eigenvalues were determined.[30] The eigenvalue of each principal component defines the amount of variance in the data along each principal component. The results are shown in Table 2.6. Calculations based on the uncertainties in each detector's mean responses to the analytes were used to determine that the variance in principal components 7 through 14 could be accounted for mainly by random response noise. Thus, principal components 7 through 14, each with < 0.25 % of the total variance, were the result of random response noise, molecular features of the analytes that the detectors are barely able to probe, and molecular features that are barely present in the analyte set. Clearly, other orthogonal dimensions of odor space are conceivable. For example, if an array is given the task of distinguishing different chiralities of enantiomers, then recently developed detectors using chiral polymers[34] would need to be added to probe an additional orthogonal dimension of odor space.

If the array were required to identify analytes in a mixture, at variable concentrations, then in principle a minimum of one detector per analyte in the mixture

would be required assuming only the maximum detector responses were used in the analysis, although extraction of complementary information from the temporal response patterns could reduce the number of required detectors. The less controlled the environment in which the detectors were expected to perform, the more detectors would be required to calibrate out temperature and humidity fluctuations. Another reason for more detectors is the benefit of redundancy, which insures backup copies are present in case detectors fail. Additionally, it has been shown that a $\sqrt{n}$ resolution enhancement is attainable when n copies of a detector are present in an array.[24] For these reasons it seems reasonable to hypothesize that efforts to mimic the functional behavior of the mammalian olfactory system will require relatively large numbers of detectors, and that small collections of carefully chosen broadly responsive detectors will be most useful for well-defined tasks when the environmental variation is either well-controlled or is also known in advance.

Table 2.6: Principal components of the fourteen element carbon black-polymer composite detector array response data.

principal component	total variance	% of total variance	cumulative % variance
1	277.94	64.87	64.87
2	93.20	21.75	86.61
3	41.67	9.73	96.34
4	7.63	1.78	98.12
5	4.40	1.03	99.15
6	2.47	0.58	99.72
7	0.99	0.23	99.95
8	0.15	0.03	99.99
9	0.03	0.01	100.00
10	0.01	0.00	100.00
11	0.01	0.00	100.00
12	0.00	0.00	100.00
13	0.00	0.00	100.00
14	0.00	0.00	100.00

Table 2.6

B. Comparing Arrays of Different Detector Classes

One of the goals of this work was to use a well-defined metric to compare quantitatively the performance of different classes of vapor detector arrays, which use different detection mechanisms, in performing several tasks involving a sizable and broad selection of odorants. The 14 carbon black-polymer composite detectors were made from readily available polymers without prior quantitative knowledge of the sensing abilities they would provide. Eight different tin oxide detectors, selected as to be best suited for the task of resolving the solvent vapors, were purchased from a commercial supplier. The 12-element conducting polymer detector was obtained as sold by a commercial supplier. Figures 2.5, 2.7a, 2.7c, 2.8a and 2.9 show the data used in the comparison, from which one can learn strengths and weaknesses of each detector class. It is clear from these figures that the carbon black-polymer composite detectors significantly outperform the evaluated tin oxide and conducting polymer arrays in resolving both the full set of 19 analytes and in resolving subsets of these analytes, as determined by the criteria of best resolving the analytes on average or best resolving the worst resolved analyte pairs, when using the raw response data. The wide ranging chemical properties of the polymers in the carbon black-polymer composite detectors allows these arrays to probe differences between even chemically similar analytes. The tin oxide detectors exhibit responses which are similar from one analyte to the next, while the evaluated conducting polymer detector array commonly resolved polar from polar and non-polar from polar analytes with resolution factors of 10 or larger but was less capable of resolving non-polar analytes from each other (the mean resolution factor for those tasks was 3.9). The relative difficulty these particular bulk organic conducting polymer detectors encountered in resolving non-polar analytes is understandable considering the detector films are highly polar due to their ionic doping, and this polarity of the polymer backbone evidently limits the amount of nonpolar character in the solvent vapors that can be probed by the specific collection of bulk conducting organic polymer detectors evaluated in this work.

In addition to the ability to resolve analytes, other characteristics displayed by the different detector classes can be important in satisfying specific application requirements. As displayed in Figure 2.2, the response times of the tin oxide detectors were very short, and these detectors tended to achieve steady state responses consistently in under 7 s. The response times of the conducting polymer and carbon black-polymer detectors varied widely, and can in principle be tuned by varying the film thickness, but the detectors of these classes studied in this work typically required between 20 and 200 s to achieve a signal response that was within 90% of their steady state values. The response magnitudes of the tin oxide detectors tended to be approximately ten times larger than that of the carbon black-polymer composite detectors (although these response magnitudes can be increased by lowering carbon black loading[23]) and approximately 15 times larger than the responses for the bulk organic conducting polymer detectors, although this ratio varied somewhat for the different analytes evaluated during the course of this study.

To some extent, there is synergy between various implementations of detector arrays, because it is readily possible to envision use of the same collection of polymers in either an array of surface acoustic wave devices,[6-9] quartz crystal microbalances,[19,20] fiber optic micro-mirrors,[17,18] or carbon black-polymer composite chemiresistors,[23] for example. The fundamental analyte classification and identification performance of these arrays would be expected to be very similar, because all of these devices rely on the polymer film's sorption of the vapor in order to produce the desired detection signal. Choosing between these various types of detector arrays then primarily requires assessment of more practically-related issues such as the signal-to-noise ratio of a given type of signal transduction mechanism, manufacturability of the detectors, integration with the processing electronics, detector cost and power requirements, as opposed to which type of detector system displays the best resolving power for a given collection of polymer films, assuming that the number and composition of the detector films is constant in each type of array being compared.

CONCLUSIONS

For the task of best resolving solvent pairs in a fixed analyte test set or in subsets thereof, increased resolving power was observed as the number of detectors was increased in the arrays of tin oxide, bulk conducting organic polymer, or carbon black-polymer composite chemically sensitive vapor detectors. Use of a larger number of detectors is beneficial for resolving, on average, a generalized set of test vapors that might not all be known in advance of the array design. Thus, if the sensing task is previously undefined, variable, or if the response characteristics of the detectors to the analytes in the task are unknown, increasing the number of different detectors is expected to increase the ability to resolve the analytes. Despite the lack of selectivity designed into any single detector element, the use of an array of broadly responsive detectors has been shown to provide exceptional classification ability for certain test solvents, with resolution factors typically in excess of 100 observed for the specific sets of carbon black-polymer composite detectors and test solvents evaluated in this work. The use of a numerical measurement of the resolution factor of a detector array can thus enhance the quantitative understanding involved in adding new detectors, in deciding which chemical properties are underrepresented in a specific array obtained from a certain type of detector modality, and in evaluating other factors that are potentially important in design of arrays of vapor detectors to mimic some of the functional characteristics of the mammalian sense of olfaction.

ACKNOWLEDGEMENTS

We acknowledge Dr. Dawei Dong and Prof. Rod Goodman of Caltech for helpful suggestions regarding this manuscript. This work was supported by the National Aeronautics and Space Administration, the Army Research Office, and the Defense

Advanced Research Projects Agency. B.J.D. acknowledges the Natural Science and Engineering Research Council of Canada for a 1967 Centennial Fellowship.

REFERENCES

(1) Gardner, J. W.; Pearce, T. C.; Friel, S.; Bartlett, P. N.; Blair, N. *Sens. Actuators B* **1994**, *18*, 240.

(2) Nanto, H.; Tsubakino, S.; Ikeda, M.; Endo, F. *Sens. Actuators B* **1995**, *24-25*, 794.

(3) Pearce, T. C. *Biosystems* **1997**, *41*, 69.

(4) Pearce, T. C. *Biosystems* **1997**, *41*, 43.

(5) Doleman, B. J.; Severin, E. J.; Lewis, N. S. *Proc. Natl. Acad. Sci. U.S.A.* **1998**, *95*, 5442.

(6) Ballantine, D. S.; Rose, S. L.; Grate, J. W.; Wohltjen, H. *Anal. Chem.* **1986**, *58*, 3058.

(7) Grate, J. W.; Abraham, M. H. *Sens. Actuators B* **1991**, *3*, 85.

(8) Grate, J. W.; Rosepehrsson, S. L.; Venezky, D. L.; Klusty, M.; Wohltjen, H. *Anal. Chem.* **1993**, *65*, 1868.

(9) Nakamoto, T.; Fukuda, A.; Moriizumi, T. *Sens. Actuators B* **1993**, *10*, 85.

(10) Gardner, J. W.; Shurmer, H. V.; Corcoran, P. *Sens. Actuators B* **1991**, *4*, 117.

(11) Gardner, J. W.; Shurmer, H. V.; Tan, T. T. *Sens. Actuators B* **1992**, *6*, 71.

(12) Corcoran, P.; Shurmer, H. V.; Gardner, J. W. *Sens. Actuators B* **1993**, *15*, 32.

(13) Shurmer, H. V.; Corcoran, P.; Gardner, J. W. *Sens. Actuators B* **1991**, *4*, 29.

(14) Pearce, T. C.; Gardner, J. W.; Friel, S.; Bartlett, P. N.; Blair, N. *Analyst* **1993**, *118*, 371.

(15) Freund, M. S.; Lewis, N. S. *Proc. Natl. Acad. Sci. U.S.A.* **1995**, *92*, 2652.

(16) White, J.; Kauer, J. S.; Dickinson, T. A.; Walt, D. R. *Anal. Chem.* **1996**, *68*, 2191.

(17) Butler, M. A.; Ricco, A. J.; Buss, R. *J. Electrochem. Soc.* **1990**, *137*, 1325.

(18) Hughes, R. C.; Ricco, A. J.; Butler, M. A.; Pfeifer, K. B. *J. Biochem. and Biotechnol.* **1993**, *41*, 77.

(19) Slater, J. M.; Paynter, J. *Analyst* **1994**, *119*, 191.

(20) Slater, J. M.; Watt, E. J. *Analyst* **1991**, *116*, 1125.

(21) Keyvani, D.; Maclay, J.; Lee, S.; Stetter, J.; Cao, Z. *Sens. Actuators B* **1991**, *5*, 199.

(22) Zubkans, J.; Spetz, A. L.; Sundgren, H.; Winquist, F.; Kleperis, J.; Lusis, A.; Lundstrom, I. *Thin Solid Films* **1995**, *268*, 140.

(23) Lonergan, M. C.; Severin, E. J.; Doleman, B. J.; Beaber, S. A.; Grubbs, R. H.; Lewis, N. S. *Chem. Mater.* **1996**, *8*, 2298.

(24) Di Natale, C.; D'Amico, A.; Davide, F. A. M. *Sens. Actuators A* **1993**, *37-38*, 612.

(25) Dickinson, T. A.; Walt, D. R.; White, J.; Kauer, J. S. *Anal. Chem.* **1997**, *69*, 3413.

(26) Axel, R. *Sci. Am.* **1995**, *273*, 154.

(27) Duda, R. O.; Hart, P. E. *Pattern Classification and Scene Analysis*; John Wiley & Sons: New York, 1973.

(28) Atkins, P. *Physical Chemistry;* 5 ed.; W.H. Freeman and Company: New York, 1994.

(29) Severin, E. J.; Doleman, B. J.; Lewis, N. S. *manuscript in preparation.*

(30) Hecht, H. G. *Mathematics in Chemistry: An Introduction to Modern Methods*; Prentice Hall: Englewood Cliffs, NJ, 1990.

(31) Martinelli, G.; Carotta, M. C. *Sens. Actuators B* **1995**, *23*, 157.

(32) Gardner, J. W.; Bartlett, P. N. *Sens. Actuators B* **1996**, *33*, 60.

(33) Müller, R. *Sens. Actuators B* **1991**, *4*, 35.

(34) Severin, E. J.; Sanner, R. D.; Doleman, B. J.; Lewis, N. S. *Anal. Chem.* **1998**, *70*, 1440.

Chapter 3: Trends in Odor Intensity for Human and Electronic Noses: Relative Roles of Odorant Vapor Pressure vs. Molecularly-Specific Odorant Binding

This chapter is based on the publication: Doleman, B. J.; Severin, E. J.; Lewis, N. S. *Proc. Natl. Acad. Sci. U.S.A.* **1998**, *95*, 5442.

ABSTRACT

Response data were collected for a carbon black-polymer composite electronic nose array during exposure to homologous series of alkanes and alcohols. The mean response intensity of the electronic nose detectors, and the response intensity of the most strongly-driven set of electronic nose detectors, was essentially constant for members of a chemically homologous odorant series when the concentration of each odorant in the gas phase was maintained at a constant fraction of the odorant's vapor pressure. A similar trend is observed in human odor detection threshold values for these same homologous series of odorants. Because the thermodynamic activity of an odorant at equilibrium in a sorbent phase is equal to the partial pressure of the odorant in the gas phase divided by the vapor pressure of the odorant, and because the activity coefficients are similar within these homologous series of odorants for sorption of the vapors into specific polymer films, the data imply that the trends in detector response can be understood based on the thermodynamic tendency to establish a relatively constant concentration of sorbed odorant into each of the polymeric films of the electronic nose at a constant fraction of the odorant's vapor pressure. Similarly, the data are consistent with the hypothesis that the odor detection thresholds observed in human psychophysical experiments for the odorants studied herein are driven predominantly by the similarity in odorant concentrations sorbed into the olfactory epithelium at a constant fraction of the odorant's vapor pressure.

INTRODUCTION

Numerous attempts have been made to understand the trends in odor detection thresholds that are displayed by the human olfactory sense. High odor detection thresholds are observed for most odorants that are gases under standard pressure and temperature conditions, while odorants with low vapor pressures generally have low odor detection thresholds.[1] Quantitative structure-activity relationships have been formulated in an attempt to correlate trends in olfactory odor intensity with specific microscopic and macroscopic properties of various odorants. For example, many workers have proposed that trends in odor detection thresholds arise from the presence of important steric and functional group features in certain olfactory receptors.[2,3] Such receptors could then primarily respond to chemically specific features such as odorant molecular length and polarity.[3-6] Other workers have empirically correlated trends in human odor detection thresholds with macroscopic properties of the odorant, such as the boiling point of the liquid phase of the odorant species.[7-9] Some workers have noted the correlation between odor thresholds and the vapor pressure of the odorant.[10-14]

In this work, we have measured the response intensities of an electronic nose,[15] based on an array of carbon black polymer composite detectors, to straight chain alkanes and alcohols. We propose a fundamental, first-order explanation for the observed trends in response intensity of the detectors in the electronic nose, based on the thermodynamic tendency for odorants to partition into sorbent phases as a function of the odorant's vapor pressure. A striking resemblance has been observed in the odor intensity trends for the human and electronic olfactory systems for these series of odorants. This similarity in odor intensity behavior occurs even though the detectors in the electronic nose array have no specific receptor sites and even though the electronic nose array is not a structural model for the human olfactory system.

EXPERIMENTAL

The electronic nose is an array of vapor detectors, with each detector consisting of a dispersion of carbon black particles in a swellable, insulating organic polymer film. Swelling of each carbon black-polymer composite in response to the presence of an odorant produces a change in the electrical resistance of the detector film. The pattern of responses produced by an array of chemically different carbon black-polymer composites identifies the odorant, and the pattern height is correlated with the odorant concentration. The resistance change of a detector is reversible, is linear over at least an order of magnitude of odorant concentration, and is quite reproducible.[15] The detectors were fabricated, and their characteristics measured, as described previously,[15] except that for convenience surface mount universal boards (surfboards, part number 6012 from Capital Advanced Technologies Inc.) were used as a substrate for the composites rather than modified glass slides or capacitors. For simplicity, during this study the partial pressures of the odorants were fixed at a constant fraction of their vapor pressures at 22 °C. Vapor pressure values were calculated using accepted formulas described previously in the literature.[16]

RESULTS

Straight chain alcohols and straight chain alkanes were investigated because they define two homologous series of odorants that vary regularly in their chemical properties as the carbon chain length is increased, and because human psychophysical data on odor detection thresholds are available for these odorants.[1] Figures 3.1a and 3.1b display the responses, $\Delta R_{max}/R_b$, where R_b is the baseline resistance of the detector immediately prior to the exposure and ΔR_{max} is the amplitude of the maximum resistance change during the 5 minutes the detector was exposed to the odorant, for an array of carbon black-polymer composite detectors exposed to methanol, 1-butanol, 1-octanol, n-pentane, n-nonane and n-tetradecane at partial pressures, P, corresponding to 10% of the vapor pressure of the odorant, P^o. The different response patterns across the array of detectors correspond to

differences in odor quality data produced by the electronic nose, while the signal intensities correspond to differences in odor intensity that are obtained from the raw, unprocessed signals of the detectors.

A striking feature of the electronic nose data is that, when the mean signal intensity, defined as the mean value of $\Delta R_{max}/R_b$ that was observed for all 13 detectors in the array upon exposure to an odorant, is plotted vs. the partial pressure of odorant present in the vapor phase, the electronic nose exhibits increased sensitivity (i.e., a similar response intensity to a lesser odorant concentration) to lower vapor pressure alkanes and alcohols (Figure 3.2a). The 13 polymers in the array of detectors (poly(4-vinyl phenol), poly(α-methyl styrene), poly(vinyl acetate), poly(sulfone), poly(caprolactone), poly(ethylene-co-vinyl acetate) (82% ethylene), poly(ethylene oxide), poly(ethylene), poly(butadiene), poly(vinylidene fluoride), poly(n-butyl methacrylate), poly(epichlorohydrin) and poly(ethylene glycol)) were chosen to include a broad range of chemical properties, thereby minimizing biases that would result from averaging the responses over sets of detectors that had a limited chemical diversity.

A better analogy to detection of an odorant at the human odor detection threshold, at which the presence of an odor can be identified as compared to a moist air blank, but the quality of the odor cannot be determined, might be obtained by plotting the trends in response intensity for the most strongly-driven detectors in the electronic nose towards the series of odorants studied in this work. Such data are displayed in Figures 3.2b and 3.2c for the alkanes and alcohols, respectively. These data confirm the trend observed in Figure 3.2a, and show that the response intensity of an individual detector is essentially independent of the odorant in the series, if the odorant is present in the gas phase at a constant fraction of its vapor pressure. Thus, the electronic nose detectors produced nearly the same odor intensity from their raw signal outputs for $P=0.1 \cdot P^o$ of pentane (P=46 torr in 707 torr of air=61 parts per thousand) as they did for $P=0.1 \cdot P^o$ of tetradecane ($P=8.5 \cdot 10^{-4}$ torr in 707 torr air=1.1 parts per million).

Figure 3.3 displays human odor detection thresholds, obtained as mean values from several published sets of psychophysical data, for the 1-alcohol and n-alkane homologous series of odorants.[1] As was observed for the electronic nose signals, these mean human olfactory odor detection thresholds, when based on odorant partial pressure, increase as the vapor pressure of the odorant increases. However, when the data are referenced to the fraction of the room temperature vapor pressure of each odorant, the mean literature detection thresholds are essentially constant across this vapor pressure range for the various odorants in the series. At vapor pressures below approximately 1 torr the thresholds appear to plateau. This could be the result of difficulties in delivering equilibrium concentrations of low vapor pressure odorants to the human sensory panels,[17] or the result of steric inhibition as odorants become large relative to olfactory receptor binding sites.[18]

The trends displayed in Figures 3.2 and 3.3 were also observed in an analysis of gas chromatography data. Retention volumes[19] for odorants having a wide range of vapor pressures were converted[20] into gas/support partition coefficients, K, and the data were collated for two selected stationary phases, one polar (tricresyl phosphate) and one nonpolar (squalane) in character. The values of log K for each odorant into each sorbent phase were then regressed against log P^o for every odorant in the data set. As displayed in Figures 3.4a and 3.4b, the regressions yielded straight lines with slopes of -0.87±0.07 and -0.80±0.04 and r^2 values of 0.86 and 0.93 respectively. Taking a cut through the sample set to leave only odorants in either the alkane or alcohol homologous series yielded a much better fit to a straight line dependence of log K on log P^o. Slopes were approximately -1.0 and r^2 values were 1.0 for both the alcohol and alkane homologous series (Figures 3.5a and 3.5b). This reduction in variance is expected because the variation in chemically based gas/support partition coefficients that contribute to the variance in the entire data set is reduced when only partition coefficients for a series of homologous odorants are considered. The activity coefficients at infinite dilution for these series of alcohols and alkanes in the two stationary phases are presented in Table 3.1.[19] It is apparent that the

activity coefficients for members of each homologous series are relatively similar relative to the variation in vapor pressures, which spans many orders of magnitude, for each series of odorants.

Activity coefficient data were also culled from the literature[19,21] for some of the specific polymers in the electronic nose detectors. Data for poly(vinyl acetate), poly(ethylene oxide) and poly(ethylene glycol) are presented in Table 3.1. The activity coefficients at infinite dilution for the odorants within either the alcohol or alkane series, sorbed into these specific polymers, are clearly similar relative to the large variation in their vapor pressures.

Figure 3.1: Histograms showing the response patterns of a 13-detector array of carbon black-polymer detectors exposed in air to (a) methanol at 11 torr, 1-butanol at 0.57 torr and 1-octanol at $5.8 \cdot 10^{-3}$ torr and (b) n-pentane at 46 torr, n-nonane at 0.37 torr and n-tetradecane at $8.5 \cdot 10^{-4}$ torr. The odorant partial pressures correspond to 10% of their vapor pressures in ambient air. Each histogram bar represents the average over 6 exposures of a single detector to a single odorant for 5 minutes. The error bars represent one standard deviation in each sensor's responses. The polymers in detectors #1-13 were: poly(4-vinyl phenol), poly(α-methyl styrene), poly(vinyl acetate), poly(sulfone), poly(caprolactone), poly(ethylene-co-vinyl acetate) (82% ethylene), poly(ethylene oxide), poly(ethylene), poly(butadiene), poly(vinylidene fluoride), poly(n-butyl methacrylate), poly(epichlorohydrin) and poly(ethylene glycol).

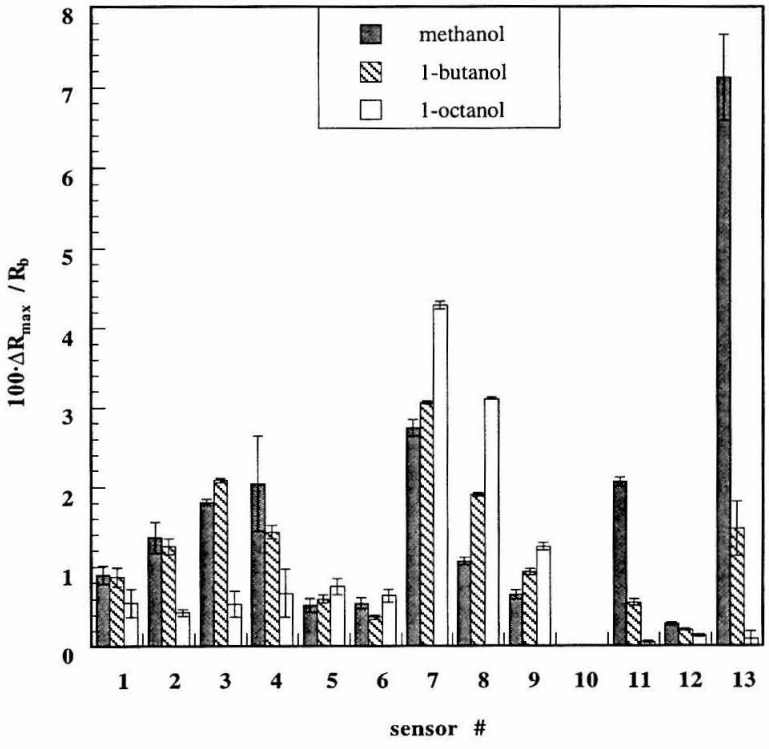
methanol
1-butanol
1-octanol
100·ΔR_max / R_b
0
1
2
3
4
5
6
7
8
1
2
3
4
5
6
7
8
9
10
11
12
13
sensor #

Figure 3.1a

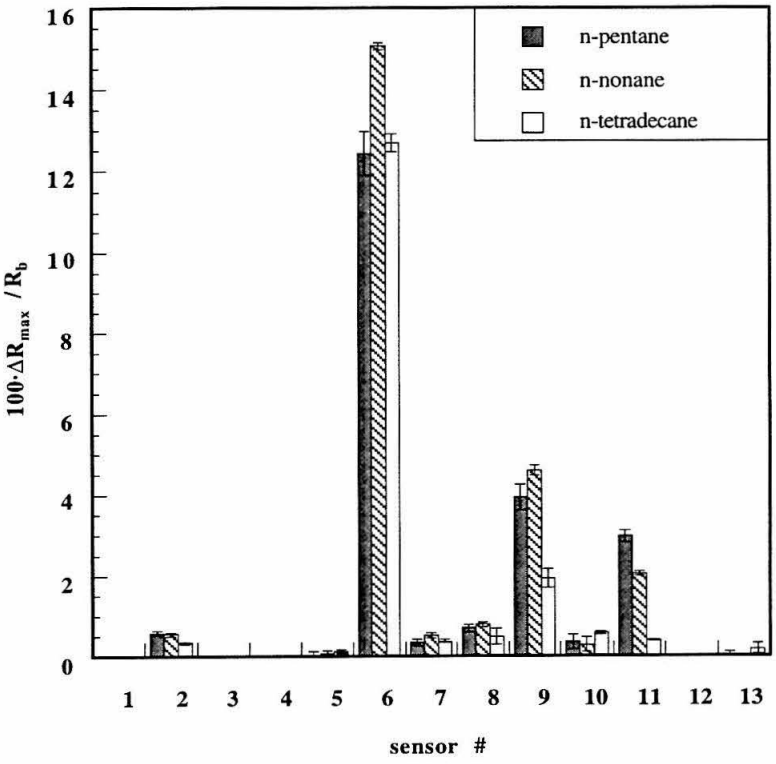
n-pentane
n-nonane
n-tetradecane
100·ΔR_max / R_b
0
2
4
6
8
10
12
14
16
1
2
3
4
5
6
7
8
9
10
11
12
13
sensor #

Figure 3.1b

Figure 3.2: (a) The mean signal intensity, $\overline{\Delta R_{max}/R_b}$, defined as the average over all thirteen detector responses in the electronic nose array to an odorant, plotted versus the partial pressures of homologous series of alkane and alcohol odorants. (b) Responses, $\Delta R_{max}/R_b$, of three individual electronic nose detectors (poly(ethylene-co-vinyl acetate), poly(butadiene) and poly(n-butyl methacrylate) which produced the largest responses to a homologous series of straight chain alkanes, plotted versus the partial pressures of the odorants in each series. (c) Responses of three individual detectors (poly(ethylene glycol), poly(ethylene oxide) and poly(vinyl acetate)), which produced the largest responses to a straight chain homologous series of 1-alcohols, plotted versus the partial pressures of the odorants in each series. The alkanes used in (a) and (b) were: n-pentane, n-hexane, n-heptane, n-octane, n-nonane, n-decane, n-dodecane and n-tetradecane. The straight chain alcohols used in (a) and (c) were: methanol, ethanol, 1-propanol, 1-butanol, 1-pentanol, 1-hexanol, 1-heptanol and 1-octanol. Each odorant was maintained at a partial pressure equivalent to 10% of its vapor pressure, and the background was ambient air. For clarity, the number of carbons in each odorant is indicated for each data point, in italics for the alcohols and plain text for the alkanes. The error bars represent one standard deviation unit in the responses to 6 exposures of each odorant.

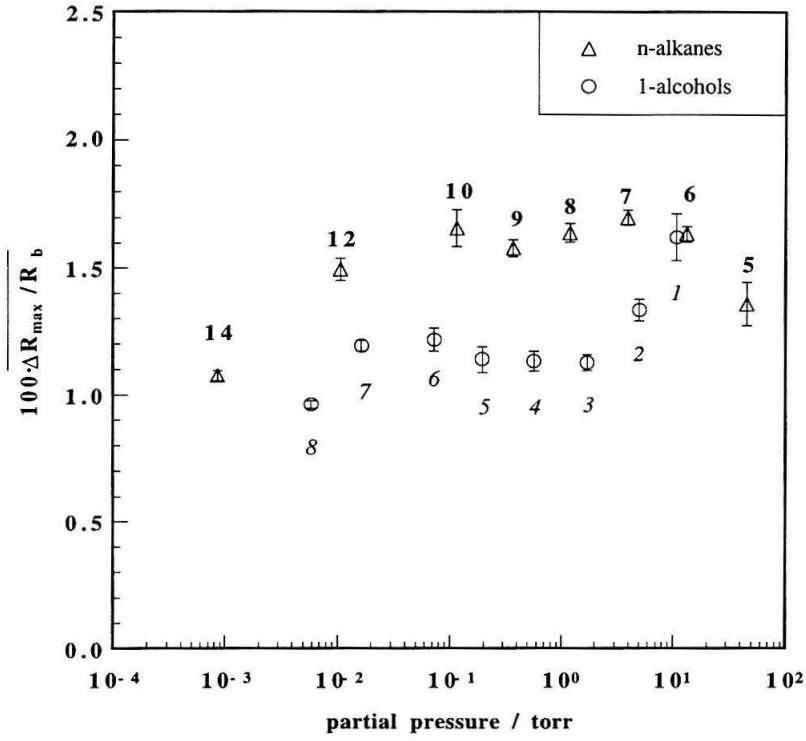
n-alkanes
1-alcohols
2.5
2.0
1.5
1.0
0.5
0.0
$100 \cdot \overline{\Delta R_{max} / R_b}$
10^{-4}
10^{-3}
10^{-2}
10^{-1}
10^{0}
10^{1}
10^{2}
partial pressure / torr
14
12
10
9
8
7
6
5
1
2
3
4
5
6
7
8

Figure 3.2a

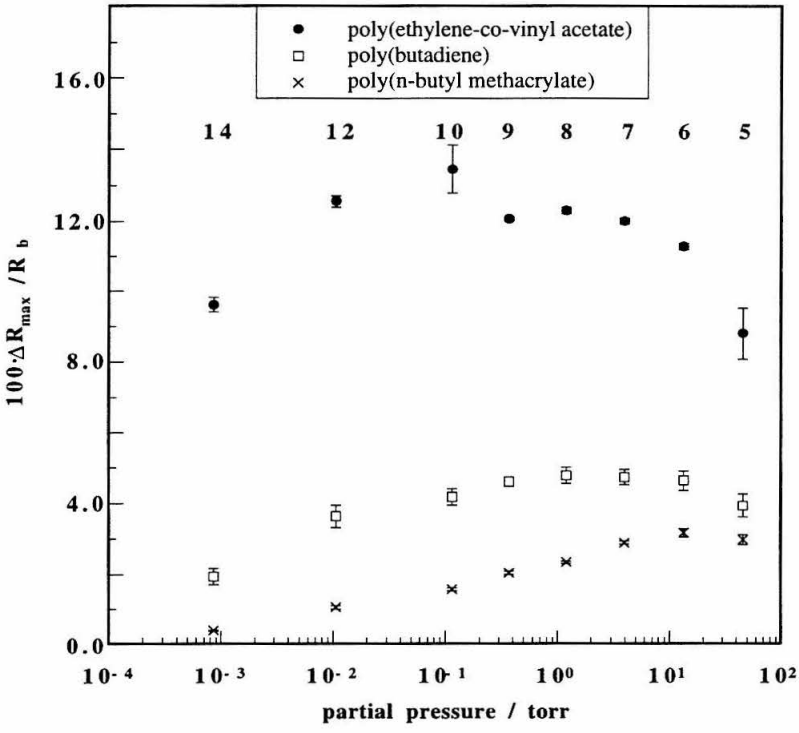
poly(ethylene-co-vinyl acetate)
poly(butadiene)
poly(n-butyl methacrylate)
14
12
10
9
8
7
6
5
16.0
12.0
8.0
4.0
0.0
100·ΔR_max /R_b
10-4
10-3
10-2
10-1
100
101
102
partial pressure / torr

Figure 3.2b

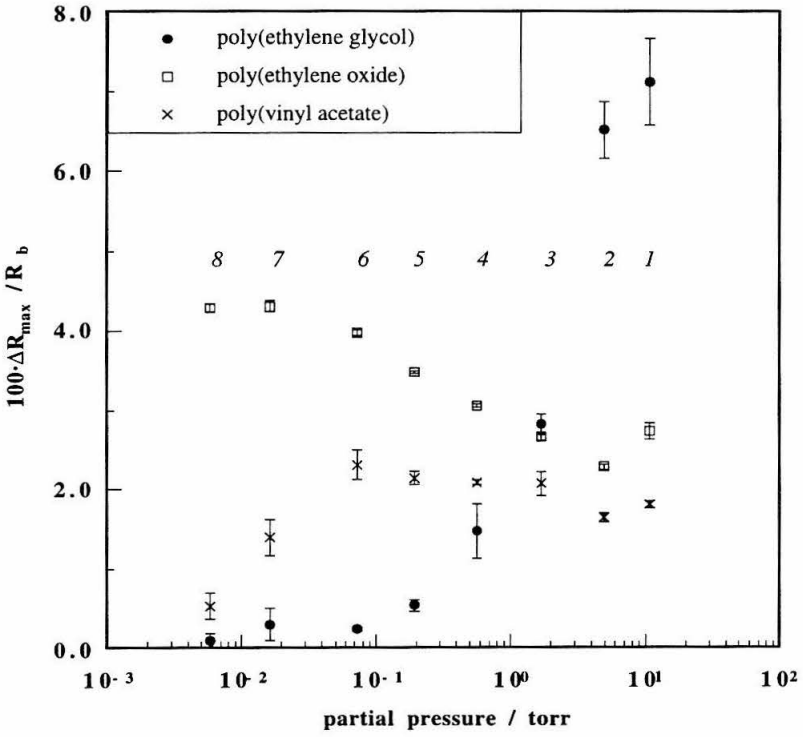
poly(ethylene glycol)
poly(ethylene oxide)
poly(vinyl acetate)
8.0
6.0
4.0
2.0
0.0
100·ΔR_max / R_b
8
7
6
5
4
3
2
1
10⁻³
10⁻²
10⁻¹
10⁰
10¹
10²
partial pressure / torr

Figure 3.2c

Figure 3.3: Plot of human olfactory detection thresholds versus the vapor pressure (at 25 °C) of a homologous series of straight chain alkanes, ranging from ethane to tridecane, and of 1-alcohols ranging from methanol to dodecanol. For clarity, the number of carbons in each odorant is indicated next to the corresponding data point, in italics for the alcohols and plain text for the alkanes. An average human can detect one odorant molecule in the number of air molecules plotted on the ordinate. The error bars represent one standard deviation unit in the standardized results reported by at least 2, and up to 20, authors.[1] A filled data point is used if only one author reported results. A best straight line fit through the alcohols from methanol to octanol gives a slope of -1.3±0.1 and an r^2 value of 0.96. Similarly, a best straight line fit through the alkanes from ethane through decane gives a slope of -0.94±0.08 and an r^2 value of 0.96.

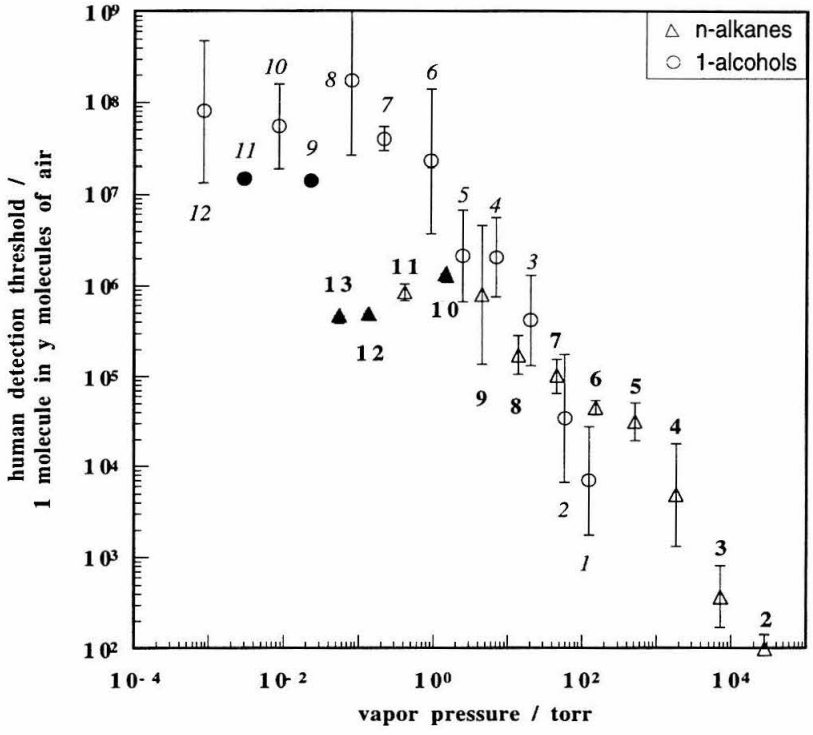
n-alkanes
1-alcohols
human detection threshold / 1 molecule in y molecules of air
vapor pressure / torr
10⁹
10⁸
10⁷
10⁶
10⁵
10⁴
10³
10²
10⁻⁴
10⁻²
10⁰
10²
10⁴

Figure 3.3

Figure 3.4: Plots of the partition coefficients, *K*, for odorants sorbing into the stationary phases (a) squalane at 100 °C and (b) tricresyl phosphate at 120 °C obtained from gas chromatography data,[19] versus odorant vapor pressure. The odorants plotted in both plots are: methanol, ethanol, n-butane, acetone, dichloromethane, 1-propanol, ethyl acetate, 2,3-dimethylbutane, n-hexane, chloroform, 1-butanol, 2-chloroethanol, tetrachloromethane, benzene, 1-pentanol, cyclopentanone, toluene, n-octane, 1-hexanol, 1-heptanol, 2-octanol, n-decane, 1-octanol and n-dodecane. Additional odorants plotted only in (a) are: ethane, m-diethylbenzene, o-diethylbenzene and o-xylene. Additional odorants plotted only in (b) are: ethylene glycol diacetate, n-hexadecane, n-tetradecane and n-octadecane. The solid lines represent the best line fits through the data points, with the fitting parameters given in the figures.

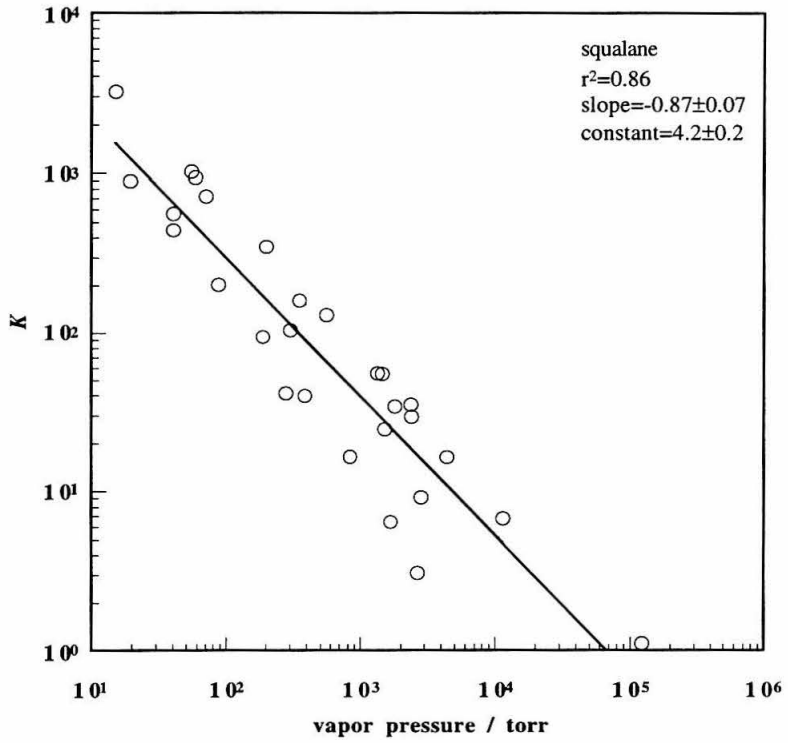
squalane
r²=0.86
slope=-0.87±0.07
constant=4.2±0.2
K
vapor pressure / torr
10⁰
10¹
10²
10³
10⁴
10⁵
10⁶

Figure 3.4a

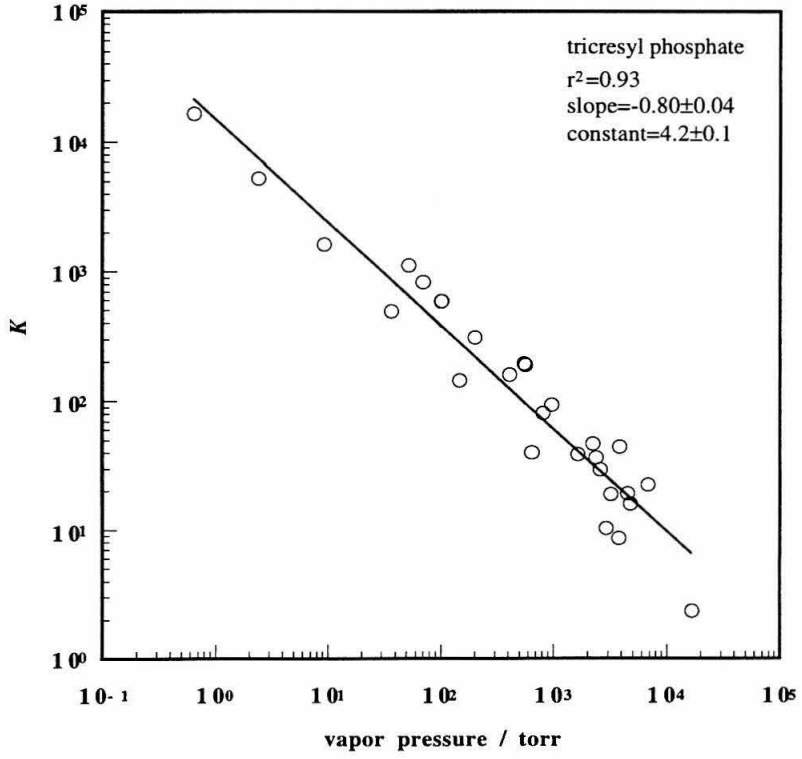
tricresyl phosphate
r²=0.93
slope=-0.80±0.04
constant=4.2±0.1
K
vapor pressure / torr

Figure 3.4b

Figure 3.5: Plots of the partition coefficient, *K*, versus the vapor pressure of homologous series of (a) 1-alcohols and (b) n-alkanes on the squalane stationary phase at 100 °C and the tricresyl phosphate stationary phase at 120 °C. The series of alcohols plotted in (a) ranged from methanol to 1-octanol inclusively. The series of alkanes plotted in (b) consisted of even carbon n-alkanes ranging from ethane to n-dodecane inclusively on the squalane stationary phase and n-butane to n-octadecane inclusively on the tricresyl phosphate stationary phase. The lines indicate the best linear fits and the fitting parameters are given in the figures.

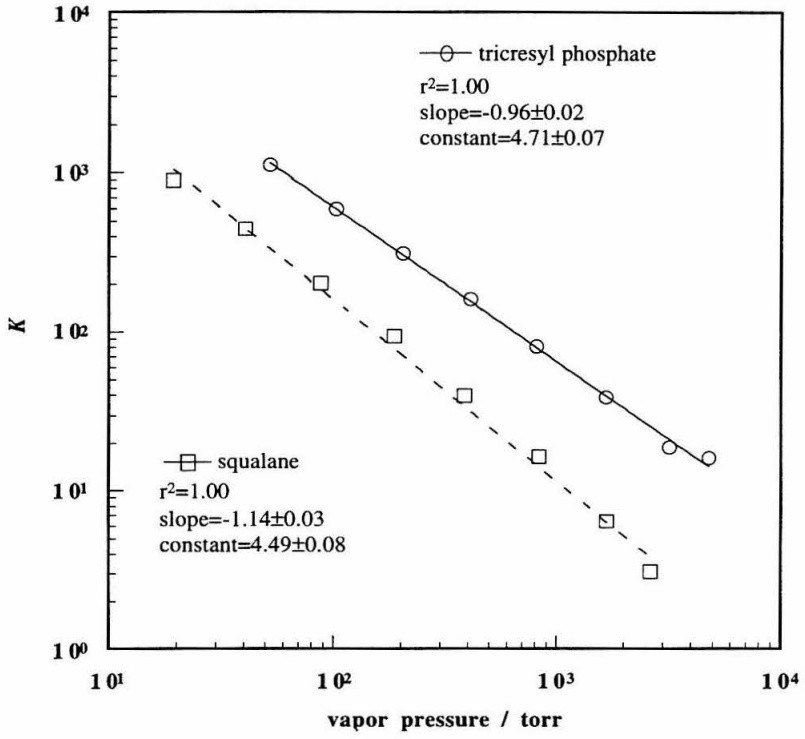
tricresyl phosphate
r²=1.00
slope=-0.96±0.02
constant=4.71±0.07
squalane
r²=1.00
slope=-1.14±0.03
constant=4.49±0.08
K
vapor pressure / torr
10⁴
10³
10²
10¹
10⁰
10¹
10²
10³
10⁴

Figure 3.5a

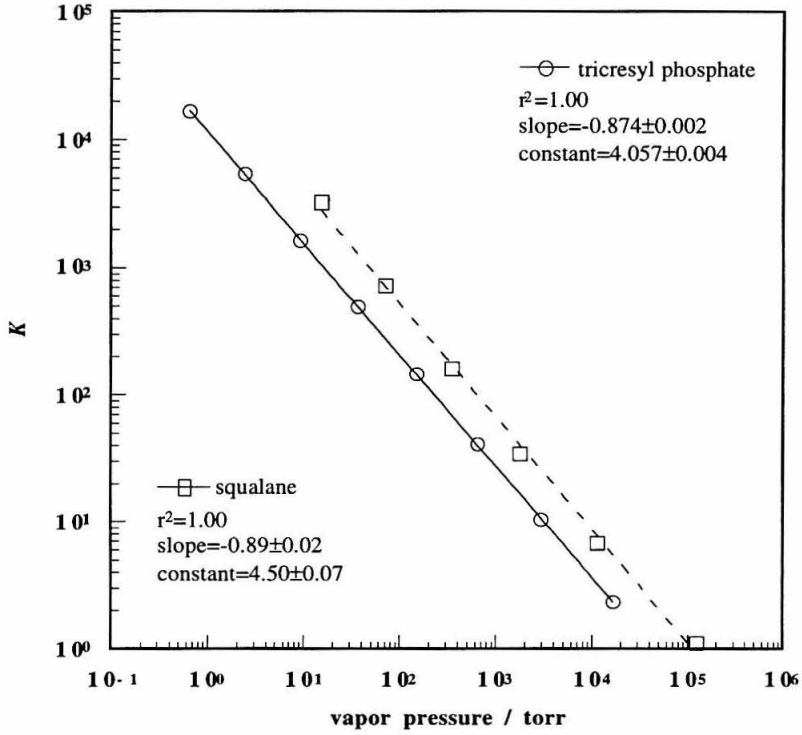
tricresyl phosphate
r²=1.00
slope=-0.874±0.002
constant=4.057±0.004
squalane
r²=1.00
slope=-0.89±0.02
constant=4.50±0.07
K
vapor pressure / torr
10⁵
10⁴
10³
10²
10¹
10⁰
10⁻¹
10⁰
10¹
10²
10³
10⁴
10⁵
10⁶

Figure 3.5b

Table 3.1: Activity coefficients for infinitely dilute straight chain alkanes and 1-alcohols in specific gas chromatography stationary phases.[19,21]

[a]Temperature = 373 K, molecular weight = 422.8 g/mol.

[b]Temperature = 393 K, molecular weight = 368.4 g/mol.

[c]Temperature = 417 K, molecular weight ≈ 500000 g/mol.

[d]Temperature = 352 K, molecular weight ≈ 1000 g/mol.

[e]Temperature = 373 K, molecular weight ≈ 300 g/mol.

Odorant	Squalane[a]	Tricresyl phosphate[b]	Poly(vinyl acetate)[c]	Poly(ethylene oxide)[d]	Poly(ethylene glycol)[e]
Ethane	0.33				
Butane	0.58	2.0			6.1
Pentane				2.1	
Hexane	0.73	2.6	0.030	2.6	12
Heptane			0.040	3.3	
Octane	0.80	2.9	0.050	4.1	18
Nonane			0.082	5.2	
Decane	0.88	3.6	0.095	6.5	27
Unedecane			0.12	8.0	
Dodecane	0.93	4.3	0.15	8.8	42
Tetradecane		5.1	0.23		66
Hexadecane		6.0	0.34		83
Octadecane		7.3			124
Methanol	5.4	1.0	0.0049		0.63
Ethanol	4.1	1.3	0.0058	0.31	0.81
Propanol	3.2	1.2	0.0081	0.29	0.93
Butanol	2.9	1.2	0.0093	0.41	1.1
Pentanol	2.5	1.2	0.011		1.2
Hexanol	2.5	1.2	0.013		1.5
Heptanol	2.5	1.3	0.015		1.8
Octanol	2.6	1.3	0.018		2.2
Decanol			0.026		

Table 3.1

DISCUSSION

The polymer-based electronic nose exhibits a characteristic displayed by the human olfactory system in that it discriminates against ambient background gases in air such as O_2, N_2, and CO_2, and is more sensitive, based on the partial pressure of odorant in the gas phase, to odorants having lower vapor pressures (Figures 3.2 and 3.3). A similar trend has also been noted previously in a qualitative study of the response of a different, polypyrrole-based, electronic nose detector array to fixed partial pressures of methanol, ethanol, 1-propanol, 1-butanol and 1-pentanol, but no explanation was advanced for the origin of the variation in mean signal response of this system.[22]

The primary trends observed in Figures 3.2, 3.4 and 3.5 can be explained using simple thermodynamic principles. At equilibrium, the chemical potential, μ, of an odorant must be equal in both the sorbed and vapor phases.[23] The equilibrium mole fraction, χ, of the odorant in the sorbed phase is therefore related to the fraction of the vapor pressure of the odorant and to the chemical potential, by the relationships:[23]

$$\mu = \mu^0 + \mathrm{RT} \ln \gamma \chi \tag{1}$$

and

$$P/P^0 = a = \gamma \chi , \tag{2}$$

where μ^0 is the chemical potential of the odorant in its saturated vapor state and also in its pure liquid state, R is the gas constant, T is the temperature, γ is the odorant activity coefficient, and a is the odorant activity. If the activity coefficients, which account for the specific solvation interactions between the sorbent phase and the odorant molecules, are similar for odorants within a homologous series being sorbed into a given polymer, then the concentration of any member of the homologous odorant series sorbed into a specific polymer will be primarily determined by the fraction of the vapor pressure of the odorant in the gas phase, as opposed to being determined primarily by the absolute concentration of the odorant in the vapor phase.

This situation is consistent with observed response trends of the electronic nose detectors to the homologous series of alkane and alcohol odorants. The data in Table 3.1 suggest that the variation in the activity coefficients, within our two homologous series of odorants sorbing into the polymers used the electronic nose, is small relative to the variation in the vapor pressures across the homologous series. The data thus indicate that the relative changes in the signals produced by the polymer composite detectors in response to exposures to members of each homologous series of odorants studied herein are, to first order, independent of specific binding features of the odorant into the polymer phase and instead depend primarily on the equilibrium concentration of the odorant that is attained in the polymeric detector material. In other words, conceptually dividing the events leading to the production of an electronic nose output signal into three components: a) sorption of the odorant into the polymeric detector material, b) binding of the dissolved odorant molecule to specific signal transduction sites, and c) molecularly-specific amplification events of the signals during the output stage, the data show that processes b) and c) are essentially constant for the electronic nose detector responses to odorants in the two homologous series that have been studied in this work.

As displayed in Figure 3.3, the mean human olfactory detection thresholds for both series of odorants show behavior which is similar to that of the electronic nose. The human data are thus consistent with the suggestion that the trends in olfactory detection thresholds for these odorants are dictated primarily by a physical sorption effect.[12] Deviations from this behavior would then be taken to indicate variations in chemical interactions between odorants and the olfactory receptors. Of course, isolation of one, thermodynamically-based, factor is difficult for the human olfactory system, in which equilibrium partitioning of the odorants in the various phases of concern may not be reached during olfaction and for which the perception of an odorant depends not only on the response of the detectors in the olfactory bulb but also on the processing of the signals in the brain. Nevertheless, the comparison between the human and electronic nose

response data is consistent with a common sorption-based effect dominating the odor intensity trends for the series of odorants studied herein.

We chose two series of odorants in this work for which we hypothesize that relatively little evolutionary pressure has been exerted on humans to develop enhanced olfactory sensitivity relative to that expected from the thermodynamically-based vapor pressure trend. The correlation of vapor pressure with odor detection threshold displayed in Figure 3.3 for the human nose would be expected to break down for hydrogen sulfide, alkylamines, and other odorants that either are related to decaying food or which are toxic gases that have been present for evolutionarily significant time periods in the atmosphere. An examination of human olfactory threshold data confirms this hypothesis, because the trend of decreasing odor intensity thresholds for odorants with lower vapor pressures is not observed for alkylamines or alkylthiols, towards which humans exhibit much increased olfactory sensitivity as compared to the alkanes or alcohols that have the same vapor pressure.[1] Additionally, recent studies by Zhao et al. indicate that an individual olfactory receptor type has significantly more specificity to odorant chain length than the detectors in the polymer-based electronic nose,[24] again indicating the differences for certain odorants that are likely to be observed between the response of the electronic nose and that of the mammalian olfactory system.

At a given odorant activity in the polymeric films (or in the epithelium for the human olfactory system), there must of course be some variation in sorbed odorant concentration, and in the resulting signal response, for different polymer (receptor) types, otherwise it would be impossible to obtain odor quality information from the output of an array of sensing elements. In the electronic nose, differential sorption of odorants, with varying activity coefficients, into the various polymers produces a differential swelling, and therefore produces the differential $\Delta R_{max}/R_b$ output pattern of signals that can be used to identify odorants (Figures 3.1a and 3.1b). Similarly, from the gas chromatographic partition coefficient data of Figures 3.5a and 3.5b, it is clear that the alcohols sorb

preferentially into the polar support (tricresyl phosphate) over the nonpolar support (squalane), while the alkanes exhibit the opposite trend and sorb preferentially into the nonpolar support relative to the polar support. These differences in signal intensity are clearly due to specific chemical interactions between the odorant and polymer molecules, as reflected in the variation in activity coefficients, that act in conjunction with the sorption effects expected for an ideal sorbent/solute system to determine the response of an individual detector in the array to the odorant of concern. The data presented herein clearly show, however, that for the odorants studied in this work, the response intensity of the electronic nose detectors is determined, to first order, by the thermodynamic activity effects that dictate the concentration of odorant into the film, while the (smaller) deviations from the mean response intensity exhibited by the various individual detectors produce the outputs that can be used to extract odor quality information from the array. Interestingly, in the electronic nose, it is clear that a fixed, and relatively constant, collection of detectors is being fired in response to the various members of a homologous series of odorants. However, the present experiments yield no information on whether the response of the human system at odor detection threshold is produced by the same, or by a significantly different, collection of receptors as the identity of the odorant is varied.

ACKNOWLEDGEMENTS

We acknowledge Prof. J. Bower and C. Chee-Ruiter of Caltech for numerous helpful discussions and for their critical comments on this work. We thank NASA, the Army Research Office, and DARPA for their support of this work, and B.J.D. acknowledges the Government of Canada for an NSERC 1967 Centennial Graduate Fellowship.

REFERENCES

(1) Devos, M.; Patte, F.; Rouault, J.; Laffort, P.; Van Gemert, L. J. *Standardized Human Olfactory Thresholds*; Oxford University Press: New York, 1990.

(2) Ohloff, G. *Scent and Fragrances, the Fashion of Odors and Their Chemical Perspectives*; Springer-Verlag: New York, 1994.

(3) Amoore, J. E. *Molecular Basis of Odour*; Charles C. Thomas: Springfield, Illinois, 1970.

(4) Dravnieks, A. In *Flavor Quality: Objective Measurement*; R. Scanlon, Ed.; American Chemical Society: Washington, 1977.

(5) Edwards, P. A.; Jurs, P. C. *Chemical Senses* **1989**, *14*, 281.

(6) Edwards, P. A.; Anker, L. S.; Jurs, P. C. *Chemical Senses* **1991**, *16*, 447.

(7) Abraham, M. H. In *Indoor Air and Human Health*; 2nd ed.; R. B. Gammage and B. A. Berven, Ed.; CRC Press: New York, 1996.

(8) Greenberg, M. J. In *Odor Quality and Chemical Structure*; H. R. Moskowitz and C. B. Warren, Ed.; American Chemical Society: Washington, 1981.

(9) Laffort, P.; Patte, F.; Etcheto, M. *Ann. N.Y. Acad. Sci.* **1974**, *237*, 192.

(10) Moulton, D. G.; Eayrs, J. T. *Quart. J. Exp. Psychol.* **1960**, *12*, 99.

(11) Cometto-Muñiz, J. E.; Cain, W. S. *Indoor Air* **1994**, *4*, 140.

(12) Cometto-Muñiz, J. E.; Cain, W. S. *Physiol. Behav.* **1990**, *48*, 719.

(13) Mullins, L. J. *Ann. New York Acad. Sci.* **1955**, *62*, 247.

(14) Ottonson, D. *Acta Physio. Scand.* **1958**, *43*, 167.

(15) Lonergan, M. C.; Severin, E. J.; Doleman, B. J.; Beaber, S. A.; Grubbs, R. H.; Lewis, N. S. *Chem. Mater.* **1996**, *8*, 2298.

(16) Yaws, C. L.; Lin, X.; Bu, L. *Handbook of Vapor Pressure*; Gulf Publishing Company: London, 1994; Vol. 1-3.

(17) Punter, P. H. *Chemical Senses* **1983**, *7*, 215.

(18) Franks, N. P.; Lieb, W. R. *Nature* **1985**, *316*, 349.

(19) McReynolds, W. O. *Gas Chromatographic Retention Data*; Preston Technical Abstracts Co.: Evanston, Illinois, 1966.

(20) Littlewood, A. B. *Gas Chromatography*; Academic Press: New York, 1962.

(21) Hao, W.; Elbro, H. S.; Alessi, P. *Polymer Solution Data Collection*; DECHEMA: Frankfurt, 1992.

(22) Hatfield, J. V.; Neaves, P.; Hicks, P. J.; Persaud, K.; Travers, P. *Sens. Actuators B* **1994**, *18*, 221.

(23) Schwarzenbach, R. P.; Gschwend, P. M.; Imboden, D. M. *Environmental Organic Chemistry*; John Wiley & Sons: New York, 1993.

(24) Zhao, H. Q.; Ivic, L.; Otaki, J. M.; Hashimoto, M.; Mikoshiba, K.; Firestein, S. *Science* **1998**, *279*, 237.

Chapter 4: Comparison of Detection Thresholds and Trends in Odorant Discrimination Abilities between Electronic and Mammalian Olfaction, and Attempts at Predicting Human Odor Quality Judgements Using Electronic Nose Response Data

ABSTRACT

Electronic nose response data were collected for the purpose of comparing quantitatively measurable phenomena in electronic and mammalian olfaction. Specifically, the detection thresholds for the electronic nose exposed to homologous series of n-alkane and 1-alcohol odorants were determined and the results were compared to detection thresholds for humans for the same odorants. Trends in the olfactory abilities of the electronic nose and mammals (humans and monkeys) in distinguishing odorant pairs within incrementally varying series of esters, carboxylic acids and alcohols were also compared. Such comparisons are of interest since biologists have proposed that the mammalian olfactory system is comprised of many differentially and broadly responsive odorant-binding receptors, conceptually similar to the electronic nose, and thus similar results in comparison tests might be observed. Quantifying such similarities is an important step in furthering the development of an electronic analogue to mammalian olfaction. Furthermore, electronic nose response data were collected for a diverse set of odorants which had previously been quantitatively characterized by human panelists according to many categories of odor quality. The responses of the electronic nose detectors were then used in attempts at predicting the human odor quality judgements.

INTRODUCTION

The development of electronic/computerized analogues to the human senses is at an advanced stage for senses such as touch, vision and hearing.[1-3] Electronic devices can transduce and record visual, audio and tactile stimuli and using advanced algorithms can process such input data to make human-like interpretations. In fact, several of these systems are approaching or have achieved a level allowing them to be interfaced with humans to help overcome various disabilities.[3] However, analogous electronic devices for the sense of olfaction have not yet achieved the same level,[4,5] in part due to the complexity of the mammalian sense of olfaction which is only recently becoming understood.[6-8]

Scientists do know that the human olfactory epithelium contains $\approx 10^6$ - 10^7 total olfactory receptor neurons which each probably contain only one of $\approx 10^3$ different types of odorant-binding receptor proteins.[6-9] Comparison of the primary structures of many putative odorant-binding receptor proteins has revealed hypervariable regions in the protein sequences which are believed to result in incremental differences in their binding specificities.[7,8,10,11] Since mammals can detect and discriminate tens of thousands of odorants, a diversity of differentially responsive odorant-binding receptor proteins is required to match the odorant diversity and each odorant-binding receptor protein is expected to be somewhat broadly responsive.[6,8,11,12] This broad and differential responsiveness has been experimentally observed using electrophysiological recordings in the mammalian olfactory epithelium and mitral/tufted cells,[13,14] and calcium imaging of active olfactory neurons.[8] Scientists have suggested that the patterns of odorant-induced receptor neuron activity allow the mammalian brain to detect and discriminate between odorants.[8,12,15]

The electronic nose is also composed of broadly responsive odorant-binding polymers which vary incrementally in their chemical properties in such a way as to obtain differential response patterns for various odorants. The detector response activity is also used to detect and discriminate between odorants. Thus, the electronic nose is conceptually

similar to the peripheral level of the mammalian olfactory system. For this reason, it is not unreasonable to expect similarities in various quantitatively measurable phenomena in electronic and mammalian olfaction. Identifying and quantifying any such similarities would be useful toward furthering the development of an electronic analogue to mammalian olfaction. Thus, one goal of this work is to compare the detection thresholds for an electronic nose and human noses as well as to compare trends in the abilities of the electronic nose and mammalian noses in distinguishing between odorants. A second goal is to use the odorant chemical information, encoded in the electronic nose detector responses, to predict human percepts of a given odorant's odor quality. The polymer-based detectors in the electronic nose and the protein-based receptors in the human nose are expected to probe mainly the same odorant chemical features. Thus, by appropriately weighting the electronic nose detector responses, attempts can be made to predict human odor quality judgements.

EXPERIMENTAL

The detector array used in determining the electronic nose detection thresholds for the homologous series of n-alkane (n-pentane, n-hexane, n-heptane, n-octane and n-nonane) and 1-alcohol (methanol, ethanol, 1-propanol, 1-butanol, 1-pentanol) odorants was composed of 20 detectors. Two detector copies were made from each of ten polymers (listed in Table 4.1) purchased from Aldrich and Polysciences. Each detector was fabricated by spin-coating mixtures containing a dissolved polymer and suspended carbon black onto a glass slide, as previously described.[16,17] The odorants were purchased from Aldrich and Pfaltz & Bauer.

A second detector array, made from the same polymers and using the same fabrication techniques, was used to test the ability of the electronic nose to pairwise discriminate between various odorants within series of esters (isopentyl acetate, isopentyl propionate, isopentyl butanoate, isopentyl pentanoate, isopentyl hexanoate, ethyl acetate, n-

propyl acetate, n-butyl acetate, n-pentyl acetate, n-hexyl acetate, n-octyl acetate, n-decyl acetate, isopropyl acetate and isobutyl acetate), alcohols (ethanol, 1-propanol, 1-butanol, 1-pentanol, 1-hexanol, 1-heptanol, 1-octanol, 2-pentanol and 3-pentanol) and carboxylic acids (n-propanoic acid, n-butanoic acid, n-pentanoic acid, n-hexanoic acid, n-heptanoic acid, isobutanoic acid, isopentanoic acid and isohexanoic acid). The odorants were purchased from Aldrich and Pfaltz & Bauer.

A third detector array, made using the same fabrication techniques and containing the polymers listed in Table 4.2, was used to test the ability of the electronic nose to predict human odor quality judgements. The odorants used in this experiment were 1-butanol, 1-hexanol, 1-heptanol, 1-octanol, ethyl propionate, ethyl butanoate, propyl butanoate, pentyl butanoate, isopentyl acetate, isopentanoic acid, n-pentanoic acid, n-hexanoic acid, toluene, anisole, phenyl ethanol, phenyl acetylene, tetrahydrothiophene, thiophene, dipropyl sulfide, pyridine, citral and (R)-(+)-limonene. The odorants were purchased from Aldrich and Pfaltz & Bauer.

Throughout this chapter, an automated system, consisting of LabVIEW software, a pentium computer, a Keithley channel switcher, a Keithley multimeter, and electronically controlled solenoid valves and mass flow controllers, was used to deliver selected concentrations of solvent vapors and monitor the detector resistances, as described previously.[17] A flame ionization detector (Model 300 HFID from California Analytical Instruments, Inc.) was used to verify the delivered concentrations when extremely low concentrations were required.

Table 4.1: Polymers contained in the detectors of the first two electronic nose arrays.

Detector #	Polymer
1	poly(4-vinyl phenol)
2	poly(*N*-vinylpyrrolidone)
3	poly(sulfone)
4	poly(methyl methacrylate)
5	poly(caprolactone)
6	poly(ethylene-*co*-vinyl acetate), 82% ethylene
7	poly(ethylene oxide)
8	poly(ethylene)
9	poly(vinylidene fluoride)
10	poly(ethylene glycol)

Table 4.1

Table 4.2: Polymers contained in the detectors of the third electronic nose array.

Detector #	Polymer
1	poly(4-vinyl phenol)
2	poly(*N*-vinylpyrrolidone)
3	poly(sulfone)
4	poly(methyl methacrylate)
5	poly(caprolactone)
6	poly(ethylene-*co*-vinyl acetate), 82% ethylene
7	poly(ethylene oxide)
8	poly(ethylene)
9	poly(vinylidene fluoride)
10	poly(ethylene glycol)
11	poly(vinyl acetate)
12	poly(styrene)
13	poly(butadiene)
14	poly(styrene-*co*-allyl alcohol)
15	poly(α-methylstyrene)
16	hydroxypropyl cellulose
17	poly(styrene sulfonic acid)
18	poly(carbonate bisphenol A)
19	poly(epichlorohydrin)
20	poly(styrene-*co*-butadiene)

Table 4.2

RESULTS AND DISCUSSION

A. Determination of Detection Thresholds for the Electronic Nose and Comparison with Human Olfaction

1. Determination of Detection Thresholds for the Electronic Nose

The detection threshold of the electronic nose array, for a given odorant, was defined as the lowest concentration at which any detector in the array had a response with a signal to noise ratio of 3. Thus, at the detection threshold an odorant is detected but would generally not be identifiable, due to the lack of responses from multiple detectors which is necessary to generate an odorant-identifying response pattern. This definition of the detection threshold was employed previously in a study of surface acoustic wave (SAW) vapor detectors, which used a different set of polymer coatings than those used herein.[18] In the present case, a detector response was taken as the maximum resistance increase relative to the baseline resistance during the 10-minute exposure to odorant-carrying air flow. The 10-minute odorant exposure was always preceded by, and followed by, a 2-minute exposure to air flow from the general laboratory source. The noise of a given detector was defined as the standard deviation in the residuals about a 9-point moving average of the baseline resistance values, spanning approximately 35 seconds. The resistance values were measured by a Keithley Model 2002 multimeter which attempted to record each resistance value to 8.5 significant digits (i.e., 29 bits) by integrating over a measurement aperture of 167 ms. However, the actual resistance measurements were limited to a lesser number of significant digits by noise inherent in the individual detectors and the overall electrical system. The expected detection thresholds were roughly estimated based on the noise levels typical of the better detectors (i.e., slightly less than 10 parts per million for the detectors containing poly(ethylene oxide), poly(ethylene) and poly(ethylene glycol) which had baseline resistances of approximately $1.3 \times 10^4\ \Omega$, $1.2 \times 10^4\ \Omega$ and $4.0 \times 10^3\ \Omega$ respectively over the course of the experiment) and the knowledge that detector response magnitudes generally vary linearly as a function of odorant concentration.[17,19,20]

Each of the ten odorants was then delivered one at a time at each of 3 concentrations generally spanning approximately an order of magnitude near the expected detection threshold. For each odorant, the largest signal to noise ratio of any of the detectors, at the lowest concentration where a signal was detected, was used to determine the detection threshold by linearly extrapolating down to a signal to noise ratio of 3. The extrapolations were never larger than a factor of 5 and were typically less than a factor of 3.

The detection thresholds obtained for the electronic nose, on exposure to homologous series of alkanes (n-pentane to n-nonane) and alcohols (methanol to 1-pentanol) are shown in Figures 4.1a and 4.1b. In all cases, the electronic nose detection threshold concentrations decrease with decreasing odorant vapor pressure along a homologous odorant series, as expected from a previous study which showed that lower vapor pressure odorants have larger partition coefficients for sorption into polymers.[21] In the case of the homologous series of n-alkanes, detectors containing poly(ethylene oxide) and poly(ethylene) exhibited similar signal to noise ratios and were the detectors that defined the detection threshold of the array. In the case of the homologous series of 1-alcohols, a poly(ethylene glycol) based detector exhibited the largest signal to noise ratios for methanol, ethanol and 1-propanol while a poly(ethylene oxide) based detector exhibited the largest signal to noise ratios for 1-butanol and 1-pentanol. Therefore, the specific detector which allows the array to detect the lowest concentration of a given odorant, defining the array detection threshold, will vary depending on the affinity of the detectors for the given odorant.

2. Comparison of Detection Thresholds for Human and Electronic Noses

The detection threshold data for humans in detecting the homologous series of n-alkanes and 1-alcohols were obtained from the literature.[22] These literature values, plotted in Figure 4.1, represent detection thresholds averaged over the work of many authors in testing many humans.[22] The definition of the human detection thresholds is such that an

average human would be able to detect the odorant but not necessarily be able to identify it, which is consistent with the definition employed for the electronic nose. In fact, it can be postulated that in the case of humans, odorant detection at the detection threshold likely involves the brain receiving a signal from only the olfactory receptor or receptors most strongly responsive to a given odorant. This is also consistent with the electronic nose detection threshold, as defined above.

From the data in Figure 4.1, it is apparent that the electronic nose detection thresholds are typically lower than the human detection thresholds, with the sole exception being n-pentane, where humans have only a slightly lower detection threshold. Typically, the electronic nose detection thresholds are lower by a factor ranging from 2 to 10. In terms of thermodynamic activities, the fraction of a given odorant's vapor pressure (i.e., the partial pressure of the odorant, P, relative to its vapor pressure, P^0) at which the detection threshold lies for the electronic nose is in the range of 2.0×10^{-5} to 6.0×10^{-5} for the studied odorants. The minimum fraction of the odorant vapor pressures detectable by the average human, for the same set of test odorants, is in the range of 4.9×10^{-5} to 9.0×10^{-4}.

It is worth noting that the electronic nose exhibits similar response magnitudes when exposed to most odorants at a constant fraction of their vapor pressure.[21] Thus, the electronic nose would be expected to exhibit similar detection thresholds for most odorants in terms of the minimum detectable fraction of vapor pressure (i.e., $P/P^0 \approx 4.0 \times 10^{-5}$). To a slightly lesser extent, due to the relative complexity of human olfaction, humans also exhibit an odorant fraction of vapor pressure range slightly above that of the electronic nose within which the detection thresholds for many odorants lie. However, there are many significant exceptions, notably in the cases of thiols and amines where humans can be several orders of magnitude more sensitive as a possible result of evolutionary pressure to detect certain toxins that are present in decaying food.

Figure 4.1: Plots of the detection threshold in parts per million (ppm) of odorant in air, for the average human[22] and the electronic nose, versus odorant vapor pressure for homologous series of (a) alkanes from n-pentane through n-nonane and (b) alcohols from methanol through 1-pentanol.

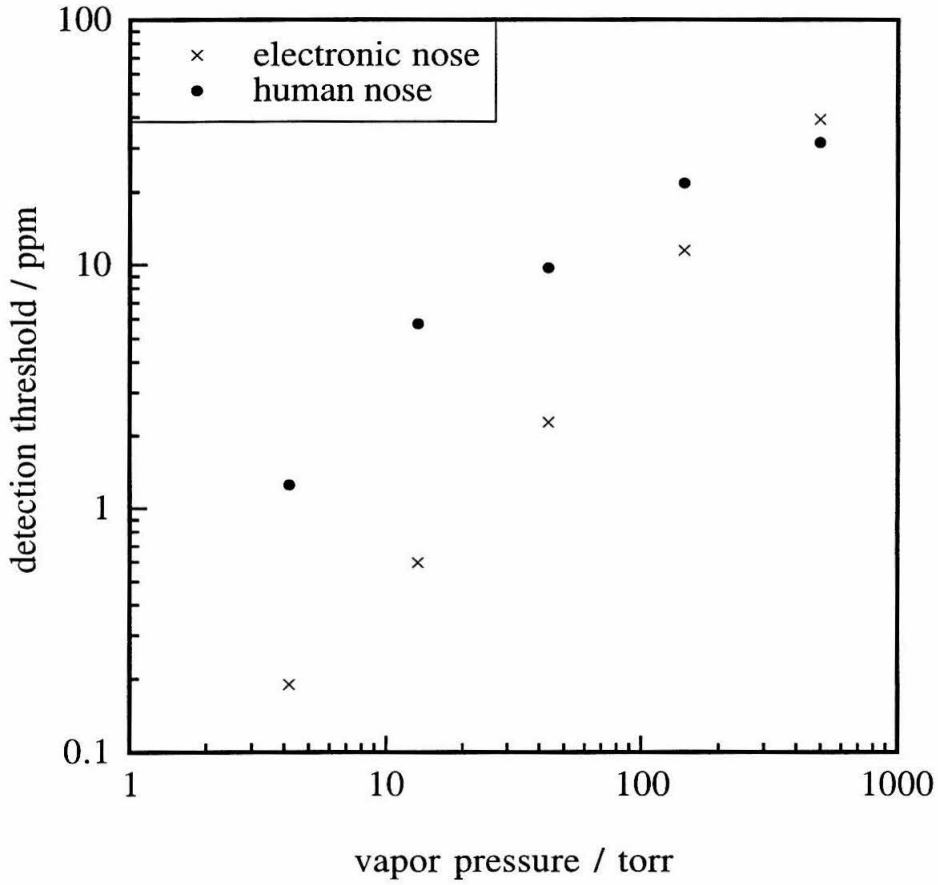
100
10
1
0.1
detection threshold / ppm
electronic nose
human nose
1
10
100
1000
vapor pressure / torr

Figure 4.1a

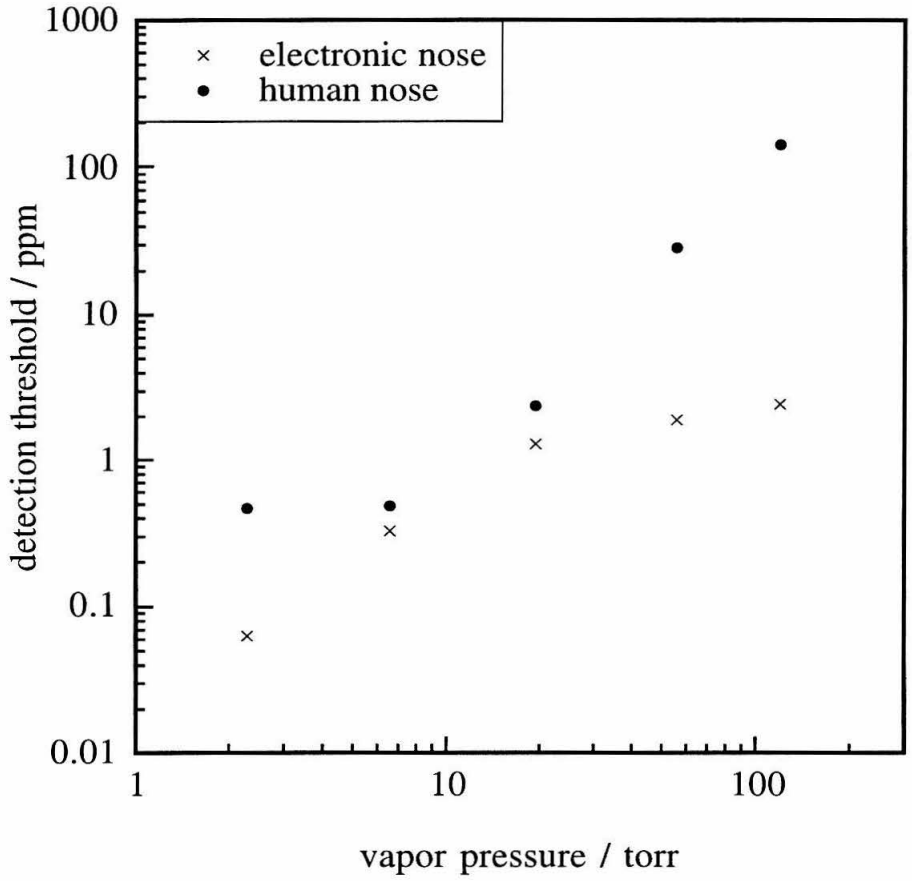
1000
100
10
1
0.1
0.01
detection threshold / ppm
electronic nose
human nose
1
10
100
vapor pressure / torr

Figure 4.1b

B. Determination of the Ability of the Electronic Nose to Pairwise Discriminate between Odorants in Homologous Series and Comparison of the Trends with Mammalian Olfaction

1. Determination of the Electronic Nose Odorant Discrimination Ability

The electronic nose was exposed to each of the odorants to be discriminated 10 times in a randomized order within subsets of a maximum of 8 odorants, because the automated odorant delivery apparatus was limited to handling 8 odorants at a time. The experimental protocol for each exposure was 5 minutes of clean air flow, followed by 5 minutes of air flow containing the odorant at a partial pressure corresponding to 1% of its vapor pressure, followed by another 5 minutes of clean air flow. The data was then processed to extract the response signals as described previously.[16,17]

Since the 20-detector array contained two copies of nominally the same 10-detector array, random combinations of 10 detectors (constrained to each contain exactly one of each of the 10 polymer types) could be used in order to obtain a measure of variability in the ability of a 10-detector electronic nose to discriminate odorants. For each randomly selected 10-detector array, the response signals were normalized and then the Fisher linear discriminant method was used to quantify the ability of the electronic nose to distinguish the odorants.[17] The resolution factor (rf) for resolving a given odorant pair was then taken as the mean rf over the results from 10 randomly selected 10-detector arrays.

Using this methodology, the electronic nose containing 10 detectors was able to pairwise discriminate between all tested odorants with a resolution factor of at least 3.7. The minimum value was observed for the case of n-hexanoic acid vs. isohexanoic acid. The median rf across all tested odorant pairs was 29. If it is assumed that the statistical distributions of the collected data samples are representative of the actual statistical distributions, then an rf $\geq$ 3.0 corresponds to a probability $\geq$ 98% of correctly identifying an odorant as *a* or *b* as a result of a single presentation. Hence the electronic nose can easily discriminate between all the test odorant pairs.

2. Comparison of the Trends in Discrimination Abilities between Electronic and Mammalian Olfaction

The data on the abilities of monkeys (*Saimiri sciureus*) and humans to pairwise discriminate between various ester, alcohol and carboxylic acid odorants were obtained from Laska et al.[23-25] In those experiments, an average probability of correctly distinguishing between a given pair of odorants was determined by averaging across multiple trials and multiple test monkeys or humans. The odorants were presented at a perceived intensity-matched concentration arrived at via dilution of the pure odorants in virtually odorless diethyl phthalate solvent. The dilution ratios were commonly ≈ 1:100, which was the same as the gas phase dilution ratio used in the electronic nose tests.

Since the electronic nose has virtually a 100% probability of correctly distinguishing every tested analyte pair, the measure of distinguishing ability for the electronic nose was taken as the resolution factor, which scales based on the separation of the clustered odorant responses relative to the widths of the clusters in detector space. The measure of distinguishing ability for the humans and monkeys was taken as the percentage of correct decisions in distinguishing an odorant pair. The results are plotted in Figures 4.2, 4.3 and 4.4 for odorant discrimination of isopentyl acetate from series of other esters, isopentanoic acid from series of other carboxylic acids, and n-pentanol from a series of other alcohols.

In several instances in Figures 4.2, 4.3 and 4.4, the trends in the abilities of the electronic, monkey and human olfactory systems are correlated. In most cases, as expected, odorants become easier to discriminate for the electronic nose, monkeys and humans as they become more chemically dissimilar. For example, in Figure 4.2a the task of discriminating between isopentyl acetate versus isopentyl propionate, isopentyl butanoate, isopentyl pentanoate and finally isopentyl hexanoate becomes progressively easier for all three olfactory systems as the odorants become progressively dissimilar.

Similarly, in Figure 4.3b, n-pentanoic acid is more difficult for each of the three olfactory systems to discriminate from isopentanoic acid than from either of isobutanoic acid or isohexanoic acid.

There are also subtle differences in the discrimination trends. For example, in discriminating n-pentanoic acid from each of n-propanoic acid, n-butanoic acid, n-hexanoic acid and n-heptanoic acid (Figure 4.3a), the electronic nose has more difficulty in discriminating n-pentanoic acid from the longer chain acids relative to the shorter chain acids. Conversely, both mammals can more easily discriminate n-pentanoic acid from n-hexanoic acid than from n-butanoic acid. A similar observation can be made from Figure 4.4 where monkeys more easily discriminate 1-pentanol from 1-heptanol and 1-octanol than from 1-propanol and ethanol while the opposite is true for the electronic nose. Typically, the chemical difference between consecutive molecules in a homologous series decreases with the addition of each additional carbon atom. Thus, the relative difficulty of the electronic nose is discriminating longer chain molecules versus shorter chain molecules, which differ by the same number of carbon atoms, is understandable. The opposite observation in specific instances for mammals could be speculatively attributed to odorant receptor proteins with geometrically defined binding sites which more effectively differentiate between certain odorant geometries than the amorphous polymeric detectors of the electronic nose. Observations confirming the differential responses of an olfactory receptor neuron as a function of odorant chain length have recently been published.[8,14]

Figure 4.2: Plots of trends in the abilities of the electronic nose, monkeys and humans to discriminate isopentyl acetate from various series of other ester odorants with incremental chemical differences and from isopentyl alcohol and 1-pentanol. The electronic nose data is plotted with reference to the left scale and the data points represent a mean resolution factor (rf). The monkey and human data are plotted with reference to the right scale and represent the mean probability of correctly discriminating between each specific pair of odorants averaged over 20 humans and five monkeys as experimentally determined by Laska et al.[25] The error bars represent 1 standard deviation unit of confidence in the mean values.

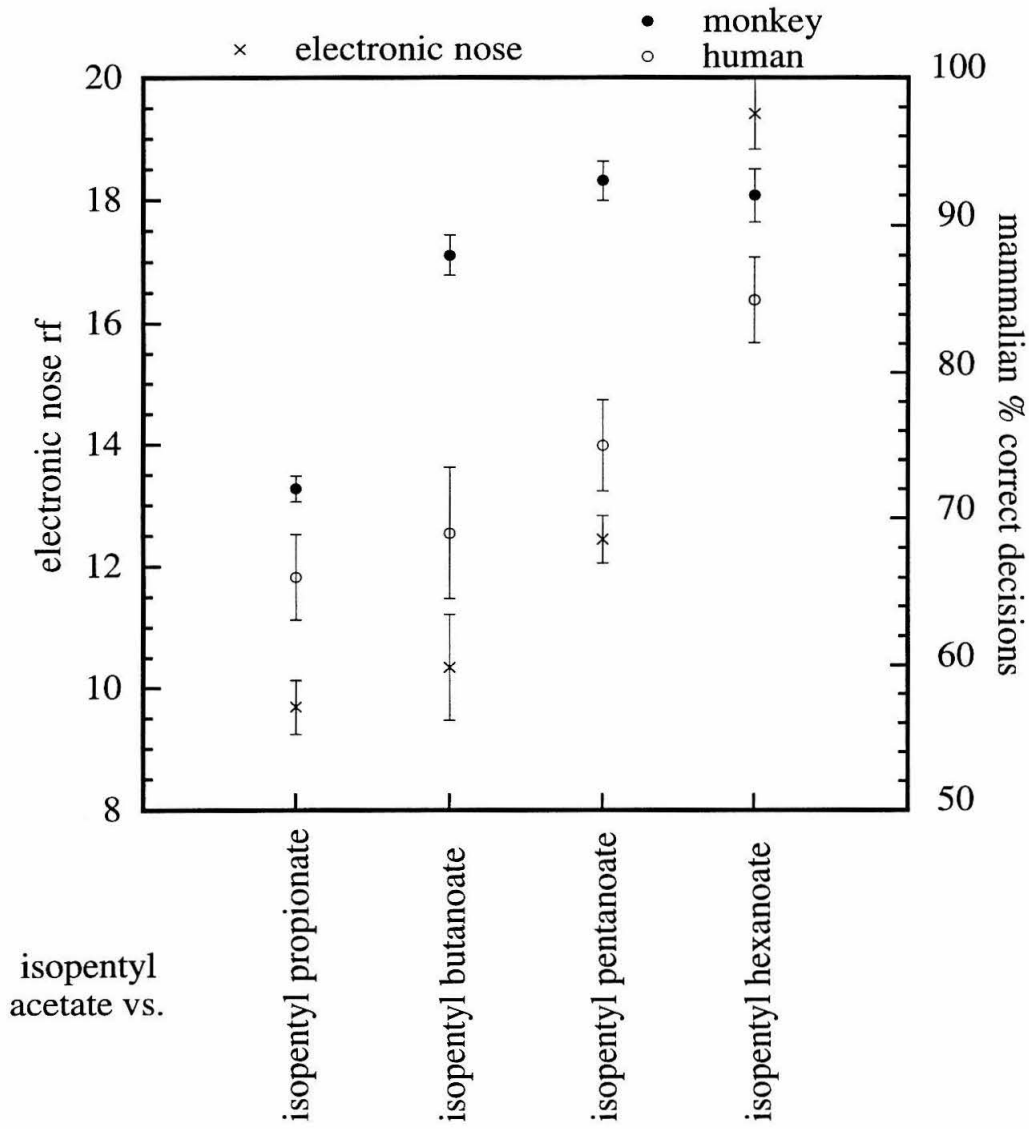
× electronic nose
• monkey
○ human
electronic nose rf
mammalian % correct decisions
20
18
16
14
12
10
8
100
90
80
70
60
50
isopentyl acetate vs.
isopentyl propionate
isopentyl butanoate
isopentyl pentanoate
isopentyl hexanoate

Figure 4.2a

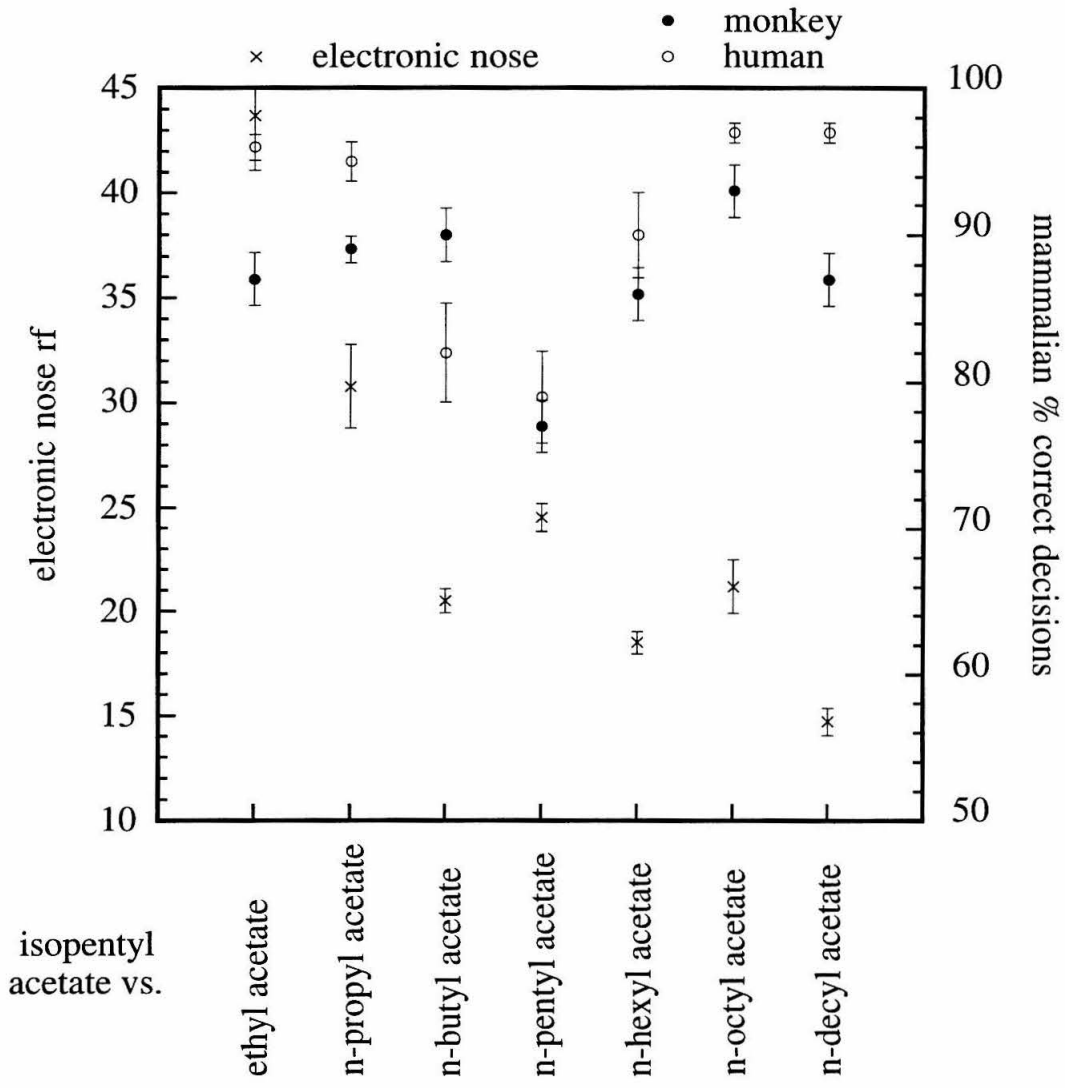
monkey
human
electronic nose
electronic nose rf
mammalian % correct decisions
45
40
35
30
25
20
15
10
100
90
80
70
60
50
isopentyl acetate vs.
ethyl acetate
n-propyl acetate
n-butyl acetate
n-pentyl acetate
n-hexyl acetate
n-octyl acetate
n-decyl acetate

Figure 4.2b

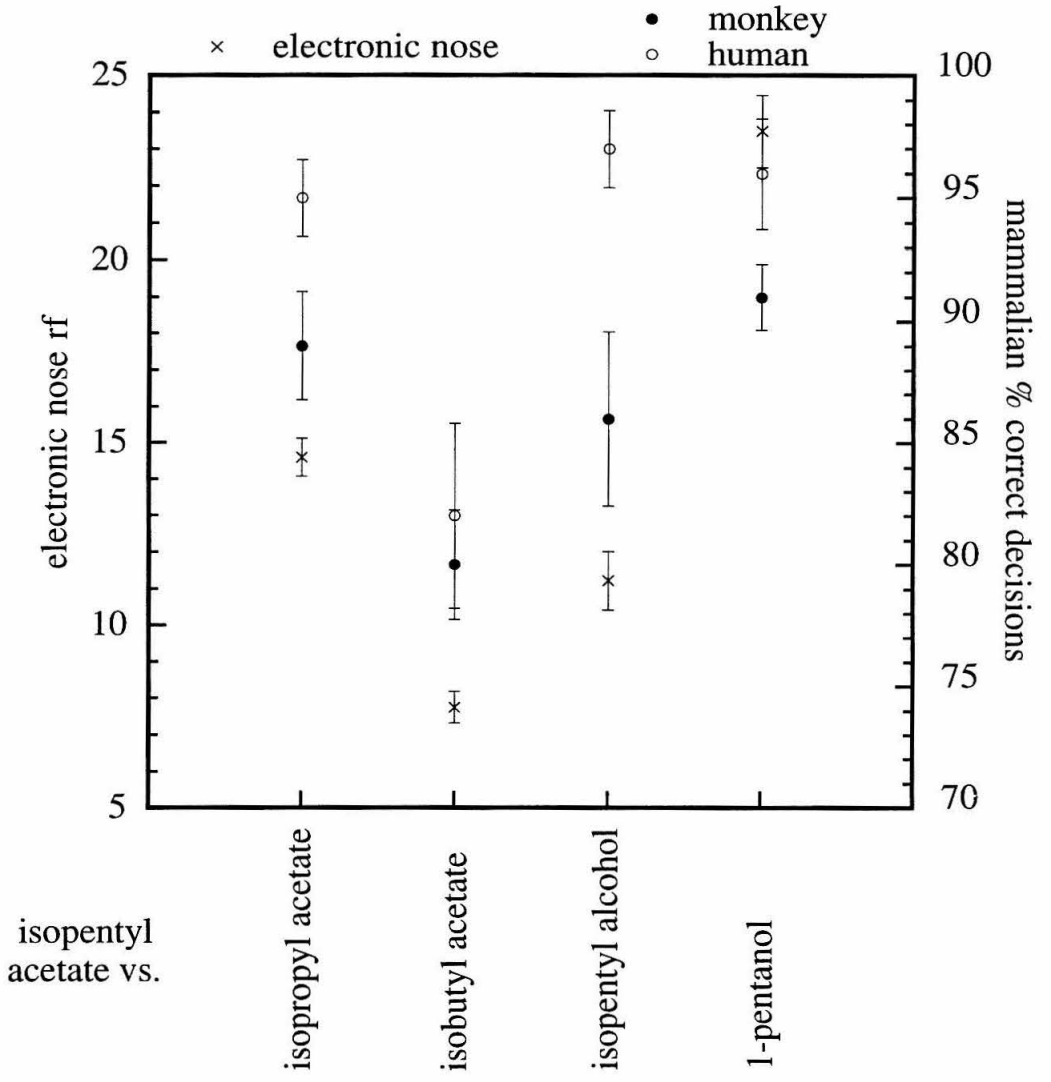
× electronic nose
• monkey
○ human
electronic nose rf
mammalian % correct decisions
25
20
15
10
5
100
95
90
85
80
75
70
isopentyl acetate vs.
isopropyl acetate
isobutyl acetate
isopentyl alcohol
1-pentanol

Figure 4.2c

Figure 4.3: Plots of trends in the abilities of the electronic nose, monkeys and humans to discriminate between n-pentanoic acid and two series of other carboxylic acid odorants with incremental chemical differences. The electronic nose data is plotted with reference to the left scale and the data points represent a mean resolution factor (rf). The monkey and human data are plotted with reference to the right scale and represent the mean probability of correctly discriminating between each specific pair of odorants averaged over ten humans and 4 monkeys as experimentally determined by Laska et al.[24] The error bars represent 1 standard deviation unit of confidence in the mean values.

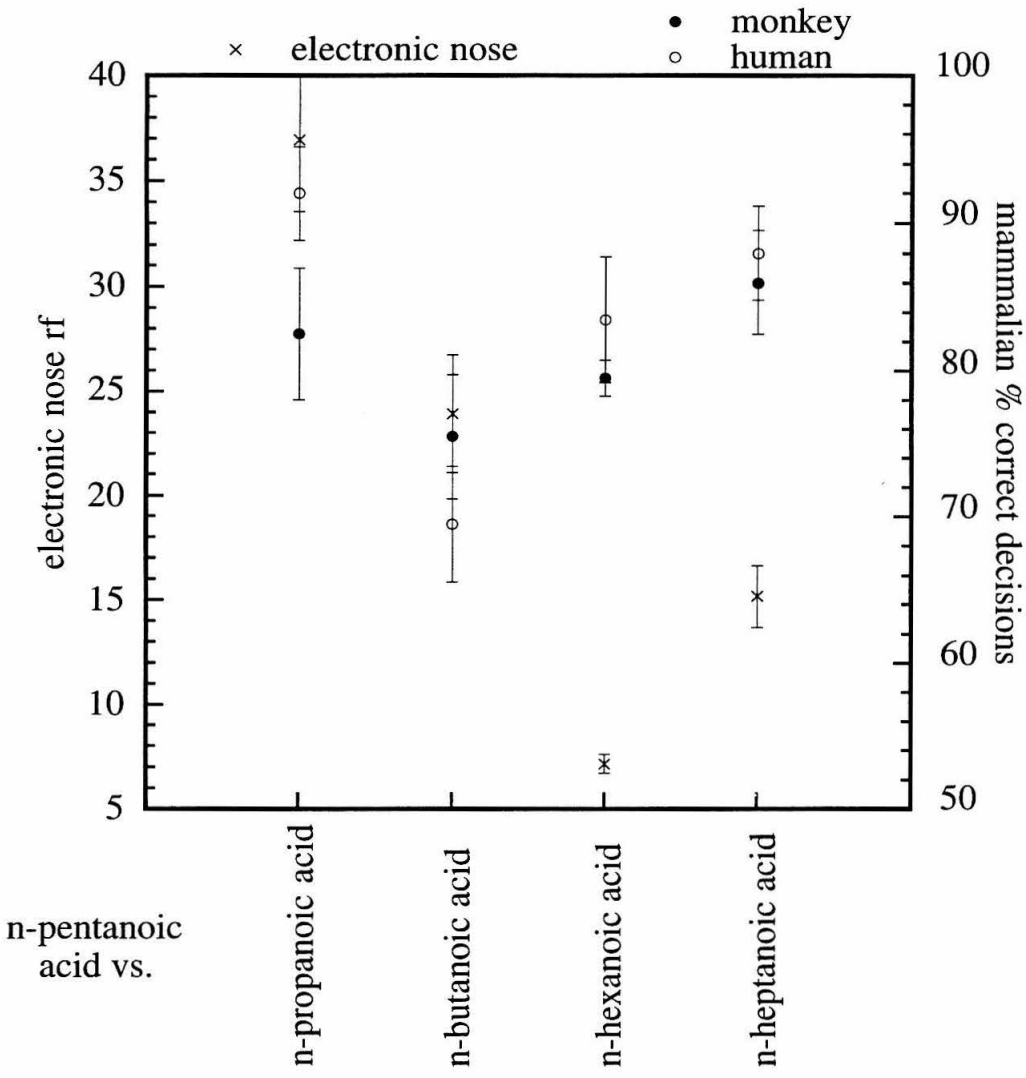
monkey
human
electronic nose
electronic nose rf
mammalian % correct decisions
40
35
30
25
20
15
10
5
100
90
80
70
60
50
n-pentanoic acid vs.
n-propanoic acid
n-butanoic acid
n-hexanoic acid
n-heptanoic acid

Figure 4.3a

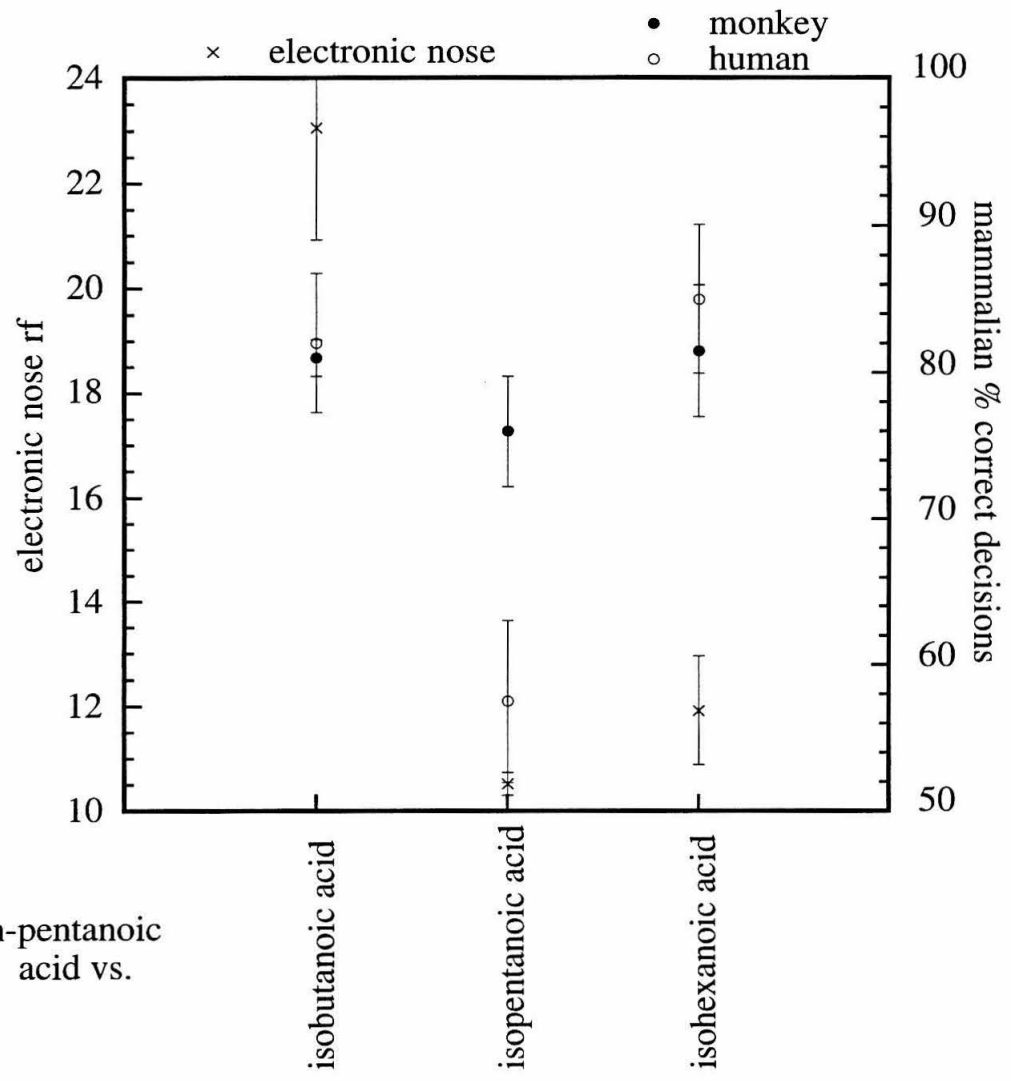
× electronic nose
• monkey
○ human
electronic nose rf
mammalian % correct decisions
24
22
20
18
16
14
12
10
100
90
80
70
60
50
n-pentanoic acid vs.
isobutanoic acid
isopentanoic acid
isohexanoic acid

Figure 4.3b

Figure 4.4: Plots of trends in the abilities of the electronic nose, monkeys and humans to discriminate between 1-pentanol and a series of other alcohol odorants with incremental chemical differences. The electronic nose data is plotted with reference to the left scale and the data points represent a mean resolution factor (rf). The monkey and human data are plotted with reference to the right scale and represent the mean probability of correctly discriminating between each specific pair of odorants averaged over ten humans and 4 monkeys as experimentally determined by Laska et al.[23] The error bars represent 1 standard deviation unit of confidence in the mean values.

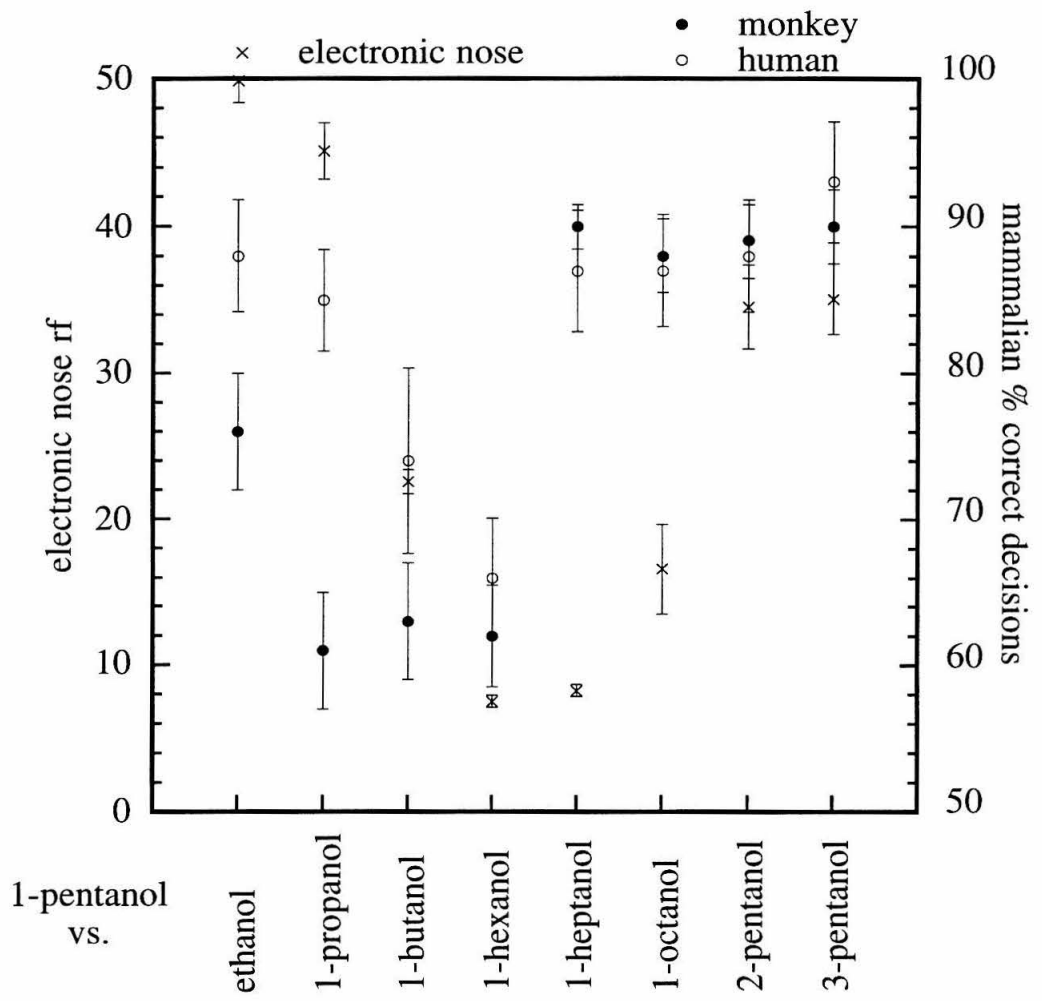
electronic nose
monkey
human
electronic nose rf
mammalian % correct decisions
50
40
30
20
10
0
100
90
80
70
60
50
1-pentanol
vs.
ethanol
1-propanol
1-butanol
1-hexanol
1-heptanol
1-octanol
2-pentanol
3-pentanol

Figure 4.4

C. Attempts at Predicting Human Odor Quality Judgements Using Electronic Nose Response Data

Electronic nose response data were collected from 22 odorants (1-butanol, 1-hexanol, 1-heptanol, 1-octanol, ethyl propionate, ethyl butanoate, propyl butanoate, pentyl butanoate, isopentyl acetate, isopentanoic acid, n-pentanoic acid, n-hexanoic acid, toluene, anisole, phenyl ethanol, phenyl acetylene, tetrahydrothiophene, thiophene, dipropyl sulfide, pyridine, citral and (R)-(+)-limonene), all of which have been quantitatively characterized based on their odor qualities by human panelists in a previous study.[26] The experimental protocol for each odorant exposure was 5 minutes of clean air flow, followed by 5 minutes of air flow containing the odorant at a partial pressure corresponding to 5% of its vapor pressure, followed by another 5 minutes of clean air flow. The electronic nose detectors were exposed to each odorant a minimum of 10 times. The data was then processed to extract the response signals as described previously.[16,17] For each detector, only the last 5 exposures to a given odorant were averaged to obtain the response value used in predicting odor qualities.

The human odor quality judgement data used in this study were obtained from a publication by Dravnieks.[26] In that study, each of the 22 odorants was evaluated by at least 120 panelists spanning a wide range of ages, including both sexes, and including smokers such that the percepts should be consistent with those of the generalized human population. For each odorant, each panelist judged the degree (on a scale of 0 through 5) to which the unknown odorant resembled a list of odor categories. For example, a particular panelist could perceive an odorant as having a rating of 3 in the "etherish, anesthetic" category, 1 in the "minty" category and 0 in several other odor categories. The author then combined all the human judgements for a given odorant's resemblance of a given odor category, and reported a quantitative applicability rating which is used herein as the observed odor quality.

The responses of the 20 electronic nose detectors to the 22 odorant molecules were used to build a different quantitative structure activity relationship (QSAR) for predicting human odor quality judgements for each of several odor categories ("etherish, anesthetic," "sharp, pungent," "oily, fatty," "minty," "putrid, foul, decayed," "fruity, non-citrus," "floral" and "gasoline, solvent"). Each QSAR equation is a linear combination of descriptors (i.e., detector responses) whose coefficients are obtained by a least squares fitting of predicted to observed odor quality data through multiple linear regression. The procedure employed for selecting the optimal detectors for the QSAR models involved the use of a genetic function algorithm[27] which generates a final count of 100 equations as described by Vaid et al.[28] The calculations were performed using the Cerius^2 software package (Molecular Simulations, Inc.) on a Silicon Graphics O_2 computer. A QSAR equation for a specific odor category has the general form,

$$y_n = a + b\cdot\mathbf{D1_n} + c\cdot\mathbf{D2_n} + d\cdot\mathbf{D3_n} + \ldots + u\cdot\mathbf{D20_n}\,, \qquad (1)$$

where y_n is the predicted rating in the specific odor category of the n^{th} odorant, $\mathbf{D1_n}$ through $\mathbf{D20_n}$ are the responses of the 20 detectors to the n^{th} odorant, and a through u are coefficients which are optimized by fitting y_n(predicted) onto y_n(observed). In practice, most of the coefficients are set to zero since only a subset of the 20 detectors can be used in any given QSAR equation without over-fitting the 22 odorant data set. The optimized equations generated by the genetic function algorithm typically used less than five detectors. The best equations generated for predicting human odor quality judgements within the odor categories of "etherish, anesthetic," "sharp, pungent," "oily, fatty," "minty," "putrid, foul, decayed" and "fruity, non-citrus" are shown in Figure 4.5 along with the corresponding plots of predicted versus observed odor quality. All of these equations were tested using cross-validation to ensure that each squared correlation coefficient, R^2, was approximately equal to the corresponding cross-validated R^2, C.V.R^2, thus providing evidence that the limited predictive ability implied in the plots is real. The fitting statistics for each plot, R^2 and C.V.R^2, are included in Figure 4.5.

The plots of predicted versus observed odor quality in Figure 4.5 show that the electronic nose does have some predictive ability, especially in the cases of the "etherish, anesthetic" and "sharp, pungent" odor categories, despite the significant amount of scatter in the plots. Only a marginal predictive ability exists in the cases of the "oily, fatty," "minty," "putrid, foul, decayed" and "fruity, non-citrus" odor categories. Specifically, the R^2 statistic defines the fraction of the variance in the observation data which can be accounted for based on the QSAR model predictions.[29] Thus, the models which predict the "etherish, anesthetic" and "sharp, pungent" odor qualities account for 65% and 72% of the variance in the respective observations. However, the remaining QSAR models each account for 52%, or less, of the variance in the observations.

While the predictive ability of the models is not particularly compelling, this study does represent a reasonable first step toward developing an electronic nose which may eventually predict the perceptual qualities of an odor, in addition to identifying the odor and quantifying its concentration. Further progress may be realized by using of nonlinear fitting algorithms. However, the subjective nature of the human odor quality data compounded by the variation in the olfactory percepts between individuals can lead to uncertainties in the observations which may ultimately limit the generalized predictive ability of any model.

Figure 4.5: Plots of the predicted odor qualities versus observed human odor quality judgements for a group of 22 odorants classified by their applicability to the (a) "etherish, anesthetic," (b) "sharp, pungent," (c) "oily, fatty," (d) "minty," (e) "putrid, foul, decayed" and (f) "fruity, non-citrus" odor categories. The human odor quality judgement data was obtained from the literature.[26] The predicted odor qualities were obtained by fitting the responses of the electronic nose detectors to the human data. The specific fitting equations and fitting statistics are given in each figure.

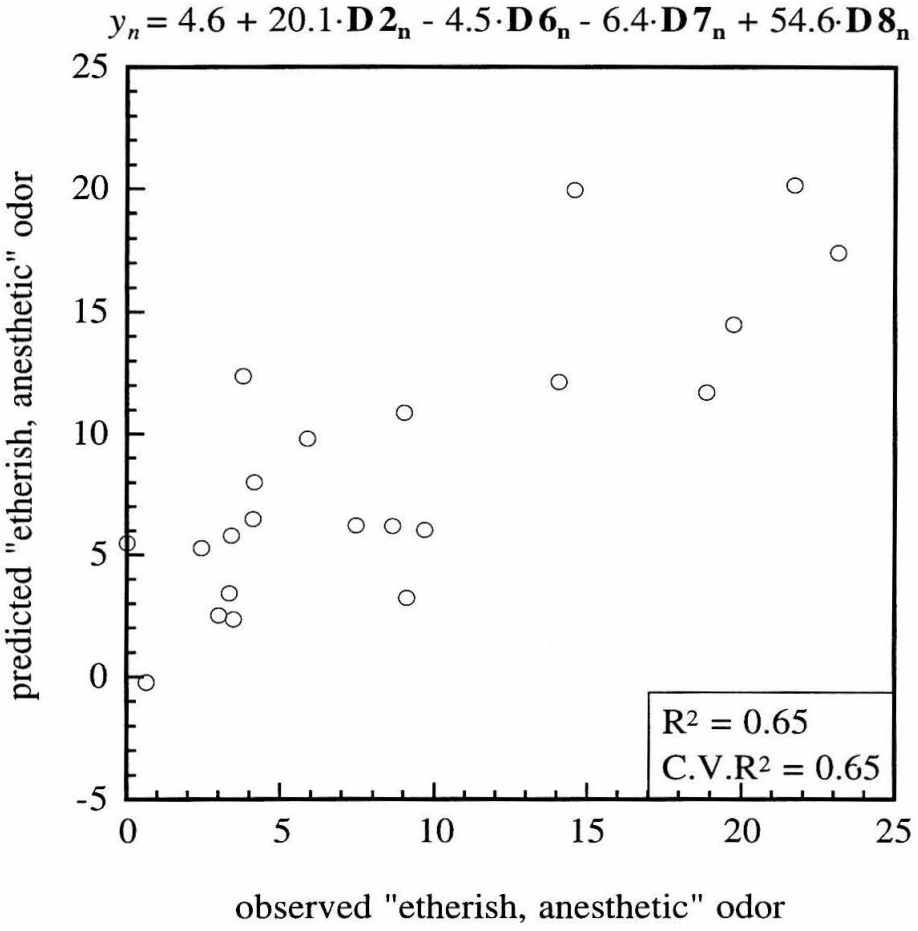
$y_n = 4.6 + 20.1 \cdot \mathbf{D2_n} - 4.5 \cdot \mathbf{D6_n} - 6.4 \cdot \mathbf{D7_n} + 54.6 \cdot \mathbf{D8_n}$
predicted "etherish, anesthetic" odor
observed "etherish, anesthetic" odor
25
20
15
10
5
0
-5
0
5
10
15
20
25
R² = 0.65
C.V.R² = 0.65

Figure 4.5a

$$y_n = 8.5 - 55.2 \cdot \mathbf{D3}_n + 31.0 \cdot \mathbf{D12}_n + 154.9 \cdot \mathbf{D14}_n + 52.1 \cdot \mathbf{D17}_n$$

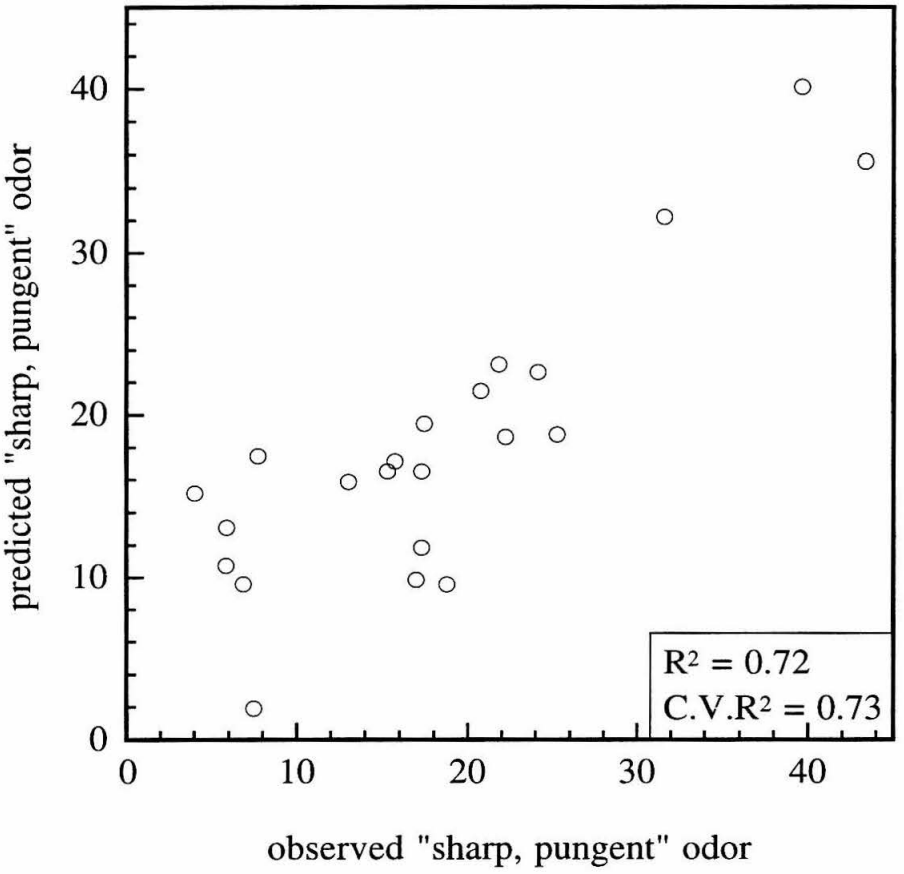

Figure 4.5b

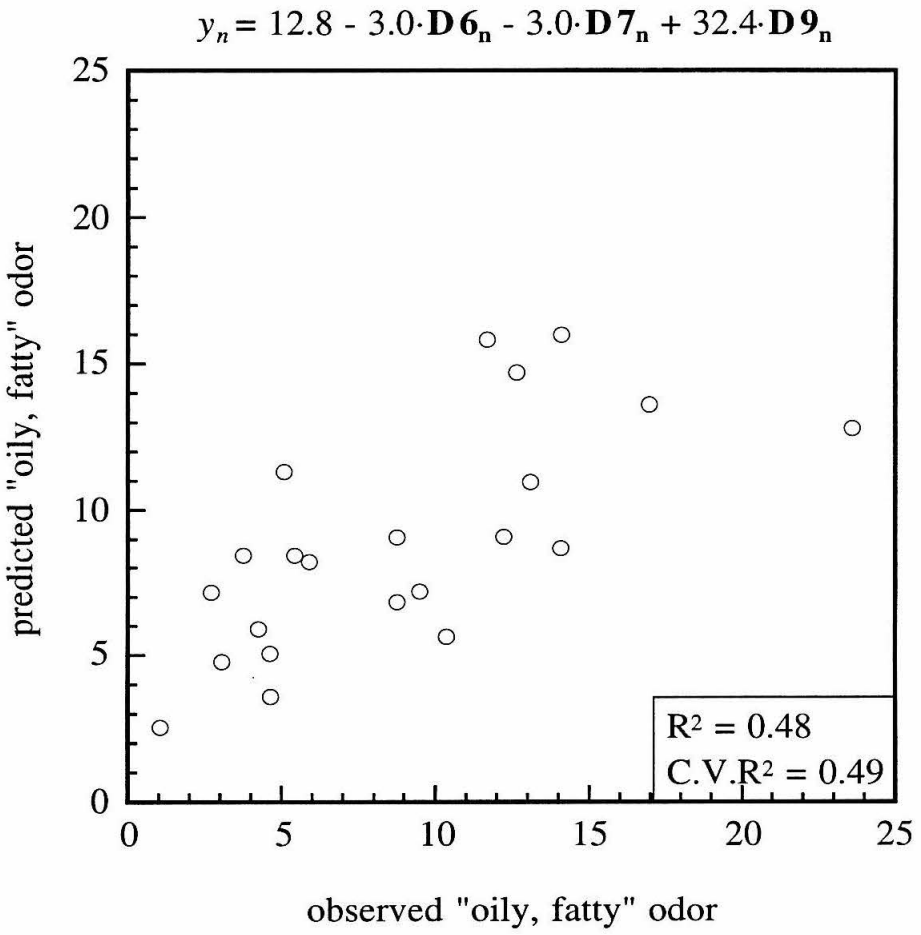
y_n = 12.8 - 3.0·**D6**$_n$ - 3.0·**D7**$_n$ + 32.4·**D9**$_n$
predicted "oily, fatty" odor
observed "oily, fatty" odor
R² = 0.48
C.V.R² = 0.49
0
5
10
15
20
25

Figure 4.5c

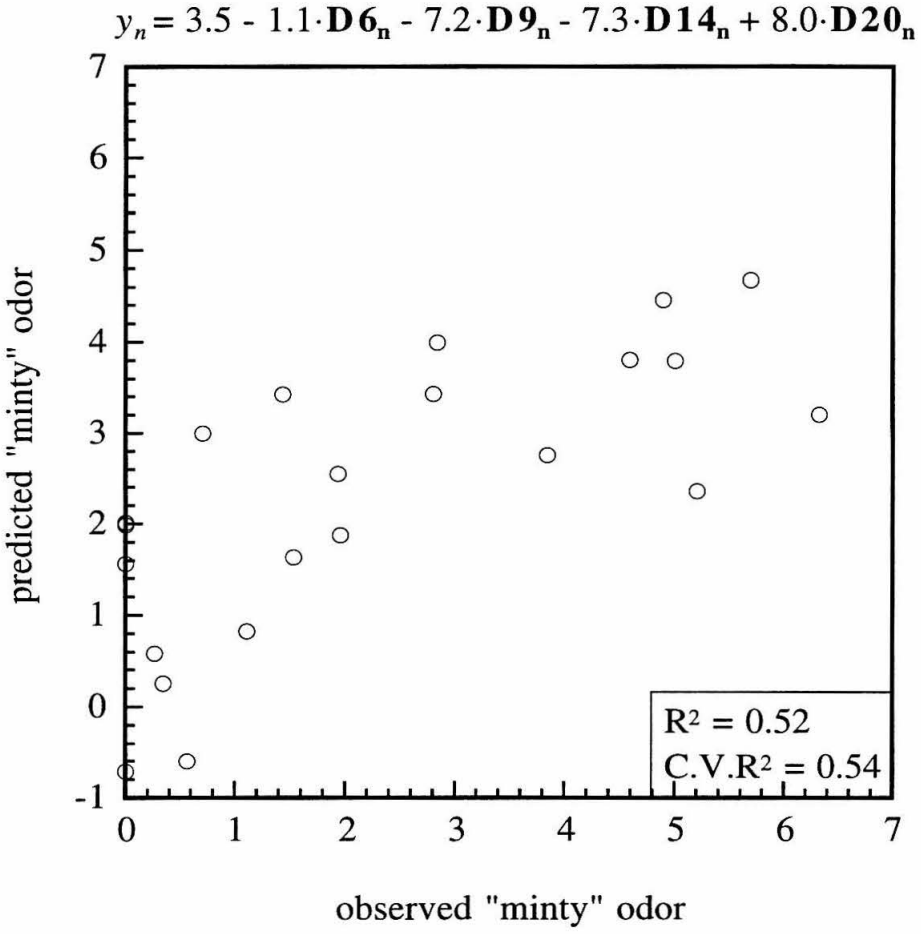
$y_n = 3.5 - 1.1 \cdot \mathbf{D6}_n - 7.2 \cdot \mathbf{D9}_n - 7.3 \cdot \mathbf{D14}_n + 8.0 \cdot \mathbf{D20}_n$
predicted "minty" odor
observed "minty" odor
R² = 0.52
C.V.R² = 0.54
7
6
5
4
3
2
1
0
-1
0
1
2
3
4
5
6
7

Figure 4.5d

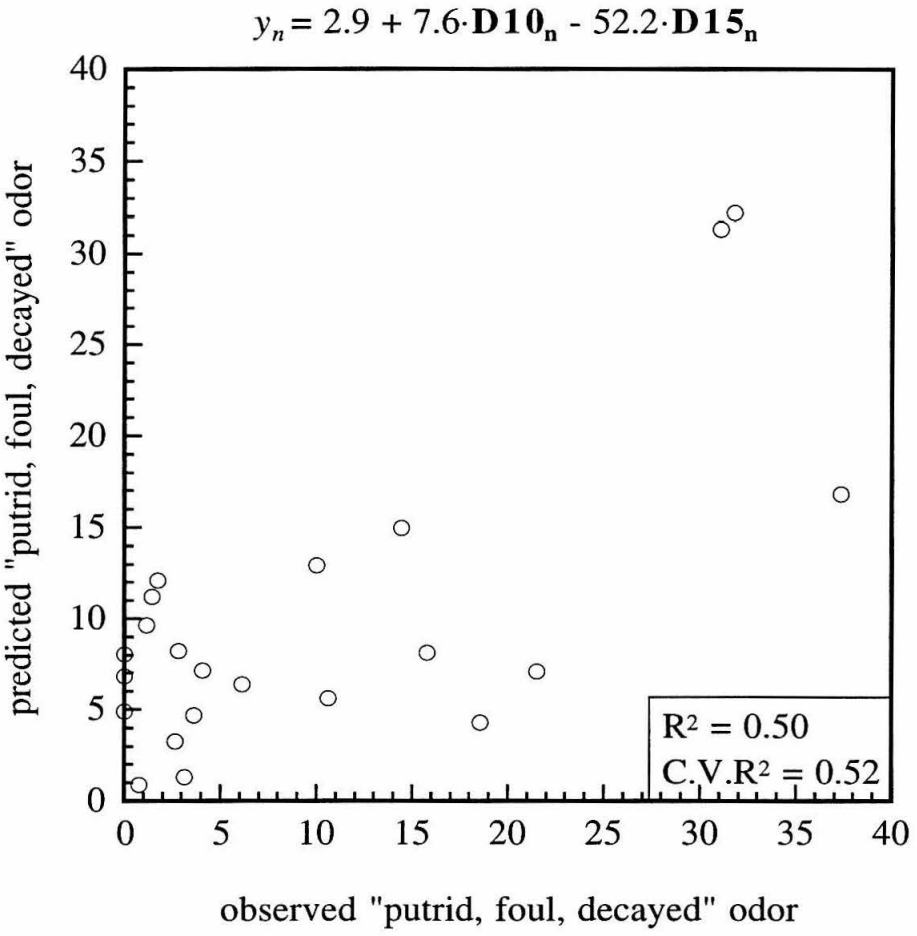
$y_n = 2.9 + 7.6 \cdot \mathbf{D10_n} - 52.2 \cdot \mathbf{D15_n}$
predicted "putrid, foul, decayed" odor
observed "putrid, foul, decayed" odor
0
5
10
15
20
25
30
35
40
R² = 0.50
C.V.R² = 0.52

Figure 4.5e

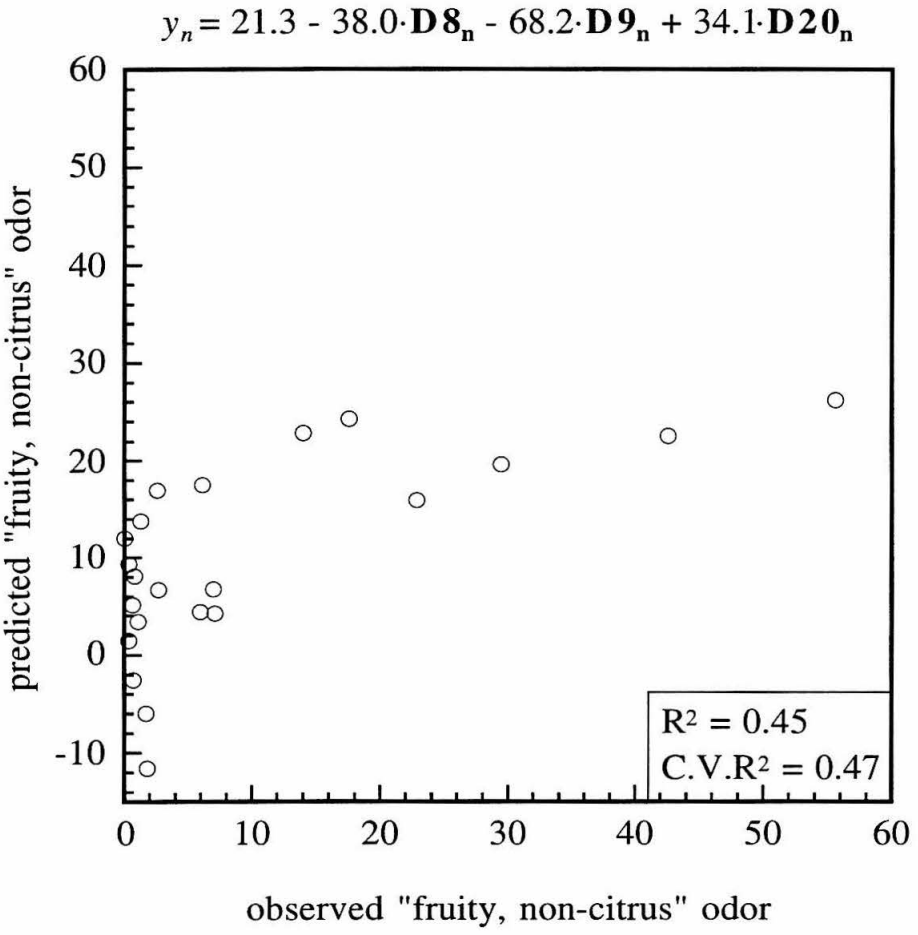
$y_n = 21.3 - 38.0 \cdot \mathbf{D8_n} - 68.2 \cdot \mathbf{D9_n} + 34.1 \cdot \mathbf{D20_n}$
predicted "fruity, non-citrus" odor
observed "fruity, non-citrus" odor
R² = 0.45
C.V.R² = 0.47
60
50
40
30
20
10
0
-10
0
10
20
30
40
50
60

Figure 4.5f

CONCLUSION

The results presented herein show several similarities in the basic abilities and trends in the abilities of the electronic nose compared to mammalian olfaction. Some degree of similarity was anticipated, despite the complex signal processing in the brain, since both systems ultimately rely on binding odorants with chemically diverse sets of broadly responsive polymer/protein-based detectors. Specifically, the absolute detection thresholds and trends in the detection thresholds of the current generation of the electronic nose are similar to those of humans across the tested odorants. The electronic nose can typically detect a minimum odorant partial pressure of approximately $4 \times 10^{-3}\%$ of the odorant's vapor pressure and humans are typically within an order of magnitude less sensitive. In addition, the trends in the odorant discrimination abilities of the electronic nose compared to the monkey and human olfactory systems are correlated as odorants typically become easier to discriminate for all three systems as they become more chemically dissimilar. In terms of predicting human odor quality judgements, the electronic nose results were not generally compelling. Only in the cases of the "etherish, anesthetic" and "sharp, pungent" odor categories were reasonably predictive models obtained.

The quantitative comparisons between the electronic nose and mammalian olfaction provided in this study are an important contribution toward the ambitious goal of designing an electronic analogue to the mammalian olfactory sense. Significant additional work by other scientists in the field will also contribute to this goal by endowing the electronic nose with increased sensitivity to specific odorant classes, such as amines and thiols, to further mimic the mammalian olfactory sense.

ACKNOWLEDGEMENTS

We sincerely thank Dr. Matthias Laska and his coworkers from the Department of Medical Psychology at the University of Munich Medical School for providing us with their data on the odorant discriminating ability of humans and monkeys. We thank NASA, the Army Research Office and DARPA for their support of this work, and B.J.D. acknowledges the Government of Canada for an NSERC 1967 Centennial Graduate Fellowship.

REFERENCES

(1) Lenarz, T. *Am. J. Otol.* **1997**, *18*, s2.

(2) Kovrigin, Y.; Chernyshov, V. *Opt. Eng.* **1998**, *37*, 3039.

(3) Heiduschka, P.; Thanos, S. *Prog. Neurobiol.* **1998**, *55*, 433.

(4) Shurmer, H. V. *IEE Proc.-G* **1990**, *137*, 197.

(5) Gardner, J. W.; Bartlett, P. N. *Sens. Actuators B* **1994**, *18*, 211.

(6) Axel, R. *Sci. Am.* **1995**, *273*, 154.

(7) Breer, H.; Wanner, I.; Strotmann, J. *Behav. Genet.* **1996**, *26*, 209.

(8) Malnic, B.; Hirono, J.; Sato, T.; Buck, L. B. *Cell* **1999**, *96*, 713.

(9) Buck, L.; Axel, R. *Cell* **1991**, *65*, 175.

(10) Ostrowski, J.; Kjelsberg, M.; Caron, M.; Lefkowitz, R. *Annu. Rev. Pharmacol. Toxicol.* **1992**, *32*, 167.

(11) Lancet, D.; Ben-Arie, N. *Curr. Biol.* **1993**, *3*, 668.

(12) Nef, P. *News Physiol. Sci.* **1998**, *13*, 1.

(13) Mori, K.; Mataga, N.; Imamura, K. *J. Neurophysiol.* **1992**, *67*, 786.

(14) Zhao, H. Q.; Ivic, L.; Otaki, J. M.; Hashimoto, M.; Mikoshiba, K.; Firestein, S. *Science* **1998**, *279*, 237.

(15) Pearce, T. C. *Biosystems* **1997**, *41*, 43.

(16) Doleman, B. J.; Sanner, R. D.; Severin, E. J.; Grubbs, R. H.; Lewis, N. S. *Anal. Chem.* **1998**, *70*, 2560.

(17) Doleman, B. J.; Lonergan, M. C.; Severin, E. J.; Vaid, T. P.; Lewis, N. S. *Anal. Chem.* **1998**, *70*, 4177.

(18) Zellers, E. T.; Park, P.; Hsu, T.; Groves, W. A. *Anal. Chem.* **1998**, *70*, 4191.

(19) Severin, E. J.; Doleman, B. J.; Lewis, N. S. *manuscript in preparation.*

(20) Lonergan, M. C.; Severin, E. J.; Doleman, B. J.; Beaber, S. A.; Grubbs, R. H.; Lewis, N. S. *Chem. Mater.* **1996**, *8*, 2298.

(21) Doleman, B. J.; Severin, E. J.; Lewis, N. S. *Proc. Natl. Acad. Sci. U.S.A.* **1998**, *95*, 5442.

(22) Devos, M.; Patte, F.; Rouault, J.; Laffort, P.; Van Gemert, L. J. *Standardized Human Olfactory Thresholds*; Oxford University Press: New York, 1990.

(23) Laska, M. *submitted for publication.*

(24) Laska, M.; Teubner, P. *Am. J. Physiol.-Reg. I.* **1998**, *43*, R1639.

(25) Laska, M.; Freyer, D. *Chem. Senses.* **1997**, *22*, 457.

(26) Dravnieks, A. *Atlas of Odor Character Profiles*; American Society for Testing and Materials: Baltimore, 1985.

(27) Rogers, D.; Hopfinger, A. J. *J. Chem. Comput. Sci.* **1994**, *34*, 854.

(28) Vaid, T. P.; Lewis, N. S. *manuscript in preparation.*

(29) Freund, R. J.; Wilson, W. J. *Statistical Methods*; Academic Press: San Diego, 1997.